

AFWL-TR-87-92

AFWL-TR-
87-92

2

AD-A198 843



CHEMICAL PUMP SOURCES FOR IF(B)

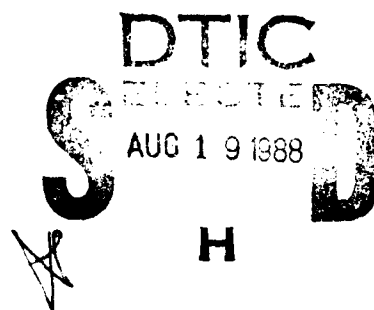
S. J. Davis, et al

Physical Sciences Incorporated
Research Park
Andover, MA 01810

June 1988

Final Report

Approved for public release; distribution unlimited.



AIR FORCE WEAPONS LABORATORY
Air Force Systems Command
Kirtland Air Force Base, NM 87117-6008

88 8 18 0 3 3

This final report was prepared by Physical Sciences, Inc, Andover, Massachusetts under Contract F29601-86-C-0017, Job Order ILIR8604 with the Air Force Weapons Laboratory, Kirtland Air Force Base, New Mexico. Leonard Hanko (ARBI) was the Laboratory Project Officer-in-Charge.

When Government drawings, specifications, or other data are used for any purpose other than in connection with a definitely Government-related procurement, the United States Government incurs no responsibility or any obligation whatsoever. The fact that the Government may have formulated or in any way supplied the said drawings, specifications, or other data, is not to be regarded by implication, or otherwise in any manner construed as licensing the holder or any other person or corporation; or as conveying any rights or permission to manufacture, use or sell any patented invention that may in any way be related thereto.

This report has been authored by a contractor of the United States Government. Accordingly, the United States Government retains a nonexclusive, royalty-free license to publish or reproduce the material contained herein, or allow others to do so, for the United States Government purposes.

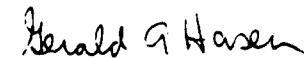
This report has been reviewed by the Public Affairs Office and is releasable to the National Technical Information Service (NTIS). At NTIS, it will be available to the general public, including foreign nations.

If your address has changed, if you wish to be removed from our mailing list, or if your organization no longer employs the addressee, please notify AFWL/ARBI, Kirtland AFB, NM 87117-6008 to help us maintain a current mailing list.

This technical report has been reviewed and is approved for publication.

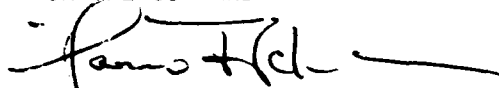


LEONARD HANKO
Project Officer



GERALD A. HASEN
Major, USAF
Chief, Advanced Chemical Laser Br

FOR THE COMMANDER



HARRO ACKERMANN
Lt Col, USAF
Chief, Laser Science & Technology Ofc

DO NOT RETURN COPIES OF THIS REPORT UNLESS CONTRACTUAL OBLIGATIONS OR NOTICE ON A SPECIFIC DOCUMENT REQUIRES THAT IT BE RETURNED.

UNCLASSIFIED

SECURITY CLASSIFICATION OF THIS PAGE

REPORT DOCUMENTATION PAGE				
1a. REPORT SECURITY CLASSIFICATION UNCLASSIFIED		1b. RESTRICTIVE MARKINGS		
2a. SECURITY CLASSIFICATION AUTHORITY		3. DISTRIBUTION / AVAILABILITY OF REPORT Approved for public release; distribution unlimited.		
2b. DECLASSIFICATION / DOWNGRADING SCHEDULE				
4. PERFORMING ORGANIZATION REPORT NUMBER(S) PSI-2000/TR-689		5. MONITORING ORGANIZATION REPORT NUMBER(S) AFWL-TR-87-92		
6a. NAME OF PERFORMING ORGANIZATION Physical Sciences, Inc	6b. OFFICE SYMBOL (If applicable)	7a. NAME OF MONITORING ORGANIZATION Air Force Weapons Laboratory		
6c. ADDRESS (City, State, and ZIP Code) P.O. Box 3100, Research Park Andover, Massachusetts 01810		7b. ADDRESS (City, State, and ZIP Code) Kirtland Air Force Base, NM 87117-6008		
8a. NAME OF FUNDING / SPONSORING ORGANIZATION	8b. OFFICE SYMBOL (If applicable)	9. PROCUREMENT INSTRUMENT IDENTIFICATION NUMBER F29601-86-C-0017		
8c. ADDRESS (City, State, and ZIP Code)		10. SOURCE OF FUNDING NUMBERS		
		PROGRAM ELEMENT NO. 61101F	PROJECT NO. ILIR	TASK NO. 86
				WORK UNIT ACCESSION NO. 04
11. TITLE (Include Security Classification) CHEMICAL PUMP SOURCES FOR IF(B)				
12. PERSONAL AUTHOR(S) Davis, Steven J.; Woodward, Anne M.; Piper, Lawrence G.; and Marinelli, William J.				
13a. TYPE OF REPORT Final	13b. TIME COVERED FROM 1 Mar 86 to 4 May 87	14. DATE OF REPORT (Year, Month, Day) 1988 June	15. PAGE COUNT 94	
16. SUPPLEMENTARY NOTATION				
17. COSATI CODES		18. SUBJECT TERMS (Continue on reverse if necessary and identify by block number)		
FIELD	GROUP	SUB-GROUP		
20	05		Singlet molecular oxygen. Visible chemical laser.	
			Chemiluminescence Energy transfer	
			Iodine monofluoride Bimodal vibrational distribution.	
19. ABSTRACT (Continue on reverse if necessary and identify by block number)				
<p>Excitation of iodine monofluoride (X) by singlet molecular oxygen was studied. Mechanistic investigations revealed that two excitation routes are active, and both require an intermediate state which is most likely iodine monofluoride (A⁻). The two models hypothesized and tested are described by: (1) iodine monofluoride reacts with singlet sigma oxygen producing the IF(A⁻) state, this state reacts with singlet delta oxygen producing IF(B), (2) vibrationally hot iodine monofluoride reacts with singlet sigma oxygen to produce the IF(A⁻) this reacts with singlet sigma oxygen and produces IF(B). ✓</p> <p>Chemiluminescence results showed that [IF(B)] scaled linearly with singlet sigma when IF(X, v=0) was excited. In contrast when IF was excited by singlet delta, the [IF(B)] scaled as the square of the concentration of singlet delta, consistent with a two step mechanism. Detailed laser induced fluorescence (LIF) measurements indicated that [IF(B)] scaled linearly with [IF(X, v">=9)] when singlet delta was the pump source. Preliminary (over)</p>				
20. DISTRIBUTION / AVAILABILITY OF ABSTRACT <input checked="" type="checkbox"/> UNCLASSIFIED/UNLIMITED <input type="checkbox"/> SAME AS RPT. <input type="checkbox"/> DTIC USERS		21. ABSTRACT SECURITY CLASSIFICATION UNCLASSIFIED		
22a. NAME OF RESPONSIBLE INDIVIDUAL LEONARD HANKO		22b. TELEPHONE (Include Area Code) (505) 844-0661	22c. OFFICE SYMBOL ARBI	

DD FORM 1473, 84 MAR

83 APR edition may be used until exhausted.
All other editions are obsolete.SECURITY CLASSIFICATION OF THIS PAGE
UNCLASSIFIED

SECURITY CLASSIFICATION OF THIS PAGE

estimates for key excitation rate coefficients are also presented.

Accusation Form

NAME	LAST	FIRST	MIDDLE	SUFFIX
DATE OF BIRTH				
PLACE OF BIRTH				
EDUCATION				
CITY				
STATE				
COUNTRY				
RELIGION				
POLITICAL PARTY				
PROFESSION				
INDUSTRY				
RESIDENCE				
TELEPHONE				
STREET ADDRESS				
CITY				
STATE				
COUNTRY				
POSTAL CODE				
DATE OF ARREST				
PLACE OF ARREST				
ARRESTING OFFICER				
CHARGE				
REMARKS				

A-1

CONTENTS

		<u>Page</u>
Paragraph 1	INTRODUCTION	1
1.1	IF as a chemical laser.	1
1.2	Chemical production of IF(B).	3
1.3	Energy transfer from excited O ₂ to IF(B).	4
1.3.1	Background and previous investigations.	4
2	CHEMILUMINESCENT STUDIES	11
2.1	Flow tube description	11
2.2	Preliminary investigations.	13
2.2.1	O ₂ ¹ Σ quenching studies.	13
2.2.2	IF(B) excitation studies.	15
2.3	O ₂ ¹ Σ studies.	19
2.3.1	Apparatus	19
2.3.2	Results of O ₂ ¹ Σ studies	21
2.4	O ₂ (¹ Δ) studies.	25
2.5	Estimation of rate coefficients	31
2.5.1	O ₂ ¹ Σ + IF	31
2.5.2	O ₂ (¹ Δ) + IF	32
2.6	Other experiments	33
3	LASER INDUCED FLUORESCENCE STUDIES	37
3.1	Introduction.	37
3.1.1	LIF apparatus	37
3.1.2	Flow tube apparatus	39
3.1.3	IX sample preparation	39
3.1.4	Analysis of LIF data.	40
3.1.5	Filter calibration.	45
3.2	Results	46
3.2.1	Initial LIF results	46
3.2.2	LIF results: complete study.	52
3.2.3	Analysis of results	52
3.3	Chemiluminescence from IF ⁺ + O ₂ [*]	65
3.4	Comparison with previous results.	72
4	MISCELLANEOUS STUDIES.	77
4.1	LIF from D' + A'.	77
4.2	Removal of IF(X,v) by O ₂ [*]	77
4.3	Rotational temperature.	77
4.4	Vibrational relaxation.	78
5	CONCLUSIONS.	81
6	REFERENCES	83

FIGURES

		Page
FIGURE	1. Energy level diagram of IF and O ₂	7
	2. Plot of detailed rate constants, k_v , for partitioning of vibrational energy in IF(X) formed from F + CF ₃ I . .	9
	3. Plot of detailed rate constants, k_v , for partitioning of vibrational energy in IF(X) formed from F + I ₂ reaction.	9
	4. Block diagram of flow tube apparatus used for initial O ₂ [*] /IF chemiluminescence studies.	11
	5. Dependence of relative [O ₂ (¹ Σ)] and [IF(B)] upon added [CO ₂]	15
	6. Dependence of relative [O ₂ (¹ Σ)] and [IF(B)] upon added [H ₂].	16
	7. Flow tube configuration used for O ₂ [*] - IF excitation studies	17
	8. Spectral scan showing chemiluminescence from IF(B+X) and O ₂ (b+X) system.	18
	9. Temporal profiles of IF(B+X) ₀₋₄ intensities using CF ₃ I and I ₂ as iodine donors.	19
	10. Block diagram of apparatus.	20
	11. IF(B+X) chemiluminescence from O ₂ [*] excitation	22
	12. Vibrational distributions of IF(B) for two [O ₂ (¹ Σ)]	23
	13. Plots of [IF(B)] _{CO₂} /[IF(B)] _{CO₂=0} versus CO ₂ flow rate for two reaction times.	24
	14. Plot of [IF(B)] versus [O ₂ (¹ Σ)] for a reaction time of 9 ms	25
	15. Dependence of [IF(B)] upon [O ₂ (¹ Σ)] at a reaction time of 1.0 ms.	26
	16. Energy levels of IF and O ₂ showing states relevant to model described by Reactions (19) + (24).	27
	17. Plot of [IF(B)] as a function of [O ₂ (¹ Δ)]	29
	18. Plot of [IF(B)] versus [O ₂ (¹ Δ)] ²	30
	19. Chemiluminescence from IF(B+X) produced by O ₂ [*] pumping of IF(X) formed from F + ICl.	34
	20. IF(B) as a function of flow rates of ICl and I ₂	35
	21. Block diagram of apparatus used for LIF studies	38
	22. Flow tube reactor showing new loop injector	38
	23. Schematic of ICl saturation used for ICl + F studies. . . .	40
	24. Energy level diagram indicating relevant states involved in LIF detection of IF(X,v).	41
	25. IF(X,v) distribution for IX + F reactions	42
	26. Transmission functions of bandpass filters used to collect LIF data.	45
	27. LIF signal.	47
	28. Energy level diagram indicating LIF detection scheme. . . .	48

FIGURES

	<u>Page</u>
29. Comparison of LIF excitation spectra using $\text{CF}_3\text{I} + \text{F}$ and $\text{I}_2 + \text{F}$ reactions when dye laser was probing hot vibrational levels in $\text{IF}(\text{X})$	49
30. Plot of temporal evolutions of IF^\dagger and $\text{IF}(\text{B} \rightarrow \text{X})$ chemiluminescence intensity $\text{IF}(\text{X})$ produced by $\text{I}_2 + \text{F}$ reaction	50
31. Plot of temporal evolution of $\text{IF}(\text{X}; \text{v}''=0)$ and $\text{IF}(\text{B} \rightarrow \text{X})$ chemiluminescence intensity	51
32. LIF of IF	55
33. LIF of IF	56
34. LIF of IF	57
35. LIF of IF	58
36. LIF of IF	59
37. LIF of IF	60
38. LIF of IF	61
39. LIF of IF	62
40. Vibrational distribution of $\text{IF}(\text{X})$	63
41. Vibrational distribution of $\text{IF}(\text{X})$	63
42. Vibrational distribution of $\text{IF}(\text{X})$	64
43. $\text{IF}(\text{B} \rightarrow \text{X})$ chemiluminescence from O_2^* excitation	66
44. $\text{IF}(\text{B} \rightarrow \text{X})$ chemiluminescence from O_2^* excitation	66
45. $\text{IF}(\text{B} \rightarrow \text{X})$ chemiluminescence from O_2^* excitation	67
46. $\text{IF}(\text{B} \rightarrow \text{X})$ chemiluminescence from O_2^* excitation	67
47. Temporal profiles of $\text{IF}(\text{B} \rightarrow \text{X})_{0-4}$ chemiluminescence intensity using iodine donors	68
48. Excitation spectra for $\text{IF}(\text{X})$ resulting from $\text{I}_2 + \text{F}$ reaction.	69
49. $[\text{IF}(\text{B})]$ produced by O_2^* pumping as a function of IF^\dagger at constant $\text{O}_2(^1\Delta)$	71
50. Vibrational distribution for $\text{IF}(\text{X})$ produced by $\text{IX} + \text{F}$	73
51. IF produce vibrational state distribution from the trajectory calculations for the reaction $\text{F} + \text{I}_2 \rightarrow \text{IF} + \text{I}$ at a collision energy of 8.4 kJ mol^{-1} (histograms)	75
52. Temporal profile of $\text{v}'' = 12$	78
53. Plot of temporal evolutions of IF^\dagger and $\text{IF}(\text{B} \rightarrow \text{X})$ chemiluminescence intensity $\text{IF}(\text{X})$ produced by $\text{I}_2 + \text{F}$ reaction	79
54. Semi log plot of $[\text{IF}(\text{X}, \text{v}'' = 10)]$ versus reaction time	80

1. INTRODUCTION

1.1 IF AS A CHEMICAL LASER

Following the initial flurry of activity in the search for a visible chemical laser in the early 1970's there has been a continued but somewhat subdued program for the past several years. However, since the formation of a national Strategic Defense Initiative, there has been a renewed interest in developing efficient high energy short wavelength chemically pumped laser systems. The potential is great, but no visible chemical lasers have yet been demonstrated.

One promising concept for producing a short wavelength chemical laser (SWCL) is to use energy transfer from a chemically produced metastable atom or molecule to a suitable laser species. The search for a laser system has taken two independent routes, i.e., the identification of suitable storage and laser species and the subsequent coupling of the two. A leading candidate for visible lasing is the IF (B \rightarrow X) system at $\lambda \sim 603$ nm.

The radiative and collisional properties of IF(B) are nearly perfect for chemical laser development. Reference 1 reports the radiative lifetime (τ) is ~ 7 μ s for $0 \leq v' \leq 9$. This translates into large stimulated emission cross sections (σ_{se}) for many $v' \rightarrow v''$ transitions. For example, $\sigma_{se} = 7.2 \times 10^{-17}$ cm² for the $0 \rightarrow 5$ transition. This leads to a small signal gain (γ) of $\gamma = 0.23$ percent/cm on the R(20) line for only 1 mtorr of IF(B) at 300 K. In addition to radiative lifetimes that offer large optical gains, the equilibrium internuclear separation for the B state is 10 percent greater than that for the X state. Consequently, the largest Franck-Condon Factors ($q_{v',v''}$) for IF(B \rightarrow X) terminate on high v'' facilitating the production of population inversions between $v' = 0$ and high v'' ($v'' = 4,5,6$). Interestingly, even though there is a relatively large potential shift in IF, the emission spectrum for the entire IF(B \rightarrow X) system is relatively narrow (440 to 750 nm), and, as a result, the B \rightarrow X emission oscillator strength is not so severely diluted as it is in other molecules possessing shifted potentials.

It has been demonstrated that the $IF(B + X)$ system will lase if a suitable chemical pump source can be found (Refs. 2, 3). In a pulsed optically pumped laser containing 10 torr of He, IF lased on the $(v', J') \rightarrow (v'', J'') = (0, 22) \rightarrow (4, 21)$ band, independent of which (v', J') level was pumped for $v' = 0 \rightarrow 6$. Thermalization in $IF(B)$ by He dominated all kinetic processes. Since most conceivable chemical excitation mechanisms will populate at least several v', J' levels, the observation of lasing from a thermalized distribution is evidence that relatively nonselective chemical excitation can be channeled into a single $(v'' = 0)$ level enhancing both the probability and the efficiency of lasing.

Energy transfer experiments (Refs. 4-6) have shown that V-T collisions in $IF(B)$ occur in single, $|\Delta v| = 1$, steps with rates that exceed electronic quenching by at least two orders of magnitude for all the rare gases and N_2 . Rotational relaxation occurs in large ($\Delta J \sim 10$) steps at nearly gas kinetic rates.

While the pulsed IF studies answered critical questions concerning the kinetics of the upper laser level, the recent continuous wave (CW) optically pumped demonstration provided the definitive proof that relaxation within the v, J manifold in $IF(X)$ can keep the terminal laser level essentially empty (Ref. 7).

Using these results, one can then search for pumping schemes with confidence that if an efficient chemical pumping source can be identified then lasing may indeed be achieved. Since the laser properties of the $IF(B + X)$ system are well in hand and appear favorable, it is in the area of chemical excitation kinetics that the breakthroughs necessary to produce a chemical laser must occur.

1.2 CHEMICAL PRODUCTION OF IF(B)

Chemical production of IF(B) was first observed by Durie (Ref. 8) when he reacted $I_2 + F_2$. Whitefield and Davis (Ref. 9) measured the rate coefficient for consumption of I_2 by F_2 to be $(1.9 \pm 0.4) \times 10^{-15} \text{ cm}^3/\text{molecule}^{-1}\text{-s}^{-1}$ at room temperature. This is consistent with the molecular beam results in Refs. 10 and 11 which showed that the $I_2 + F_2$ reaction has a 4.2 kcal/mole activation barrier. In addition, Valentini and Lee proposed the now accepted mechanism for the IF(B) excitation in the $I_2 + F_2$ reaction (Ref. 10):



The rate of IF(B) production via the $I_2 + F_2$ reaction appears to be limited by reaction (1), and if the activation barrier could be exceeded then the efficiency of IF(B) production might be significantly enhanced (Ref. 9).

The more promising approach to a chemical laser demonstration, energy transfer to IF(B) from metastable molecules, has also been observed for several species. For example, transfer has been observed from $O_2(^1\Delta)$ (Refs. 12 and 13), $NF(^1\Sigma)$ (Ref. 14), $N_2(A^3\Sigma)$ (Ref. 15), and active nitrogen (Refs. 16 and 17).

It has been determined that the process $N_2(A) + IF(X)$ proceeds with a rate coefficient of $2.0 \times 10^{-10} \text{ cm}^3 \text{ molecule}^{-1}\text{-s}^{-1}$ with an IF(B) pumping efficiency of 40 percent (Ref. 15). Daily, et al. (Ref. 16) and Piper (Ref. 17) have also observed that "active" nitrogen pumps IF. In their preliminary study Daily et al. (Ref. 16) estimated that as much as 10 percent of the ground state IF was excited to IF(B) by active N_2 that was produced in a microwave discharge.

Another scheme that has received considerable attention (Ref. 14) is described by Eq. (3)

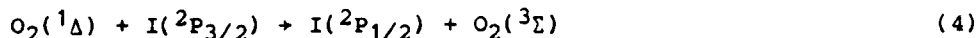


Pritt and coworkers (Ref. 14) have observed this transfer process, and the metastable molecule $\text{NF}(b^1\Sigma)$ can be chemically produced. Recent work by Setser (Ref. 18), however, has shown that $\text{NF}(b)$ is quenched by $\text{IF}(X)$ with a rate coefficient approximately two orders of magnitude faster than that for $\text{IF}(B)$ excitation by $\text{NF}(B)$. Consequently, this excitation scheme has been deemphasized.

The present study was concerned with the third excitation scheme: the energy transfer from excited singlet $\text{O}_2(a^1\Delta, b^1\Sigma)$ to $\text{IF}(B)$. The maturity of O_2^* chemical generator technology is much greater than that for either excited N_2 or NF , and there were several previous observations that had indicated that the O_2^*/IF system should be studied further.

1.3 ENERGY TRANSFER FROM EXCITED O_2 TO $\text{IF}(B)$

1.3.1 Background and previous investigations--There have been only two reported investigations in which excited oxygen was used to excite $\text{IF}(B)$. The first was by Clyne, et al. (Ref. 12) in 1972 when they reacted $\text{I} + \text{F} + \text{O}_2(^1\Delta)$. Although they proposed no definitive mechanism, they favored the process



where M was a rare gas atom. The $\text{I}(^2\text{P}_{1/2})$ and F might be expected to have an efficient three-body formation rate to $\text{IF}(B)$ because they are the separated atom correlations of $\text{IF}(B)$.

In more recent experiments Whitefield, Shea, and Davis (Ref. 13) examined chemiluminescence from three reactions.



The IF emission intensities were in the ratio 1/10/50 for reactions (6), (7), and (8). Defining a photon yield $\phi = \frac{\# \text{IF(B+X) photon emitted/s}}{\# \text{I}_2 \text{ molecules injected/s}}$, Whitefield et al. (Ref. 13) measured $\phi \sim 0.3$ percent for reaction (8).

There are several reasons for concluding that this yield was not optimum. First, the photon yield definition assumed complete I_2 consumption. Incomplete reaction would have decreased the measured yield. Secondly, very recent results by Wolf and Davis (Ref. 5) and by Whitefield (Ref. 19) have shown that I_2 is an efficient quencher of IF(B) ($k_Q = 3.6 \times 10^{-10} \text{ cm}^3/\text{molecule-s}$). Thus, any residual I_2 would have quenched IF(B), further reducing the yield. Finally, the measurements by Whitefield, et al. (Ref. 13) were performed over a limited range of conditions. They used a microwave discharge to produce $\sim 10^{15} \text{ O}_2(^1\Delta)/\text{cm}^3$ at a ratio $[\text{O}_2(^1\Delta)]/[\text{O}_2(^3\Sigma)]$ of only 8 percent. They found that the yields were $\text{O}_2(^1\Delta)$ limited. Even in their small scale flow tube, Whitefield, et al. produced IF(B) number densities of approximately $10^{10}/\text{cm}^3$; IF(B) densities of 10^{12} cm^{-3} would almost certainly produce lasing. Indeed, using a novel intracavity gain measurement technique Williamson, Hanks and Davis (Ref. 20) have observed small signal gain for optically excited IF(B) concentrations of $\sim 10^{12} \text{ cm}^{-3}$.

It appears that an order of magnitude increase in pumping efficiency coupled with a high yield chemical oxygen generator could produce gain or lasing in IF. The potential of this approach was demonstrated in 1985 when F_2 was injected into the $\text{I}_2 + \text{O}_2(^1\Delta)$ flow in the RECOIL laser device. Extremely intense IF(B+X) emission was observed. From Whitefield, et al. (Ref. 13) we note that injecting F in place of F_2 would probably have produced an even greater emission.

There were other kinetic data that also warranted further investigation of $O_2(^1\Delta)$ as a pump source for IF(B). Early measurements (Ref. 4) of rapid removal of IF(B; $v > 3$) by O_2 ($k = 8.5 \times 10^{-12} \text{ cm}^3/\text{molecule-s}$) were originally attributed to electronic quenching of IF(B). In a more detailed study, Wolf and Davis (Ref. 5) have shown that the actual electronic quenching rate coefficient is only $1.3 \times 10^{-12} \text{ cm}^3 \text{ molecule}^{-1}\text{-s}^{-1}$. Since the radiative rate for IF(B \rightarrow X) is $1.5 \times 10^5 \text{ s}^{-1}$, the IF laser should tolerate O_2 densities of at least $1 \times 10^{17}/\text{cm}^3$ (3 torr) if the quenching rate is indeed $\sim 1 \times 10^{-12} \text{ cm}^3 \text{ molecule}^{-1}\text{-s}^{-1}$. This has been confirmed with the observation of IF lasing in the presence of 5 torr of ground state O_2 in an optically pumped laser (Ref. 3).

Energy level diagrams of IF and O_2 are shown in Fig. 1. It is clear that neither $O_2(^1\Delta)$ nor $O_2(^1\Sigma)$ has sufficient energy to pump IF(X; $v''=0$) directly to IF(B). Sequential collisions of $O_2(^1\Sigma)$ and $O_2(^1\Delta)$ with IF(X; $v''=0$) could energetically transfer $\Delta E \sim 21100 \text{ cm}^{-1}$, which would produce IF(B; $v'=5$). Such a model involving sequential O_2^* collisions requires an intermediate energy reservoir in the IF manifold. There are two likely candidates: IF(X; $v'' \gg 0$) and IF A'($^3\Pi_2$). Since E-V energy transfer promoting IF(X; $v''=0$) to IF $^+$ (X; $v'' \gg 0$) would be expected to be improbable because of Franck-Condon considerations (Ref. 21), it is an unlikely candidate.

At the outset of this program the location of T_e for the IF(A') state was not known but had been estimated to be in the range $13,000$ to $15,000 \text{ cm}^{-1}$ (Ref. 13). Very recent results by Heaven (Ref. 22) have determined $T_e(A') = 13,250 \text{ cm}^{-1}$ in an Ar matrix. Thus, while $O_2(^1\Delta)$ cannot directly promote IF(X; $v''=0$) to the A' state, it would appear that $O_2(^1\Sigma)$ may contain sufficient energy to populate IF(A') from IF(X; $v''=0$) from which a secondary $O_2(^1\Delta)$ collision could produce IF(B).

In order that $O_2(^1\Delta)$ pump IF(X) to IF(A'), IF(X) must be vibrationally excited. If IF(A') has $T_e \sim 13,250 \text{ cm}^{-1}$ then only IF $^+$ (X; $v'' \gg 9$) can be pumped to IF(A') by $O_2(^1\Delta)$ collisional transfer. If T_e is higher then even more IF vibrational excitation is needed. It seems reasonable to expect that IF(A') can be pumped to IF(B) by an energy transfer collision from $O_2(^1\Delta)$. The

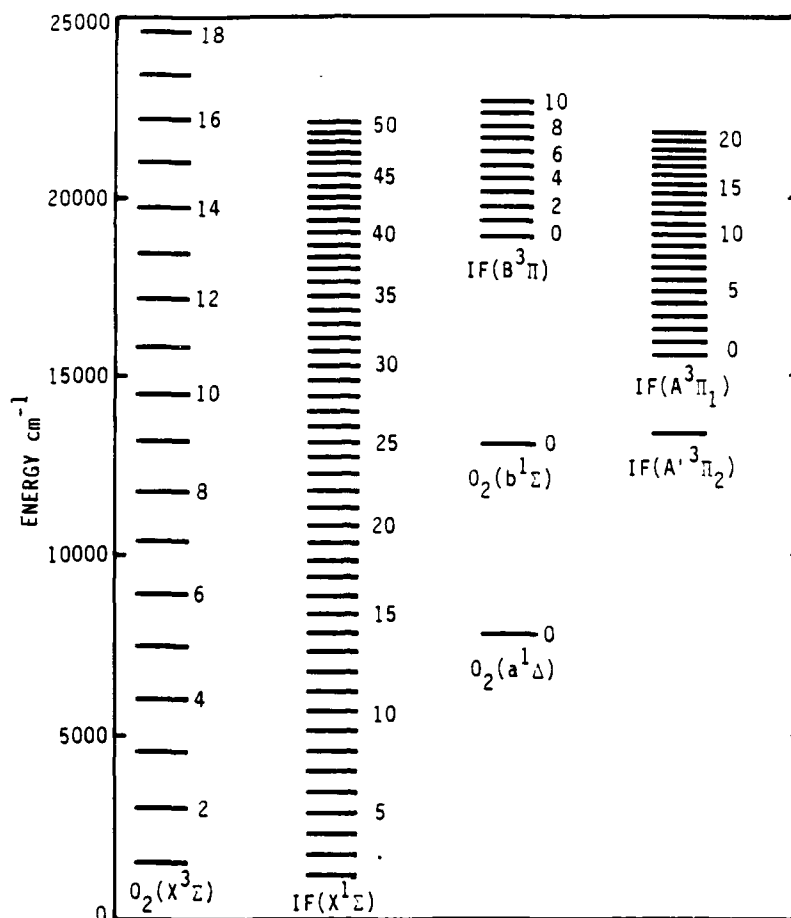


Figure 1. Energy level diagram of IF and O₂.

efficiency of IF(B) production could critically depend upon the formation rate of IF(A'). Indeed, the rates for IF(A') formation could be considerably different depending upon whether O₂(¹Δ) or O₂(¹Σ) is involved.

From these considerations one can postulate two plausible models for IF(B) excitation by O₂(¹Σ, ¹Δ). The first involves O₂(¹Σ) pumping of IF(X, v"=0) to IF(A') followed by promotion to IF(B) via an O₂(¹Δ) energy transfer collision. The second possible mechanism would use two O₂(¹Δ) molecules. As described in subsequent sections it is well known that the reactions $F + IX \rightarrow IF + X$ (X = I, Cl, Br), all partition energy into vibration of the IF(X) product. It is energetically possible for O₂(¹Δ) to promote high lying IF(X, v) to the A' state. A secondary O₂(¹Δ) collision could produce IF(B).

Although no experimental evidence existed to support the $O_2(^1\Sigma)$ mechanisms, the results of Whitefield et al. (Ref. 13) were consistent with the $IF(X,v)$ mechanism. They found that the $IF(B + X)$ emission was most intense when the three reactants were mixed at one spatial position in the flow tube. When the I_2 and F were mixed upstream of the $O_2(^1\Delta)$ the emission was much less intense. This suggested that the IF formed in the $F + I_2$ reaction initially contained internal energy that relaxed before it reached the $O_2(^1\Delta)$, (approximately 10 cm downstream.) It is likely that this internal energy was partitioned as vibrationally excited IF which we label IF^\dagger .

In 1986 VanBentham and Davis (Ref. 23) reported that vibrationally excited $I_2^\dagger(X; 33 < v'' < 44)$ is produced when $O_2(^1\Delta)$ is reacted with I_2 . The I_2^\dagger is thought to be an energy carrier in the dissociation of I_2 by $O_2(^1\Delta)$. (Interestingly, I_2^\dagger could also surmount the barrier of reaction (1).) By analogy it was inviting to speculate that highly excited $IF(X, v'' > 9)$ could also be utilized by $O_2(^1\Delta)$ to pump $IF(B)$.

The detailed work of Wanner and coworkers (Refs. 24-28) had shown that IF^\dagger is indeed produced in reactions between F and I_2 , ICl and IBr . For all three reactions they observed bimodal vibrational distributions in $IF(X)$. The population displayed a peak at $v'' = 0$ then rapidly diminished for $v'' < 5$. A secondary peak at higher v'' was also observed. Trickl and Wanner (Ref. 26) also showed that the degree of internal vibrational energy in $IF(X)$ was highly dependent upon the precursors used for $IF(X)$ production. They reported that the fraction of IF^\dagger produced is an order of magnitude greater using ICl and IBr than for I_2 . They also found (Ref. 27) that $CF_3I + F$ produces very little IF^\dagger . For illustration some of their results are presented in Figs. 2 and 3. If vibrationally excited $IF(X)$ is important in the $O_2(^1\Delta)$ pumping process then one might expect to observe significant differences in the $IF(B)$ production efficiencies for the three iodine donors: I_2 , IBr , ICl . For example, based on the results of Ref. 26, IBr should produce a significant enhancement over I_2 . CF_3I on the other hand should produce essentially no IF^\dagger and our proposed IF^\dagger model would predict essentially no $IF(B)$ production. It was clear that a systematic study of $IF(B)$ production as a function of IX precursor would directly address several aspects of the proposed $O_2(^1\Delta)$ pumping scheme that involved IF^\dagger .

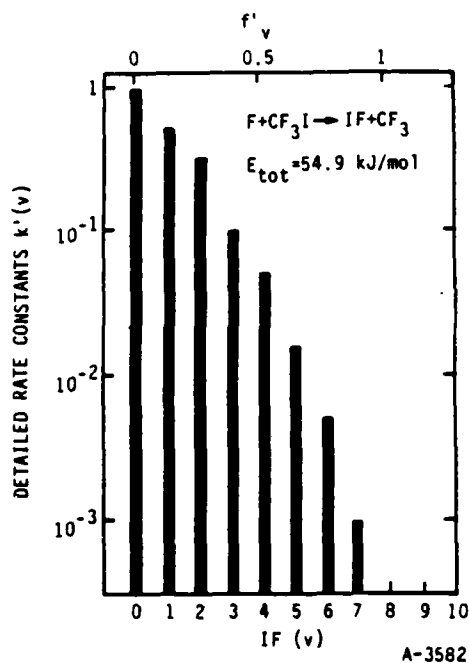


Figure 2. Plot of detailed rate constants, k_v , for partitioning of vibrational energy in IF(X) formed from F + CF₃I. Data taken from Ref. 27

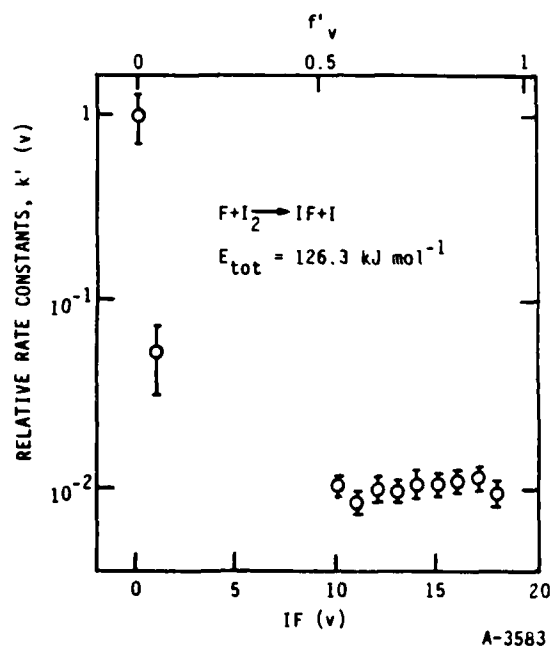
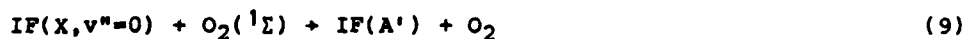


Figure 3. Plot of detailed rate constants, k_v , for partitioning of vibrational energy in IF(X) formed from F + I₂ reaction. Data taken from Ref. 26

Of necessity, the experimental program involved several studies designed to address key issues relevant to the two models. The remainder of this report is previewed by briefly describing the major experiments associated with each model.

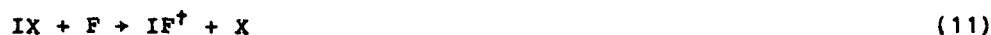
The O₂¹Σ model is summarized in Eqs. (9) and (10):



This model was tested by adding IF(X, v''=0) to a flow of O₂(¹Σ, ¹Δ) and monitoring IF(B) as a function of [O₂(¹Σ)] at a constant O₂(¹Δ) number density using

chemiluminescence techniques. The $[O_2(^1\Sigma)]$ was changed by adding species that selectively quenched $O_2(^1\Sigma)$ while having no effect on $[O_2(^1\Delta)]$.

The model involving IF^\dagger is described by Eqs. (11) through (13):



Chemiluminescence techniques and laser induced fluorescence (LIF) were used to test this mechanism. The formation of IF^\dagger from reaction (11) was confirmed using LIF. Population distributions in $IF(X,v)$ were mapped out, and $O_2(^1\Delta)$ was added to the flow. The subsequent production of $IF(B)$ was monitored using chemiluminescence as a monitor. In this manner the causal relationship between IF^\dagger and $IF(B)$ production was demonstrated. Some studies also probed the dependence of $IF(B)$ production upon $[O_2(^1\Delta)]$.

Several other miscellaneous experiments are also described. These include preliminary studies of IF^\dagger relaxation by Ar and O_2 and rotational temperatures in the IF^\dagger manifold.

The program consisted of two tasks. The first was to examine whether $O_2(^1\Sigma)$ could be used as an IF excitation source, while the second task examined the mechanistic role of vibrationally excited $IF(X)$ in the excitation of $IF(B)$ by O_2^+ .

The remainder of this report is arranged as follows. Section 2 describes the chemiluminescence studies involving both $O_2(^1\Delta)$ and $O_2(^1\Sigma)$. Section 3 contains our LIF results with emphasis on IF^\dagger . Section 4 contains results of a series of other experiments including evidence of IF^\dagger relaxation.

2. CHEMILUMINESCENCE STUDIES

2.1 FLOW TUBE DESCRIPTION

The fast flow reactor was completed and tested during the first quarter of the program. The tube was constructed from 5 cm i.d. Pyrex, and the observation region was a 5 cm i.d. stainless steel chamber coated with Teflon (Dupont Poly TFE #852-201). Prior to Teflon coating the entire observation chamber was painted with a flat black primer. The black primer/Teflon combination serves two functions. The primer reduces scattered light which facilitates all spectroscopic observations. The Teflon also reduces wall reactions and recombinations. The entire flow tube is shown in Fig. 4.

As indicated in Fig. 4, the flow tube was modular and configuration changes were conveniently made. All gas flows were monitored by electronic mass flowmeters. The flowmeters were calibrated by measuring the change in pressure versus time of gas flows into a standard volume (6.5l or 12.0l flasks). The pressure change was measured using a Validyne pressure transducer that had been calibrated against a mercury or oil manometer.

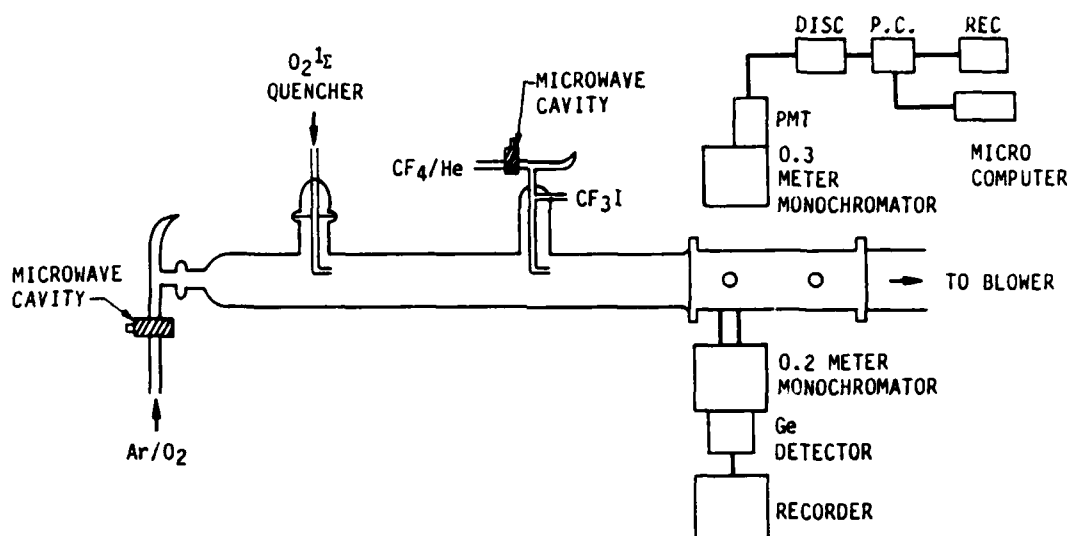


Figure 4. Block diagram of flow tube apparatus used for initial O₂^{*}/IF chemiluminescence studies.

The pressure in the flow tube was measured using a Baratron 0 to 100 torr capacitance manometer. Typical flow tube pressures ranged from 0.13 to 2.5 torr. Flow velocities could be varied from 500 to 5300 cm/s. The flow velocity was determined using the mass flow equation:

$$v = \frac{1}{A\rho}(f) \quad (14)$$

where

$f \equiv$ gas flow rate in number of molecules s^{-1}

$\rho \equiv$ total number density in the flow tube

$A \equiv$ flow tube area

$v \equiv$ bulk gas velocity.

The term f is measured with the mass flowmeter and ρ is calculated from the capacitance manometer pressure reading using Eq. (15).

If the total pressure in the flow tube is P_T (torr) at temperature T (K), then the number density of reactant i is given by:

$$N_i = \frac{f_i}{\sum_i f_i} \left(\frac{P_T N_O}{RT} \right) \quad (15)$$

where f_i = flow rate of reactant i , $\sum f_i$ total flow rate of all reactants in flow tube, N_O is Avogadro's number, and R is the gas constant.

Two configurations were used during the current program. For the chemiluminescence studies, emissions from $O_2(^1\Sigma)$ and $IF(B)$ were monitored with a 0.3m McPherson monochromator and a Hamamatsu (R943-02) GaAs PMT. Imaging of the chemiluminescence radiation was accomplished with a single lens that provided one to one imaging with an f number of 5.3 (equivalent to that of the monochromator).

The $O_2(^1\Sigma)$ was produced by passing a flow of Ar/O_2 through a microwave cavity as shown in Fig. 4. Detection of $O_2(^1\Sigma)$ was accomplished by monitoring the $b^1\Sigma \rightarrow X^3\Sigma$ system at 760 nm.

Reactions (16) and (17) were used to produce IF(X).



Although both reactions are fast, ($k_{16} = (1.2 \pm 0.6) \times 10^{-10} \text{ cm}^3 \text{ molecule}^{-1} \text{ s}^{-1}$) (Ref. 27) and ($k_{17} = (4.3 \pm 1.1) \times 10^{-10} \text{ cm}^3 \text{ molecule}^{-1} \text{ s}^{-1}$) (Ref. 29) they are known to produce drastically different vibrational distributions of IF(X;v). Detailed molecular beam work (Refs. 26,27) demonstrated that the vibrational distribution from reaction (16) is Boltzmann in nature while reaction (17) produces a bimodal distribution.

2.2 PRELIMINARY INVESTIGATIONS

2.2.1 O₂¹Σ quenching studies--One can investigate the potential role of O₂(¹Σ) as a pump source by studying the behavior of [IF(B)] as a function of [O₂(¹Σ)]. In the initial studies, a quencher gas was added to the O₂(¹Σ) flow and monitored the chemiluminescence originating from both O₂(¹Σ) and IF(B). Since the radiative lifetime (Ref. 1) of IF(B) is $\sim 7 \times 10^{-6} \text{ s}$ it radiates essentially instantaneously in the viewing region. As a result any [IF(B)] produced from excitation by O₂¹Σ is in steady state with respect to O₂¹Σ.

For these quenching investigations IF(X) was prepared in a sidearm by reacting F + CF₃I with F in excess. The F atoms were produced by a microwave discharge of a CF₄/He flow. The discharge conditions were identical to those used in a previous program (Ref. 17). Under these conditions the IF(X) flow was equal to the CF₃I flow. The ground state IF molecules flowed from the sidearm into the flow tube through a 1-cm-dia injector. When produced in this manner the IF(X) is expected to be vibrationally cold when it enters the flow tube.

For the present study two quenching gases were used: H_2 and CO_2 . The chemiluminescence intensities of both the $O_2(b^1X)$ and $IF(B^1X)$ systems were monitored as a function of added quencher gas. In these experiments a fixed port injector for the $O_2(^1\Sigma)$ quencher was used. Knowledge of the distance (D) between the quenching gas injector to the observation port and the bulk gas velocity (v) determined from Eq. (14) allows determination of the reaction time $t = D/v$. Under pseudo first order conditions with the quencher gas in large excess, a kinetic analysis yields a working equation for determining the quenching rate coefficient:

$$\frac{\Delta (\ln I_{O_2(^1\Sigma)})}{\Delta ([Q])} \left(\frac{\bar{v}}{D} \right) = k_Q \quad (18)$$

where $[Q]$ is the concentration of the quenching species and $I_{O_2(^1\Sigma)}$ is the intensity of the $O_2(b^1\Sigma + X^3\Sigma)$ emission. Some correction to this equation is required to account for imperfect radial mixing at the injector; however, this was minimal under the experimental conditions used.

A typical plot of $\ln I_{O_2(^1\Sigma)}$ versus $[CO_2]$ is shown in Fig. 5. Also shown is the corresponding plot for $[IF(B)]$. It is clear that the decay of $[IF(B)]$ is essentially identical to that for $[O_2(^1\Sigma)]$. This implies that $O_2(^1\Sigma)$ is likely involved in $IF(B)$ excitation when vibrationally cold $IF(X)$ is mixed with $O_2(^1\Sigma)$. The rate for quenching of $O_2(^1\Sigma)$ by CO_2 determined from the data in Fig. 8 is $k = 3.6 \times 10^{-13} \text{ cm}^3\text{-molecule}^{-1}\text{-s}^{-1}$. This agrees with measurements reported in a review by Setser and coworkers (Ref. 30).

A similar study was completed using H_2 as a quencher. A typical plot for these runs is shown in Fig. 6. An initial rapid depletion of $IF(B)$ was noted at low $[H_2]$ followed by a decay that approaches the slope of the $\ln[O_2(^1\Sigma)]$ versus $[H_2]$ plot. The reason for the bimodal curve of $[IF(B)]$ versus $[H_2]$ is not presently understood. However, the possibility exists that some unreacted F and CF_3I entered the flow tube from the $IF(X)$ sidearm generator. If this occurred then some $IF(X)$ could be generated in the flow tube. The rapid $H_2 + F$ reaction could consume F and therefore deplete the $[IF(X)]$ which would in turn give rise to a smaller $[IF(B)]$.

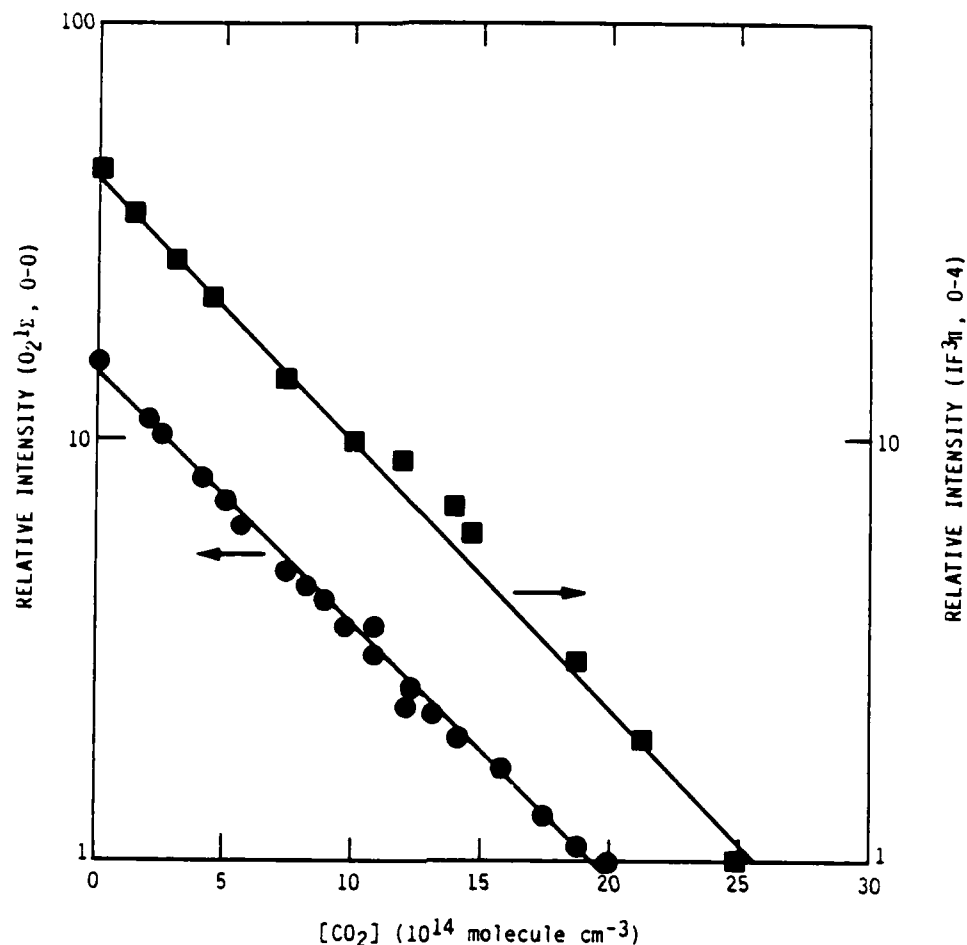


Figure 5. Dependence of relative [O₂(¹Σ)] and [IF(B)] upon added [CO₂]:
 ● - O₂(¹Σ), — IF(B).

The [IF(B)] decay at higher [H₂] does approach the slope for O₂(¹Σ) quenching by H₂. The initial results for H₂ quenching of O₂(¹Σ) yields a quenching rate of $\sim 8 \times 10^{-13} \text{ cm}^3\text{-molecule}^{-1}\text{-s}^{-1}$. This is also in reasonable agreement with the recent review (Ref. 30) and with the results of Ref. 31.

2.2.2 IF(B) Excitation Studies--The CO₂ and H₂ quenching studies (while not yet conclusive) were strongly suggestive that O₂¹Σ is directly involved in pumping vibrationally cold IF(X). However, additional chemiluminescence experiments indicated that there is a second mechanism that produces much greater concentrations of IF(B).

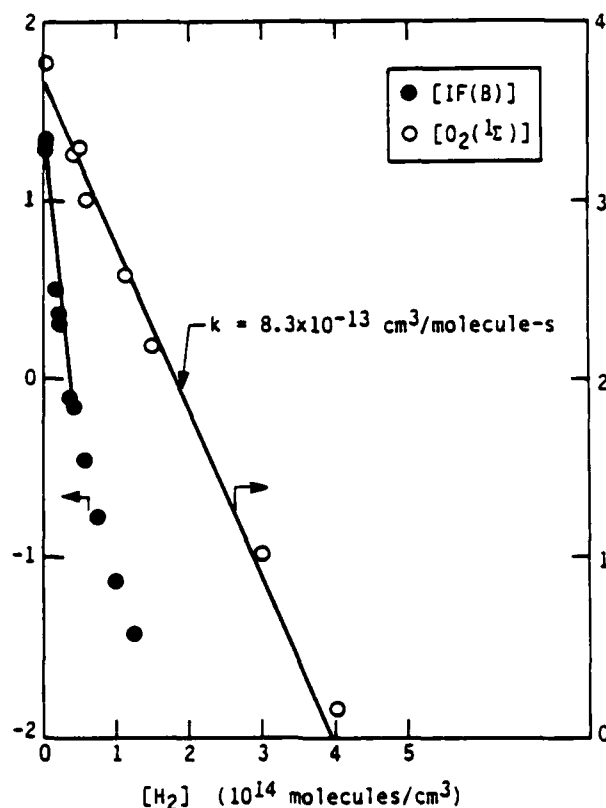


Figure 6. Dependence of relative $[O_2(^1\Sigma)]$ and $[IF(B)]$ upon added $[H_2]$:
o - $O_2(^1\Sigma)$; • - $IF(B)$.

For these additional chemiluminescence studies the $CF_3I + F$ sidearm injector was removed and the $IF(X)$ was formed directly in the flow tube using two injectors as shown in Fig. 7. This arrangement was used so that we might observe any participation of $IF^+(X;v)$, produced from the $I_2 + F$ reaction, in the pumping of $IF(B)$.

The F atom injector and O_2^* injectors were fixed while the IX ($X = CF_3, I$) injector was movable. This allowed the reaction time between $IF(X)$ formation and observation of $IF(B)$ to be varied. The I_2 flow rate was determined by an absorption technique described in Ref. 13. Several experiments were run in this configuration and the results are summarized in the following paragraphs.

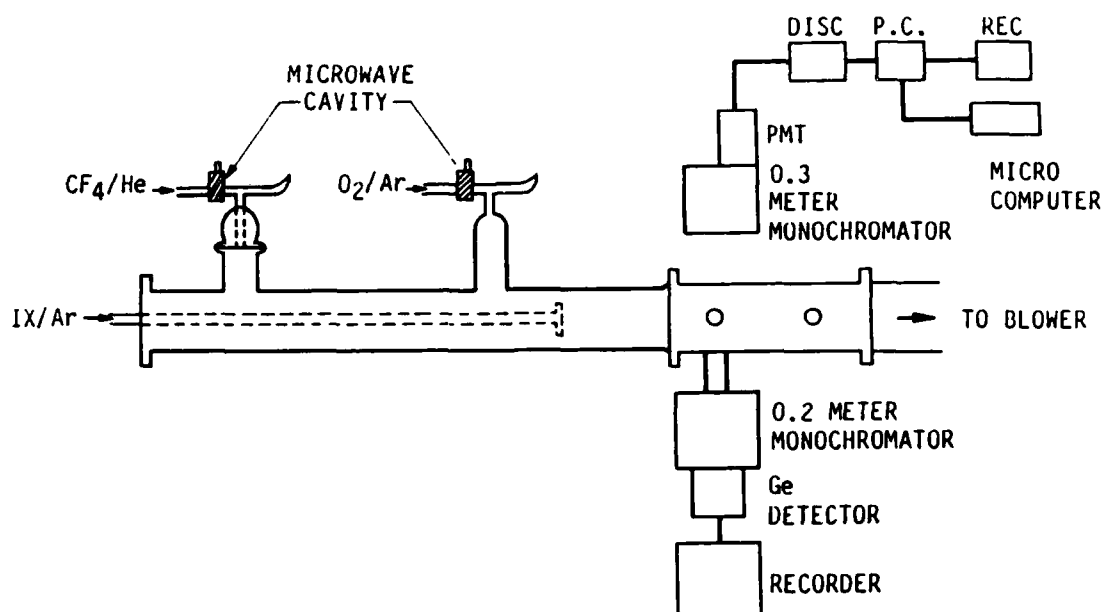


Figure 7. Flow tube configuration used for O_2^* - IF excitation studies.

A typical scan of the $IF(B+X)$ and $O_2(b+X)$ chemiluminescence spectra is shown in Fig. 8. A comparison of the $IF(B+X)_{0-4}$ chemiluminescence intensities produced using both CF_3I and I_2 as iodine donors are shown in Figure 9. The temporal profiles and the intensities of $IF(B+X)$ emissions are strikingly different for the two cases. The $[IF(B)]$ profile originating from $CF_3I + F + O_2^*$ is much flatter and at least two orders of magnitude smaller than that originating from $I_2 + F + O_2^*$. (The signal growth at short reaction times ~ 0.5 ms is ascribed to mixing.) Although difficult to discern from the plots shown in Fig. 9, the chemiluminescence intensity from the $I_2 + F + O_2^*$ reaction was only a factor of 2 greater than that from the $CF_3I + F + O_2^*$ reaction at long times (>5 ms). Thus, at long reaction times, subsequent to removal of IF^\dagger , the two reaction schemes appear to give comparable $[IF(B)]$.

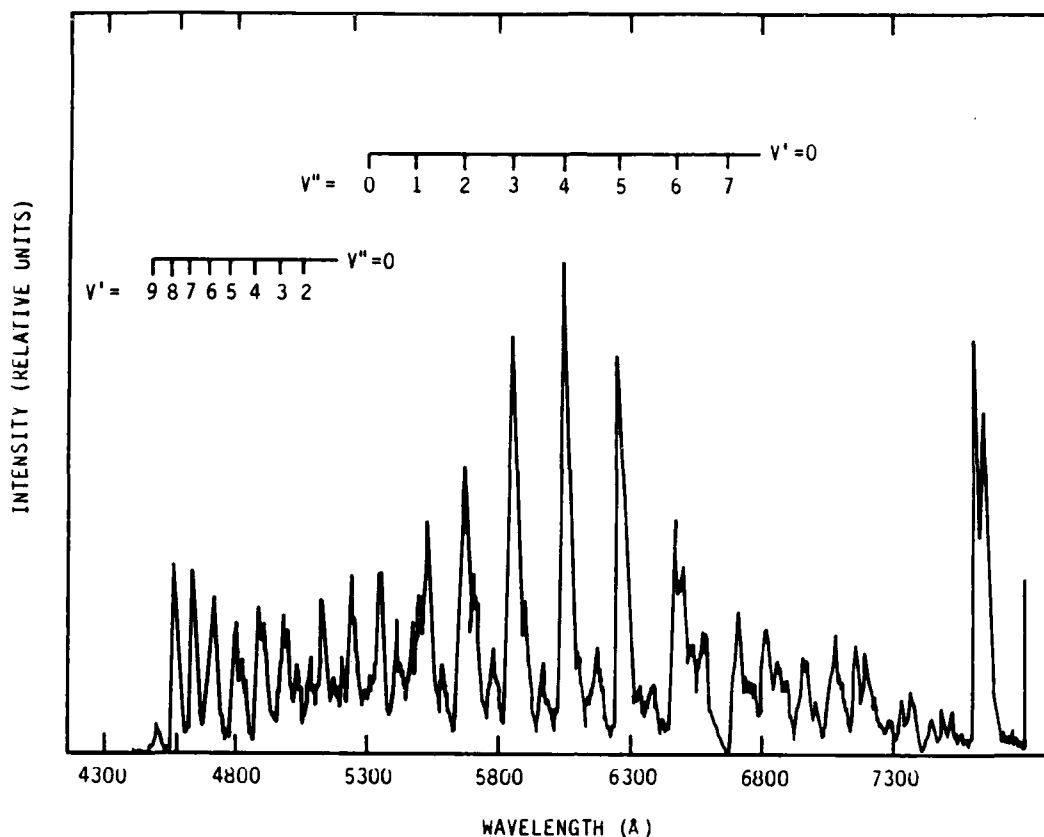


Figure 8. Spectral scan showing chemiluminescence from IF(B+X) and O₂(b+X) system. (Spectra are uncorrected for spectral response.) Total flow tube pressure 1.2 torr

These observations are consistent with vibrationally hot IF(X) being involved in the excitation process. As described previously, the vibrational distribution produced from $F + I_2$ is bimodal while $CF_3I + F$ produced a much more thermal distribution. One indeed expects larger $[IF^\dagger]$ at early reaction times since V-T relaxation will occur and reduce $[IF^\dagger]$. For the data shown in Fig. 9, the total pressure in the flow tube was 1.2 torr and some V-T relaxation will almost certainly occur at these pressures.

The initial interpretation of the data shown in Fig. 9 was that IF^\dagger produced by reaction (17) is pumped by O_2^* to IF(B) much more efficiently than is the cold IF(X) produced from reaction (16). At longer reaction times IF^\dagger is

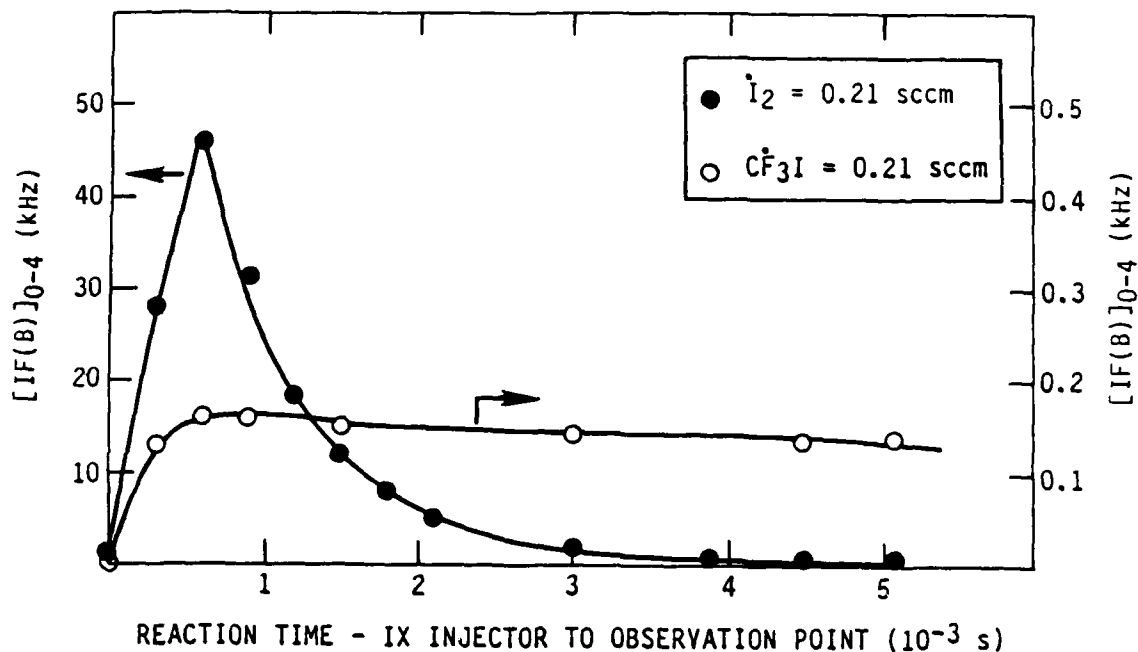


Figure 9. Temporal profiles of $IF(B+X)_{0-4}$ intensities using CF_3I and I_2 as iodine donors.

relaxed, the excitation of $IF(B)$ becomes much less efficient. When IF^+ is totally relaxed one would expect the excitation process to be identical to that using CF_3I .

Next are described a series of more detailed experiments that were performed to delineate more clearly the roles of $O_2(^1\Sigma)$ and $O_2(^1\Delta)$ in the $IF(B)$ excitation process.

2.3 $O_2^1\Sigma$ STUDIES

2.3.1 Apparatus--In the previous paragraph some preliminary measurements were discussed that indicated that $O_2(^1\Sigma)$ was involved in $IF(B)$ production when vibrationally cold $IF(X)$ was injected into a stream of $O_2(^1\Delta, ^1\Sigma)$. From quenching studies we showed that as $O_2(^1\Sigma)$ was removed, the $IF(B)$ concentration was concomitantly reduced. In these early experiments, however, we had

no monitor for $O_2(^1\Delta)$ and could not be certain that its concentration was unaffected by the $O_2(^1\Sigma)$ quencher gas. Therefore, an intrinsic germanium detector (Applied Detector Corporation Model 403) was installed to monitor the $O_2(^1\Delta + ^3\Sigma)$ band at $1.26\ \mu\text{m}$. The detector was mounted onto an Acton Research 0.2m monochromator equipped with a holographic 300 grooves/mm grating. We can easily discriminate the $O_2(^1\Delta + ^3\Sigma)$ bands at $1.26\ \mu\text{m}$ from the intense atomic iodine line at $1.315\ \mu\text{m}$. With this apparatus upgrade, we could simultaneously monitor emissions from $IF(B)$, $O_2(^1\Sigma)$, $O_2(^1\Delta)$, and I^* . The entire flow tube apparatus including the described changes is shown in Fig. 10.

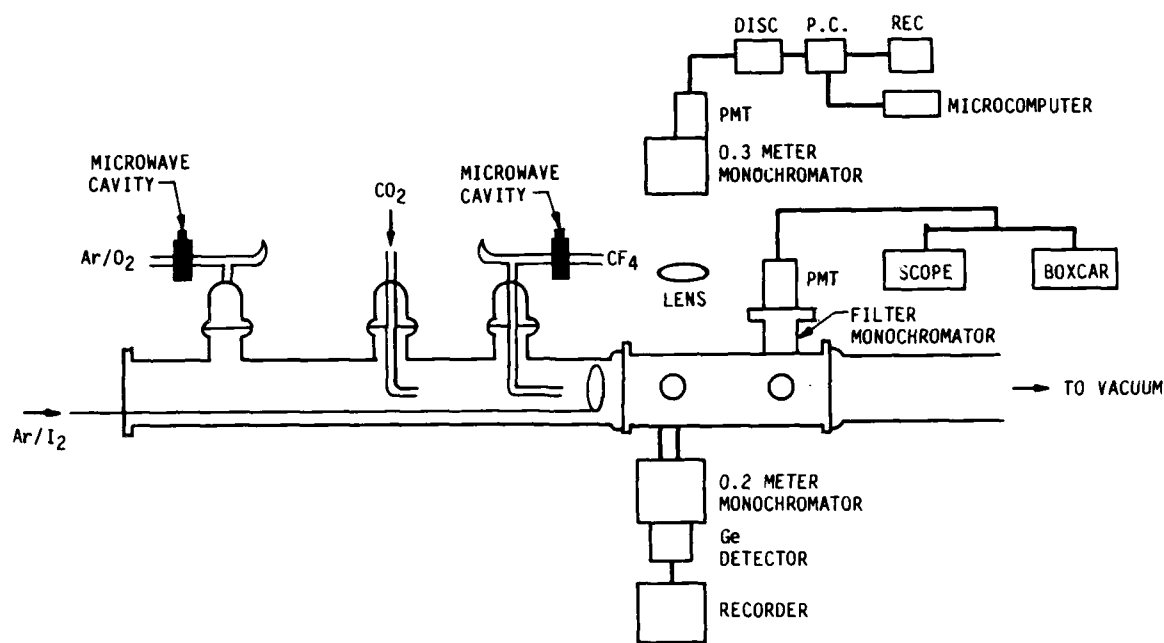


Figure 10. Block diagram of apparatus.

The chemiluminescence data were recorded on an IBM-PC microcomputer using the Lab Tech Notebook[®] software package. The digitized data were then analyzed using a spectral fitting routine. For these runs, the relative spectral response of the visible detection system was measured using a spectral irradiance lamp. The response function was put on an absolute basis using the well known $O + NO$ titration technique (Ref. 32).

The infrared detection system was calibrated by recording a blackbody spectrum on both the visible and infrared detection systems. The response of the infrared system was normalized to that of the visible detection system at 800 nm. This put the infrared system on an absolute basis. The relative response at 1.26 μm was then determined by observing the blackbody source at both 800 and 1260 nm.

To analyze the data, it is first transferred onto the microVAX system. The fitting of molecular band systems to the experimental spectra is then done in three steps. First, a high resolution spectrum covering the wavelength range and vibrational levels needed is generated by calculating the emission intensities and line positions for a given molecular system. Second, vibrational basis sets are generated by passing an appropriate slit function over the high resolution spectrum. Finally, after the data are corrected for instrument response and an average background intensity is subtracted, a least squares fit of the experimental data to the basis functions is calculated.

A sample spectrum and fit are shown in Fig. 11. Since the detector response function is also digitized and used in the spectral fitting routine, the data displayed in Fig. 11 are detector-response-function corrected. It is obvious from Fig. 11 that the $\text{IF}(X; v'' = 0) + \text{O}_2^*$ produces hot bands of $\text{IF}(B)$. In Fig. 12 we show the vibrational distribution for $\text{IF}(B)$ determined from data similar to those in Fig. 11. The non-Boltzmann distribution with a peak near $v' = 7$ is consistent with the previous work of Whitefield et al. (Ref. 13). The present feeling is that this distribution results from selective pumping of high vibrational levels of $\text{IF}(B)$ via $\text{O}_2(^1\Delta)$ possibly from $\text{IF}(A')$.

2.3.2 Results of $\text{O}_2(^1\Sigma)$ Studies--These experiments were similar to the $\text{O}_2(^1\Sigma)$ quenching studies. The $\text{IF}(X)$ source was the $\text{I}_2 + \text{F}$ reaction so that the role of IF^+ could be studied. To determine the importance of $\text{O}_2(^1\Sigma)$ in the pumping process we wish to vary $[\text{O}_2(^1\Sigma)]$ while keeping $[\text{O}_2(^1\Delta)]$ constant. Several approaches were tried and found two techniques that allow the desired variation of $[\text{O}_2(^1\Sigma)]$. One was to use a quencher gas specific to $\text{O}_2(^1\Sigma)$. Although several possible choices exist, CO_2 was used. Sources containing

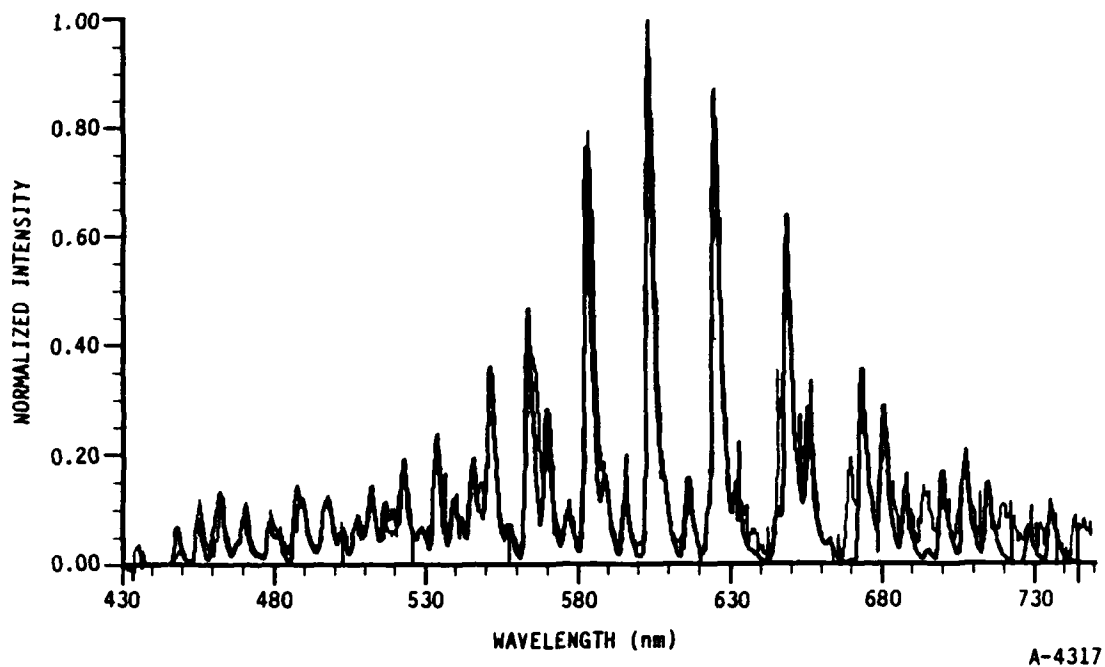
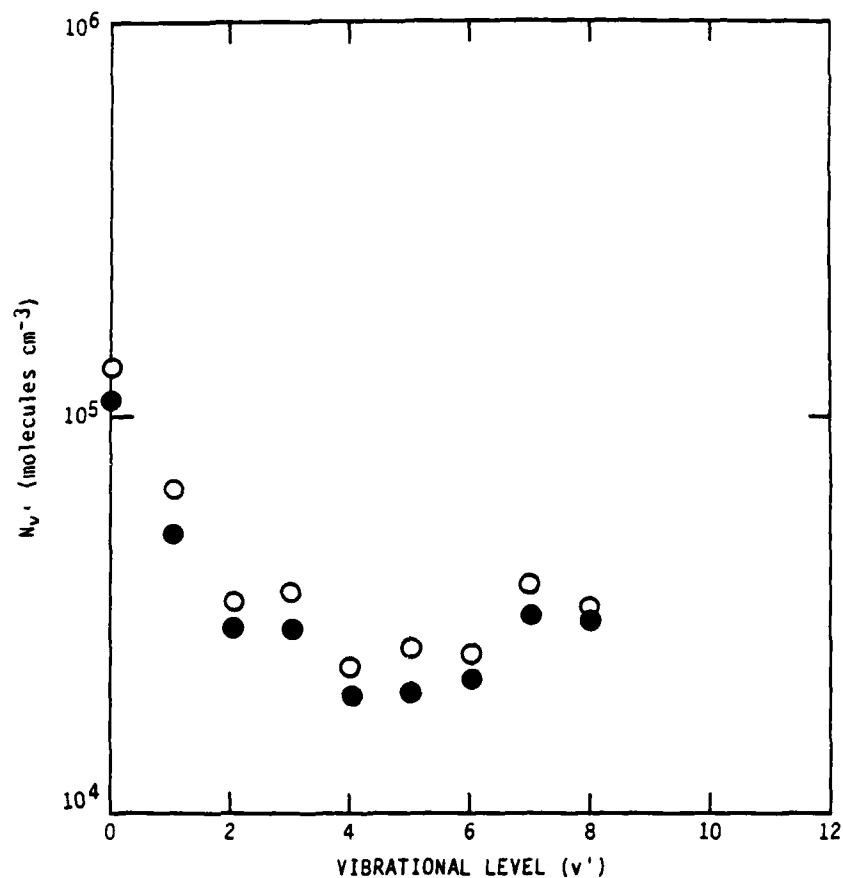


Figure 11. IF(B+X) chemiluminescence from O_2^* excitation. IF(X) was formed using $CF_3I + F$ reaction. Total pressure was 0.802 Torr. Thin line represents measured spectrum and thick line is the spectral fit

hydrogen, e.g. H_2 , cause complications because of the presence of F atoms used to form IF(X). Carbon dioxide eliminates these problems.

It was found that the amount of $O_2(^1\Sigma)$ reaching the optical detection port could be varied by changing the flow of Ar in the Ar/ O_2 discharge side-arm. As less argon is added, $[O_2(^1\Sigma)]$ is reduced; and presumably more wall collisions occur within the discharge tube.

The most reproducible $[O_2(^1\Sigma)]$ variations were obtained using the CO_2 quencher, and most of the studies were performed using this technique. The experimental arrangement is shown in Fig. 10. The IF(X) was formed in the



A-4318

Figure 12. Vibrational distributions of IF(B) for two [O₂(¹Σ)].
 o - [O₂(¹Σ)] = 3.1 × 10¹² molecules-cm⁻³,
 ● - [O₂(¹Σ)] = 2.7 × 10¹² molecules-cm⁻³
 Total pressure = 0.802 Torr.

flow of O₂^{*} and the distance (i.e., reaction time) from IF(X) formation to the observation port could be varied. The runs consisted of measuring emission intensities from IF(B), O₂(¹Σ), and O₂(¹Δ) as a function of [CO₂] added.

Two sets of data are shown in Fig. 12. The solid data points were obtained with the I₂ injector 15 cm (8.2 ms) from the observation port. As will be shown in Section 4, when the reaction time is ~8 ms, considerable relaxation of high v'' levels in IF(X) has occurred. Thus, the solid data points represent excitation from a somewhat vibrationally relaxed IF(X) distribution and is similar in behavior to cold IF(X) produced from the CF₃I + F reaction.

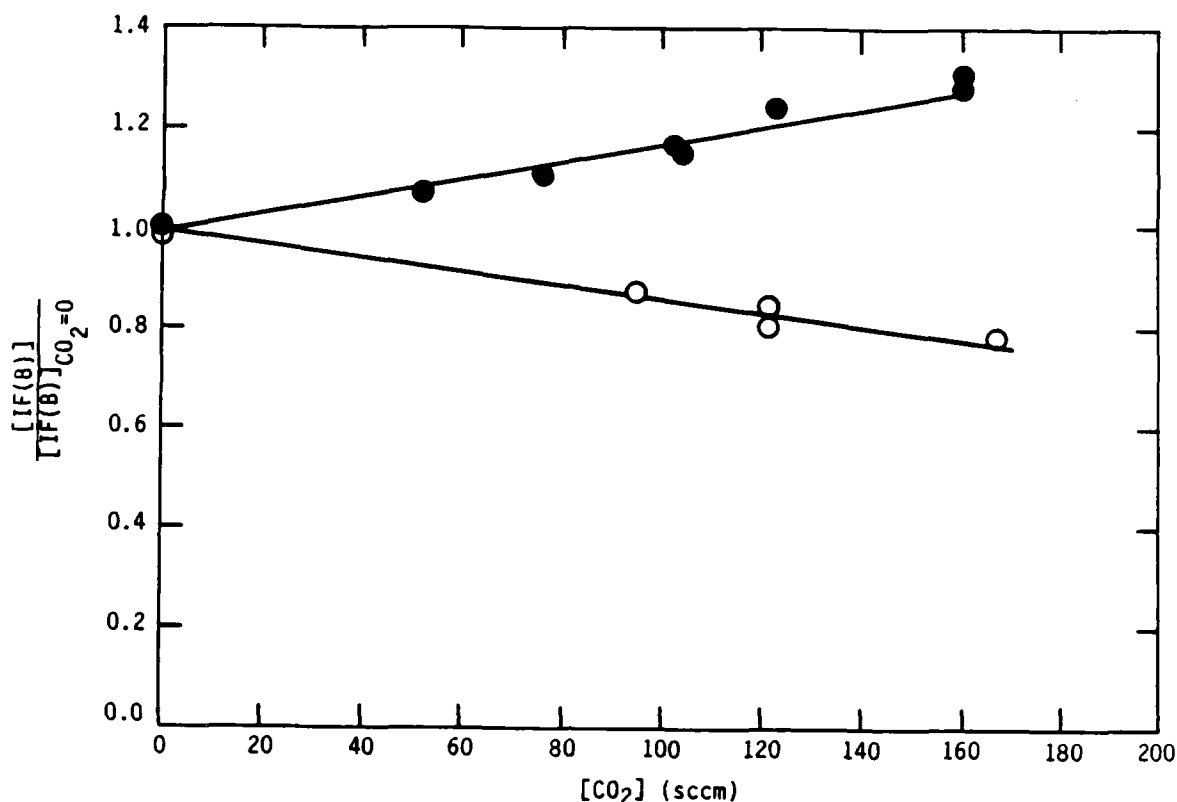


Figure 13. Plots of $[IF(B)]_{CO_2} / [IF(B)]_{CO_2=0}$ versus CO_2 flow rate for two reaction times: \circ - reaction time = 8.2 ms, \bullet - reaction time = 1.0 ms. Total pressure was 1.53 Torr.

In contrast when the reaction time was ~ 1 ms, the results represented by the solid circles in Fig. 13 were obtained. The $[IF(B)]$ actually increased as CO_2 was added. The dependencies of $[IF(B)]$ upon $[O_2(^1\Sigma)]$ for these two cases are more graphically illustrated in Figs. 14 and 15. In Fig. 14, emission from $[IF(B;v'=0)]$ is shown as a function of $[O_2(^1\Sigma)]$ for a long reaction time (9 ms).

In Fig. 15, similar data as shown for the short reaction time case, i.e., maximum $[IF^\dagger]$. The behavior is strikingly different from the data in Fig. 14. The $[IF(B)]$ is essentially independent of $[O_2(^1\Sigma)]$ and actually gets larger as $[O_2(^1\Sigma)]$ is removed. Clearly, when IF^\dagger is used, $O_2(^1\Sigma)$ is not required as an excitation source. It was concluded that $O_2(^1\Delta)$ is responsible for the $IF(B)$ excitation when IF^\dagger is present.

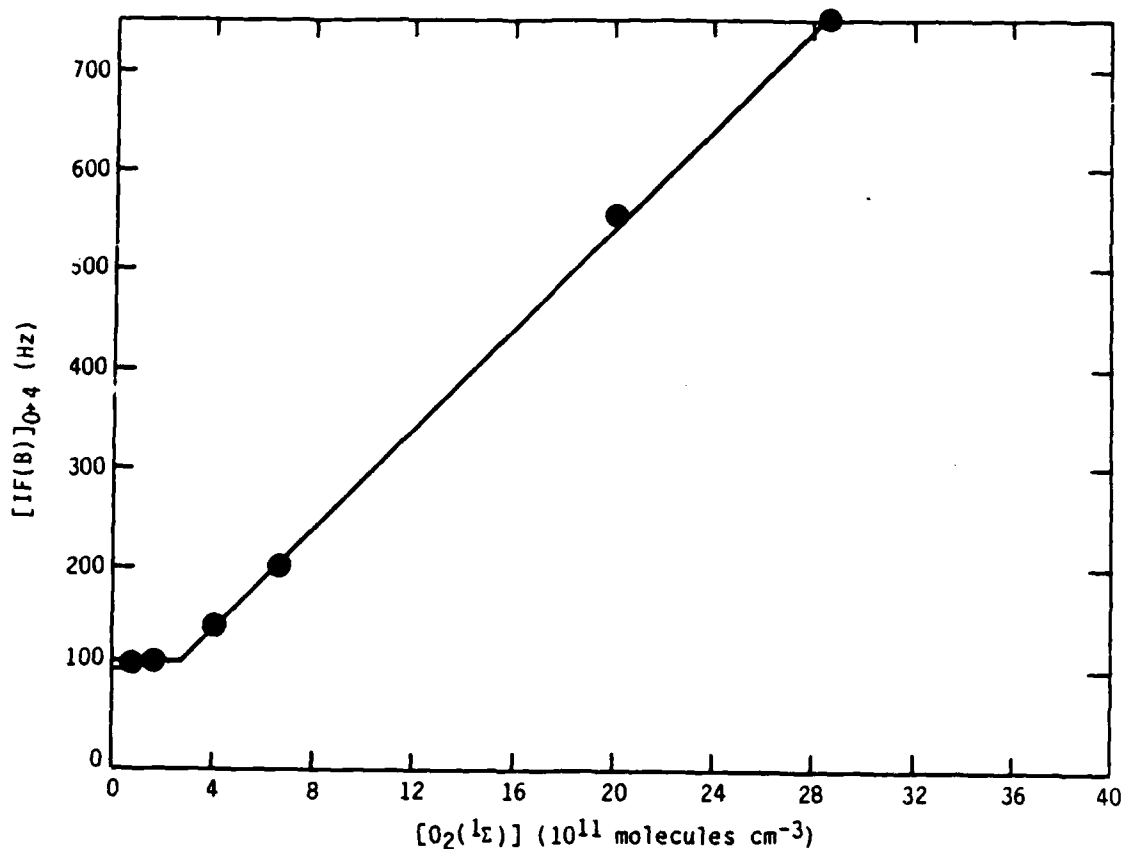


Figure 14. Plot of [IF(B)] versus [O₂(¹Σ)] for a reaction time of 9 ms.
Total pressure was 1.5 Torr.

We emphasize that in Fig. 13 the ratio of [IF(B)] with CO₂ present to [IF(B)] with CO₂ = 0 is plotted. The actual [IF(B)] for long reaction times is approximately two orders of magnitude less than that for short reaction times. This implies that the [IF(B)] excitation involving O₂(¹Σ) is less efficient than the pumping by O₂(¹Δ) at least under these conditions.

2.4 O₂(¹Δ) STUDIES

If O₂(¹Δ) is a significant excitation source for IF(B) a simplified model can be constructed to predict the expected behavior of [IF(B)] with respect to [O₂(¹Δ)]. The model is illustrated in Fig. 16. Excitation from IF⁺ to IF(A') is presumed to take place via O₂(¹Δ) energy transfer. Whitefield et al.

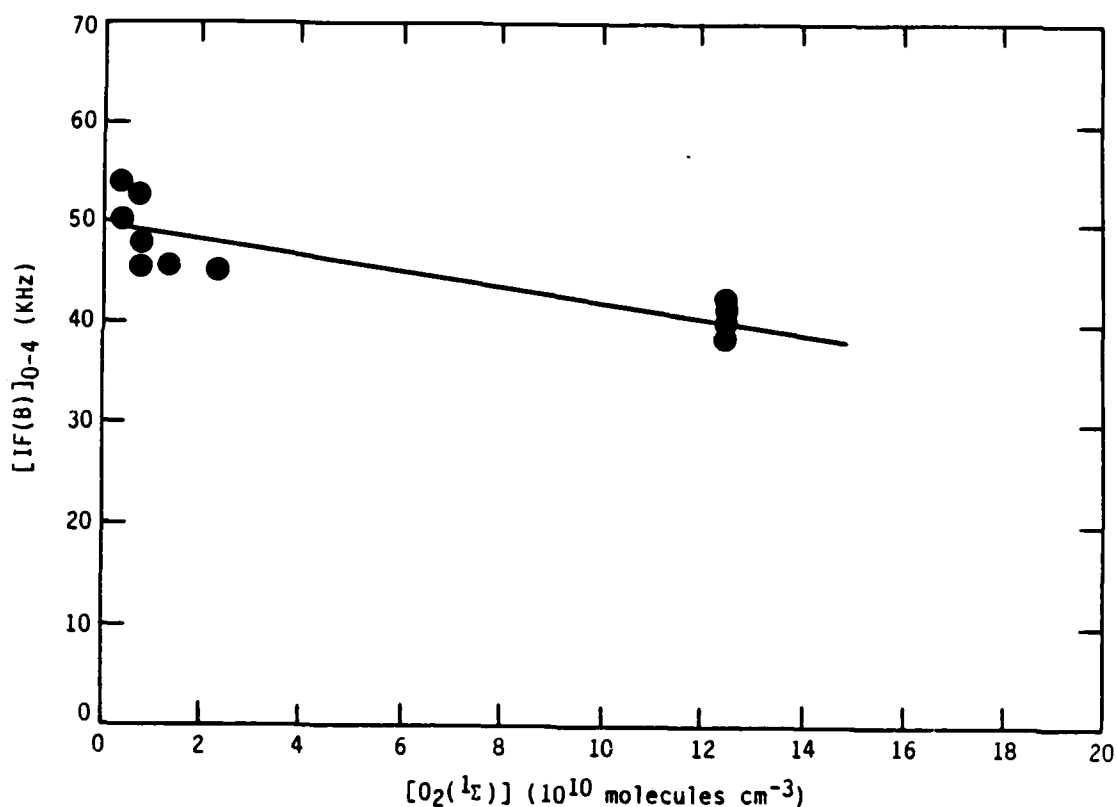


Figure 15. Dependence of $[IF(B)]$ upon $[O_2(^1\Sigma)]$ at a reaction time of 1.0 ms.
Total pressure = 1.53 Torr.

(Ref. 13) had previously estimated $T_0 \approx 13,500 \text{ cm}^{-1}$ for $IF(A')$. However, this value was obtained from indirect evidence. Recently Heaven (Ref. 22) has reported LIF excitation results for the $IF(A'+X)$ system in an Ar matrix. Results show that $T_0(A') = 13,250 \text{ cm}^{-1}$ in the matrix. The estimated gas phase value is $T_0 = 13,490 \text{ cm}^{-1}$. The small matrix shift was determined from comparison to the excitation spectra for $IF(B+X)$ in both a matrix and in the gas phase (Ref. 22).

Now that we have a much more accurate $T_0(A')$ the implications of the model in Fig. 16 can be considered. The important processes are described by reactions (19) through (24).

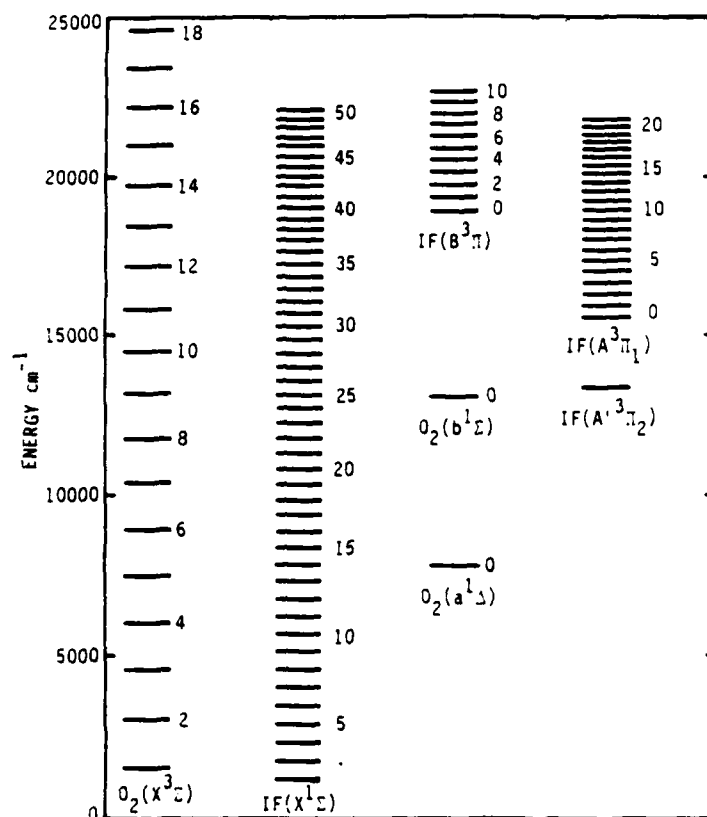
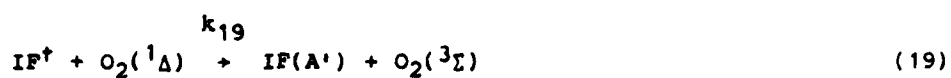
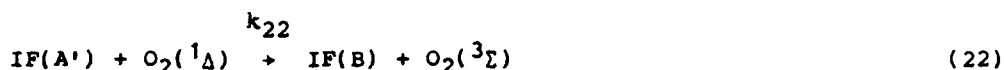


Figure 16. Energy levels of IF and O₂ showing states relevant to model described by reactions (19) + (24).





In the above reactions M represents any potential quencher, e.g., Ar or O₂.

If we assume that IF(B) is in steady-state with all other species in the optical viewing region then [IF(B)] is given by Eq. (25).

$$[\text{IF(B)}] = \frac{k_{22}[\text{IF(A')}][\text{O}_2(^1\Delta)]}{A_{B \rightarrow X} + k_{23}[\text{M}]} \quad (25)$$

But if IF(A') is in steady state

$$[\text{IF(A')}] = \frac{k_{19}[\text{IF}^\dagger][\text{O}_2(^1\Delta)]}{A_{A' \rightarrow X} + k_{21}[\text{M}] + k_{22}[\text{O}_2(^1\Delta)]} \quad (26)$$

Using Expressions (25) and (26) we get Eq. (27):

$$[\text{IF(B)}] = \frac{k_{19}k_{22}[\text{IF}^\dagger][\text{O}_2(^1\Delta)]^2}{(A_{B \rightarrow X} + k_{23}[\text{M}])(A_{A' \rightarrow X} + k_{21}[\text{M}] + k_{22}[\text{O}_2(^1\Delta)])} \quad (27)$$

Note that at low [O₂(¹Δ)], where (A_{A'→X} + k₂₁[M]) >> k₂₂[O₂(¹Δ)], [IF(B)] should scale as [O₂(¹Δ)]². As the [O₂(¹Δ)] concentration is increased [IF(B)] should eventually scale linearly with [O₂(¹Δ)].

The following sets of experiments were completed to test this hypothesis. We needed to vary [O₂(¹Δ)] in a systematic way which turned out to be a formidable task. Initially an attempt was made to vary [O₂(¹Δ)] simply by changing the microwave discharge power at a constant O₂ flow rate. The dynamic range of [O₂(¹Δ)] obtained was disappointingly small (approximately a factor of 2). In addition, instabilities in the discharge at low microwave powers were severe. This technique was disregarded and an attempt was made to vary [O₂(¹Δ)] by changing the flow rate of O₂ through the discharge cavity.

Using this method, $[O_2(^1\Delta)]$ was varied by at least a factor of 5. An initial nonlinear increase was observed in $[IF(B)]$, but it appeared to reach a limiting value. The probable cause for this is that $[IF(B)]$ was being quenched by ground state O_2 at the higher O_2 flow rates. Wolf and Davis (Ref. 6) have previously shown that ground state O_2 is a quencher of $[IF(B)]$ with $k_Q = 1.4 \times 10^{-12} \text{ cm}^3 \text{ molecule}^{-1} \text{ s}^{-1}$.

To circumvent this problem the O_2 flow was split prior to the discharge tube. Part of the O_2 flow was injected directly into the flow tube and the remainder passed through the discharge tube. By changing the fraction of O_2 passing through the discharge tube at a constant O_2 flow rate the $[O_2(^1\Delta)]$ could be varied independent of the total $[O_2]$. This was expected to minimize the effects of oxygen quenching of $IF(B)$. Sample data are presented in Fig. 17.

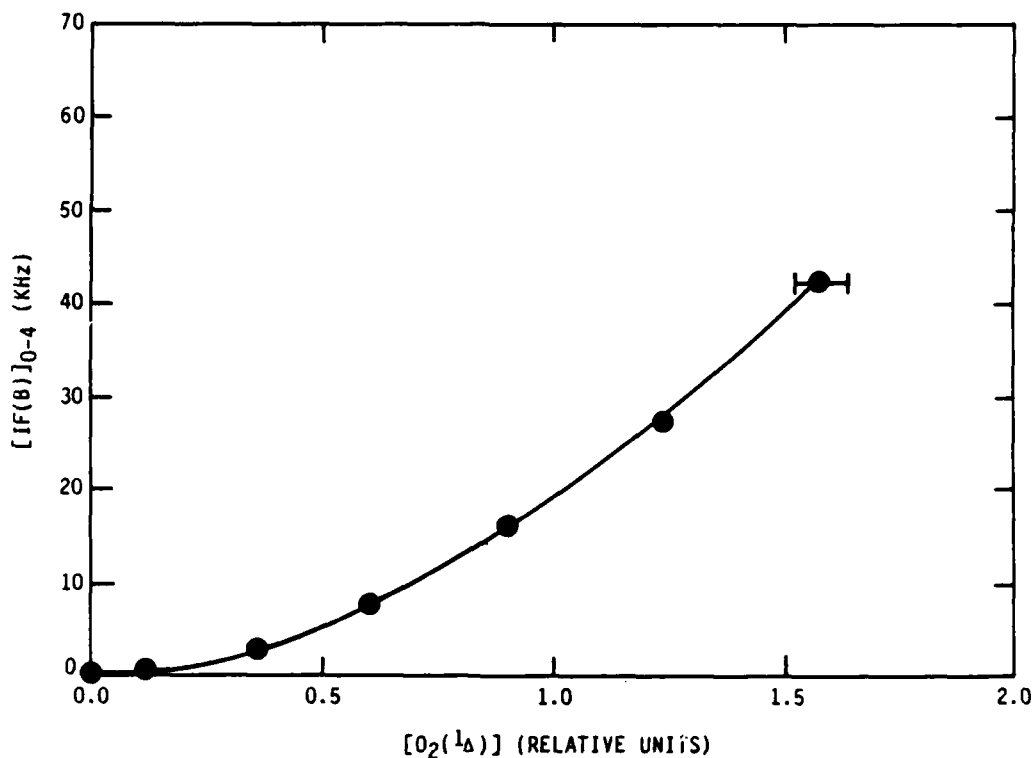


Figure 17. Plot of $[IF(B)]$ as a function of $[O_2(^1\Delta)]$. Total pressure was 1.53 Torr

The dependence of $[IF(B)]$ upon $[O_2(^1\Delta)]$ is clearly nonlinear over the entire dynamic range of $[O_2(^1\Delta)]$. In Fig. 18, $[IF(B)]$ is plotted as a function of $[O_2(^1\Delta)]^2$. The linearity is obvious and shows that under these conditions $[IF(B)]$ does scale as $[O_2(^1\Delta)]^2$ consistent with the simple model hypothesized above. To our knowledge this is the first such direct evidence of stepwise excitation of $IF(B)$ by $O_2(^1\Delta)$.

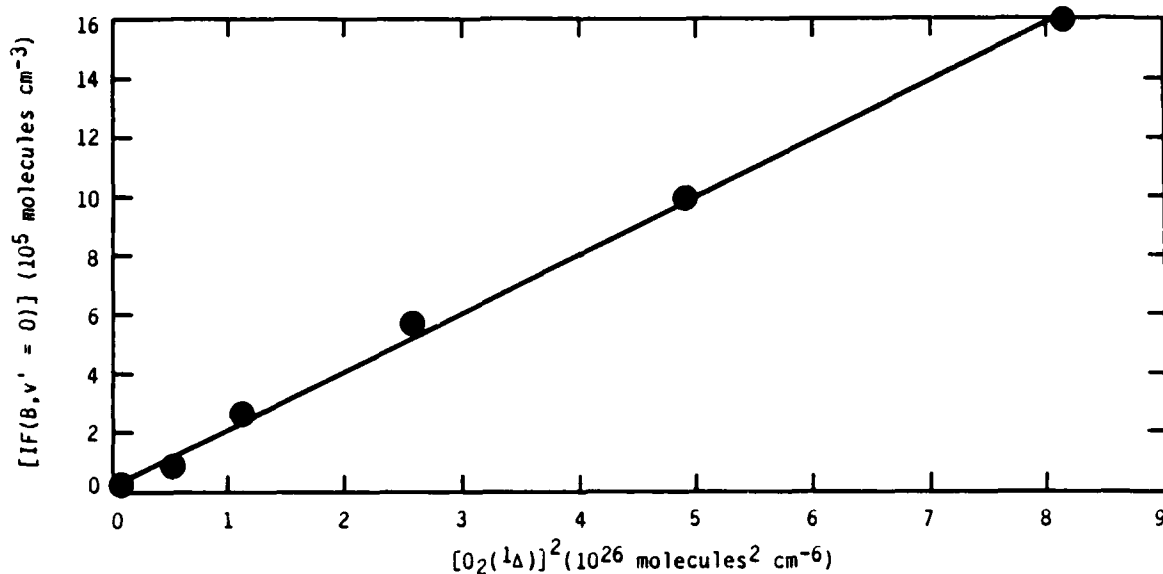


Figure 18. Plot of $[IF(B)]$ versus $[O_2(^1\Delta)]^2$. Data taken from Fig. 17

This behavior is contrasted with the data in Fig. 14 which shows $[IF(B)]$ scaling linearly with $[O_2(^1\Sigma)]$. Promotion of $[IF(X; v''=0)]$ to $IF(A')$ by $O_2(^1\Sigma)$ would be expected to require only one $O_2(^1\Sigma)$.

During these runs an interesting and significant phenomenon was observed. To insure that $O_2(^1\Sigma)$ effects were minimal we added CO_2 as a quencher. At the highest CO_2 flows we reduced $[O_2(^1\Sigma)]$ by a factor of 40. However, we noted a simultaneous approximate 10 percent increase in $[O_2(^1\Delta)]$. Since a microwave

discharge typically produces $[O_2(^1\Sigma)]/[O_2(^1\Delta)] \approx 0.10$, the implication is that CO_2 quenches $O_2(^1\Sigma)$ to $O_2(^1\Delta)$. Note that the 10 percent increase in $[O_2(^1\Delta)]$ was accompanied by a 20 percent increase in $[IF(B)]$. The CO_2 quenching of $O_2(^1\Sigma)$ to $O_2(^1\Delta)$ is the probable explanation of the behavior in Fig. 13. Note that the data presented in Fig. 17 and 18 were obtained with the $O_2(^1\Sigma)$ removed using CO_2 as a quencher gas.

2.5 ESTIMATION OF RATE COEFFICIENTS

As described earlier, the goals of this program were to determine the mechanisms of $IF(B)$ production by $O_2(^1\Delta, ^1\Sigma)$. Chemiluminescence studies provided some data that can be used to obtain preliminary estimates for rate coefficients of critical processes. In the following two sections these results are described. The derived values are only estimates and a systematic kinetic rate constant measurement program would be required to obtain reliable rate coefficients.

2.5.1 $O_2(^1\Sigma) + IF$ --As described earlier the $O_2(^1\Sigma)$ model is given by Eqs. (9), (10), and (21) through (24).



Under the experimental conditions, $k_{23}[M]$ can be neglected and process 10 can cause predissociation.

If $IF(A')$ is in steady state then the photon emission rate for $IF(B)$ is given by Eq. (28).

$$k_{24}[\text{IF(B)}] = k_9[\text{O}_2(^1\Sigma)][\text{IF}] \frac{k_{22}[\text{O}_2(^1\Delta)]}{(k_{20} + k_{21}[\text{M}] + k_{22}[\text{O}_2(^1\Delta)])} \quad (28)$$

The expression that multiplies $k_9[\text{O}_2(^1\Sigma)][\text{IF}]$ is the branching ratio of IF(A') excitation to IF(B) to total IF(A') removal. If we assume that this branching ratio is unity we can estimate a lower limit for k_9 . In this limit Eq. (28) becomes

$$k_{24} \frac{[\text{IF(B)}]}{[\text{IF}]} = k_9[\text{O}_2(^1\Sigma)]$$

A plot of $[\text{IF(B)}]$ versus $[\text{O}_2(^1\Sigma)]$ is shown in Fig. 14. For the data presented in Fig. 14 the initial I_2 concentration was approximately 2.5×10^{12} molecules cm^{-3} . Thus, $[\text{IF(X)}] < 2.5 \times 10^{12}$ molecules cm^{-3} . From this run we estimate $k_9 > 1.7 \times 10^{-15}$ cm^3 molecule $^{-1}$ s $^{-1}$. We emphasize that this is a lower limit estimate. However when one considers that $T_e(\text{IF(A')}) \approx 13490$ cm^{-1} and $T_e(\text{O}_2(^1\Sigma)) = 13195$ cm^{-1} a slow excitation rate coefficient is not unreasonable at room temperature. Clearly a more systematic study of the excitation of IF(B) using $\text{O}_2(^1\Sigma)$ is required to accurately determine k_9 .

2.5.2 $\text{O}_2(^1\Delta) + \text{IF}$ --Although time permitted only a few studies to be completed, the data presented in Fig. 18 can be used to provide estimates of the IF(B) excitation rate coefficients by $\text{O}_2(^1\Delta)$. Examination of Eq. (27) shows that a plot of $[\text{IF(B)}]$ versus $[\text{O}_2(^1\Delta)]^2$ yields a slope:

$$m = \frac{k_{19}k_{22}[\text{IF}^\dagger]}{(A_{B \rightarrow X} + k_{23}[\text{M}])(A_{A' \rightarrow X} + k_{21}[\text{M}] + k_{22}[\text{O}_2(^1\Delta)])}$$

Not all of the terms in the demoninator are known. However, if one assumes that the rate coefficients for quenching of IF(A') by O_2 and Ar are identical to those for IF(B) , then a crude estimate for the product $k_{19}k_{22}$ can be obtained. A radiative lifetime of 11 ns extrapolated from the Ar matrix value is used for the IF(A') state (Ref. 22). The plot shown in Fig. 18 is linear with respect to $[\text{O}_2(^1\Delta)]^2$. Thus, under these conditions $[k_{22}\text{O}_2(^1\Delta)]$ is apparently much less than $(A_{A' \rightarrow X} + k_{21}[\text{M}])$, so this term is neglected. Also $k_{23}[\text{M}]$ can be neglected with respect to $A_{B \rightarrow X}$.

The slope of the plot in Fig. 18 gives

$$\frac{\Delta[\text{IF}(B, v=0)]}{\Delta[\text{O}_2(^1\Delta)]^2} = 1.96 \times 10^{-21} \text{ cm}^3 \text{ molecule}^{-1} = k_{19}k_{22}[\text{IF}^\dagger] \frac{1}{(A_{B \rightarrow X})(A_{A' \rightarrow X} + k_{21}[M])}$$

Inserting the number densities for O_2 , $\text{O}_2(^1\Delta)$ and Ar we find

$$k_{19}k_{22}[\text{IF}^\dagger] \sim 4.25 \times 10^{-13} \text{ cm}^3 \text{ molecule}^{-1} \text{ s}^{-2}$$

Although $[\text{IF}^\dagger]$ is uncertain, the I_2 number density in the flow tube in the absence of F atoms would be $2.5 \times 10^{12} \text{ cm}^{-3}$ for the run shown in Fig. 18. If we assume approximately 50 percent of the I_2 is converted to IF^\dagger at the point of an observation, then the product $k_{19}k_{22} \sim 3.4 \times 10^{-25} \text{ cm}^6 \text{ molecule}^{-2} \text{ s}^{-2}$. The validity of the assumption of $[\text{IF}^\dagger]$ could not be experimentally verified, but the ratio $[\text{IF}^\dagger]/[\text{IF}] \sim 0.5$ is consistent with the LIF observations. We anticipate that $[\text{IF}^\dagger]$ is actually less than the above estimate. This would imply that $k_{19}k_{22} > 3 \times 10^{-25} \text{ cm}^6 \text{ molecule}^{-2} \text{ s}^{-2}$. In addition, this estimate is for production of $\text{IF}(B, v'=0)$. Under these conditions we find $[\text{IF}(B)] \sim 3[\text{IF}(B, v'=0)]$. Thus for $[\text{IF}(B)]$, $k_{19}k_{22} \gtrsim 1 \times 10^{-24} \text{ cm}^6 \text{ molecule}^{-2} \text{ s}^{-2}$. This value should be considered to be only preliminary since some of the rate coefficients used in its derivation were estimated and not measured.

2.6 OTHER EXPERIMENTS

Some preliminary chemiluminescence investigations have been made using ICl as the iodine donor. A problem was encountered in that ICl seemed to attack the stainless steel preparation and delivery lines readily. The lines were replaced with Teflon tubing. Using ICl we have observed $\text{IF}(B+X)$ emission excited by O_2^* . A sample spectrum and fit are shown in Fig. 19. In Fig. 20 the dependence of $[\text{IF}(B)]$ upon $[\text{ICl}]$ at constant $[\text{O}_2^*]$. Also shown is a similar plot using I_2 as a iodine source. Both plots are linear although the I_2 source seems to be much more favorable for $\text{IF}(B)$ production. Examination of the molecular beam work of Trickl and Wanner (Ref. 26) shows that the $\text{ICl} + \text{F}$ reaction produces essentially no IF^\dagger with $v'' > 9$. The energy gap between $\text{IF}(X; v''=8)$ and $\text{IF}(A'; v''=0)$ is at least 8240 cm^{-1} which is considerably greater than the energy of $\text{O}_2(^1\Delta)$ ($T_e = 7882 \text{ cm}^{-1}$).

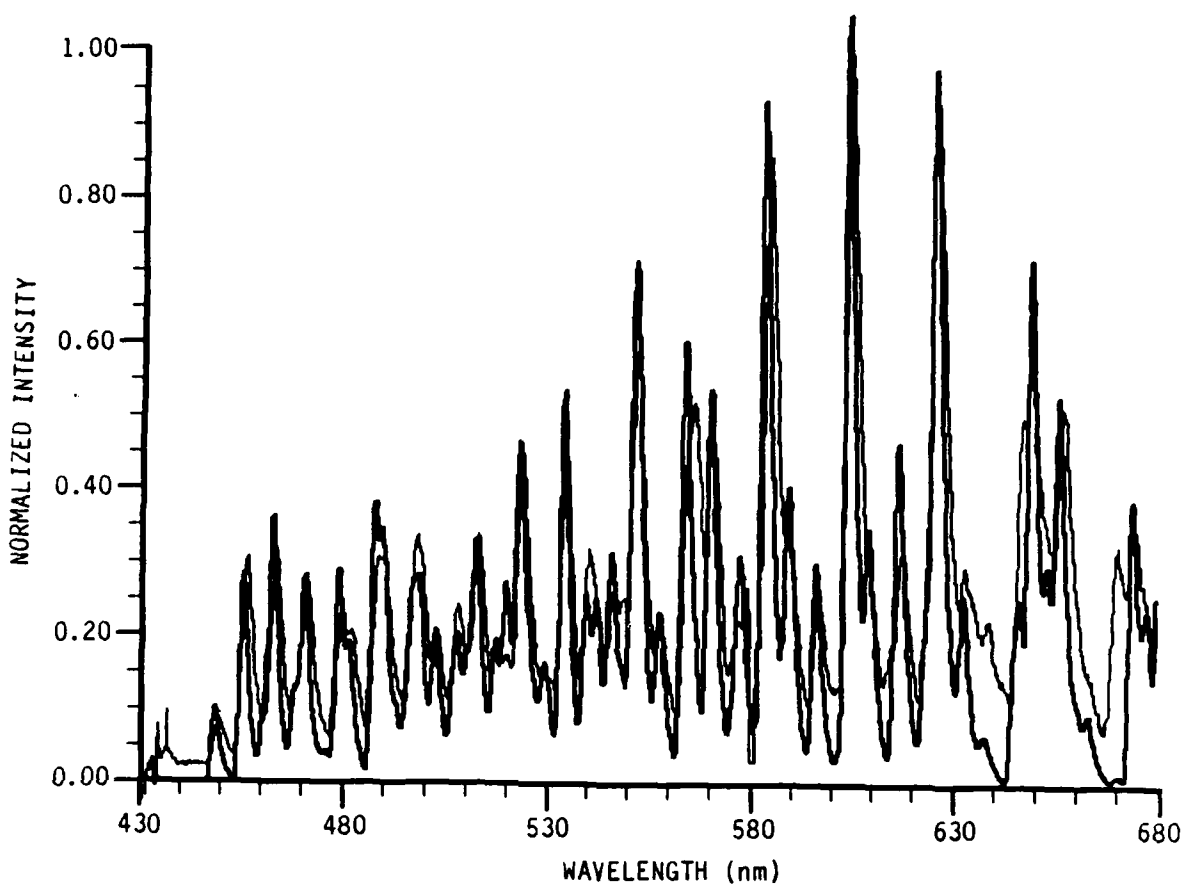


Figure 19. Chemiluminescence from IF(B \rightarrow X) produced by O₂^{*} pumping of IF(X) formed from F + ICl. Thin line is data, thick line is spectral fit. Total pressure was 0.95 Torr.

Thus, promotion of IF(X;v⁼8) to IF(A') via O₂(¹ Δ) pumping is almost certainly endothermic at room temperature; therefore, the rate coefficient at room temperature is expected to be slow. As a consequence ICl would appear to be a poor choice for an IF[†] source. This was verified, as seen in the next section which describes laser induced fluorescence results. These experiments confirmed the importance of IF[†] in the excitation of IF(B) that was hypothesized from the chemiluminescence results presented in the previous paragraphs.

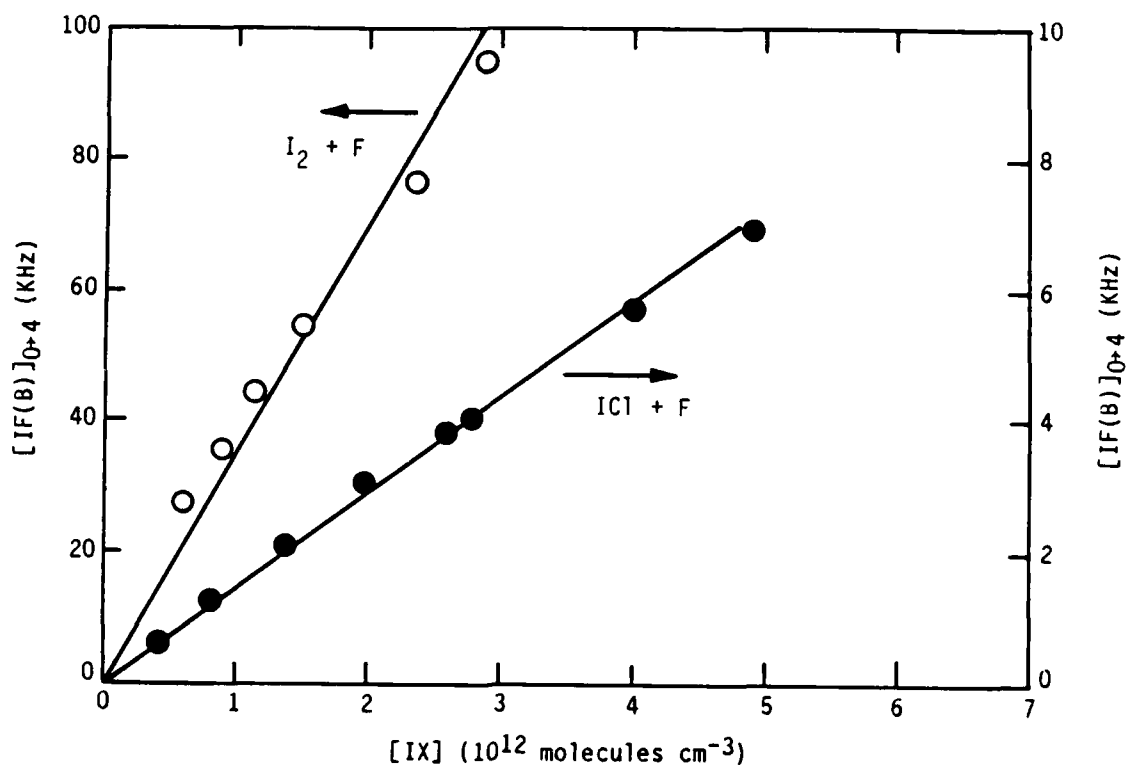


Figure 20. $IF(B)$ as a function of flow rates of ICl and I_2 : o - I_2 data; ● - ICl data. Total pressure = 0.95 Torr.

3. LASER INDUCED FLUORESCENCE STUDIES

3.1 INTRODUCTION

3.1.1 LIF apparatus--Laser induced fluorescence experiments were performed using a nitrogen-laser pumped dye laser system consisting of a Molelectron UV14 nitrogen laser and a Molelectron DL-200 dye laser. The laser has a repetition rate of 20 Hz and a pulse width of 10 ns. Several laser dyes were used to generate the large excitation wavelength range needed in these experiments. The dyes used, their lasing wavelength regions, and the v'' levels probed are given in Table 1.

TABLE 1. Summary of v'' Levels Probed.

Dye	Wavelength Region, nm	v'' Observed
Coumarin 460	453 - 467	0,1
Coumarin 480	467 - 485	0,1,2
Coumarin 500	485 - 535	0,1,2
Rhodamine 590	575 - 600	5,6,7
Rhodamine 610	600 - 630	6,7,8,9
Rhodamine 640	620 - 665	7,8,9,10
Rhodamine 640 + LD700	655 - 690	9,10,11,12,13,14
Rhodamine 640 + LD700	706 - 735	9,10,11,12,13,14

To bring the laser to the flow tube, the beam was first raised through a two mirror periscope and then turned into the flow tube by a 90 deg prism. The laser beam was passed through an iris to eliminate off axis background fluorescence from the laser. A 15 cm focal length lens was used to focus the laser into the flow tube through a Brewster window (Figs. 21 and 22). A laser precision energy meter (Model RK3230) was used to monitor the power. Laser power at the flow tube varied from 20 to 70 $\mu\text{J}/\text{pulse}$ depending on the dye.

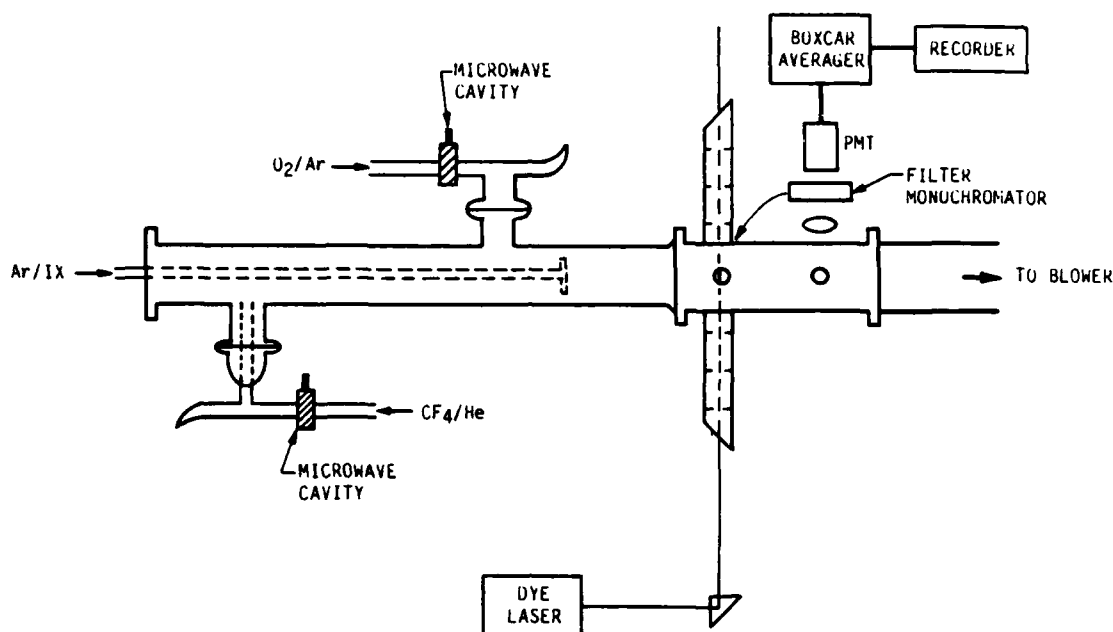


Figure 21. Block diagram of apparatus used for LIF studies. Flow tube reactor showing axial cross injector

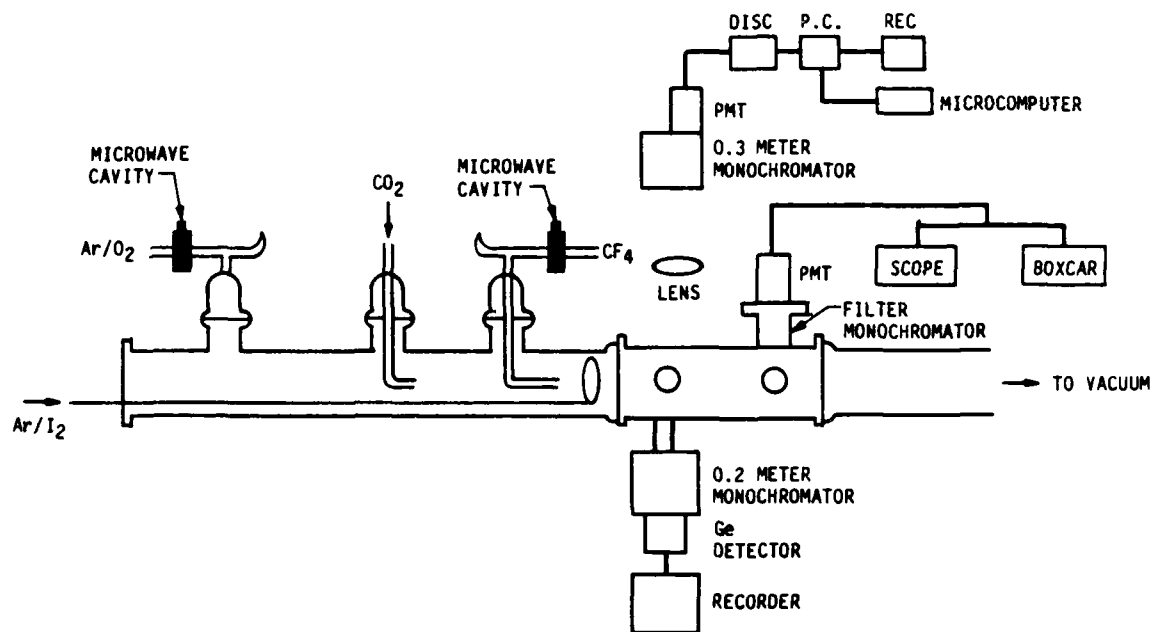


Figure 22. Flow tube reactor showing new loop injector.

The LIF signal was detected using a Hamamatsu R955 photomultiplier tube. Bandpass filters were used to remove scattered laser light from the signal. The two filters used were 500 ± 20 nm and 760 ± 5 nm. A PAR Model 160 boxcar signal averager was incorporated to analyze the signal, which was then recorded on a Soltec chart recorder. Excitation spectra were also recorded using the laboratory microcomputer as described previously.

3.1.2 Flow tube apparatus--To permit more flexibility in the flow tube apparatus the IX sample sliding injector design was modified from that used in the initial chemiluminescence experiments. The original design consisted of a Pyrex cross injector (Fig. 21). The sliding tube through which the IX was delivered traversed the center of the flow tube making it impossible to also use side-arm injectors. The new design was a loop with the delivery tube running along the bottom of the flow tube (Fig. 22). This permitted the use of the side-arm injectors up-stream from the IX loop. It also reduced F atom recombination. The tube was made of 1/4 in stainless steel tubing, and the loop injector was made from 1/8 in Teflon tubing with small holes along the inside of the loop.

3.1.3 IX sample preparation--Various IX (X = I, CF₃, Br, Cl) precursors were used to form IF. A bulb mixture of 10 percent CF₃I in helium was used with the flow measured by a mass flowmeter. The I₂ was placed in a bulb with argon flowing over the I₂. The argon flow was measured with a mass flowmeter and the I₂ flow rate was determined by an absorption technique described in Ref. 13. The introduction of IBr and ICl into the flow tube turned out to be a more difficult problem. At room temperature IBr is a solid and ICl is a liquid. Initially bulb mixtures of ICl and IBr dilute in helium were prepared. The flow of the mixture was measured with a mass flowmeter. LIF signals with ICl from $v'' = 0$ were much weaker than expected. It was suspected that the ICl flow entering the flow tube was actually much lower than indicated by the mass flowmeter. This could occur if ICl was gettered on the mass flowmeter walls or on the walls of the tubing subsequent to the mass flowmeter. When the gas lines were inspected, significant corrosion of the stainless steel in the delivery line was found. Therefore, a new delivery

system was designed and installed. A schematic of the new design is shown in Fig. 23. The ICl was placed in a glass bulb then purified by several freeze-thaw cycles at liquid N_2 temperature. A Teflon needle valve adjusted the amount of ICl flow. The ICl source was kept at ambient temperature, and argon was then mixed with the ICl. The gas mixture was fed directly into the injector. The flow of the argon diluent was measured with a mass flowmeter. Although the concentration of the ICl in the flow tube is not known, as will be described later in Subsection 3.3, the relative amount of IF produced can be measured using LIF. This delivery system was also used for IBr. While all the lines of this system were teflon, several stainless steel fittings were used. Over time even these fittings corroded. In addition over a period of several weeks the ICl and IBr became contaminated by I_2 despite repeated freeze thaw distillation cycles.

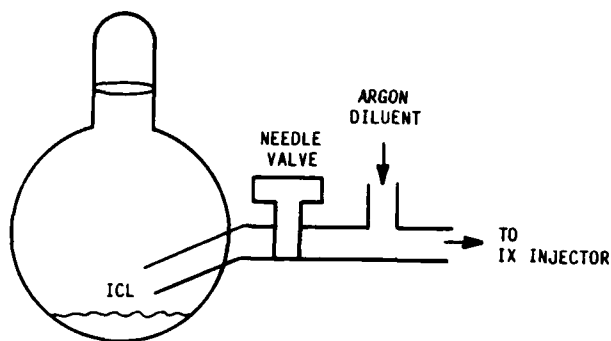


Figure 23. Schematic of ICl saturation used for ICl + F studies.

3.1.4 Analysis of LIF

data--The methodology of the LIF experiments is outlined in Fig. 24. To monitor population from low v'' the laser excited $v' \sim 3,4,5$ ($\lambda < 500$ nm) from $v' = 0,1$ and one monitors red-shifted LIF (Stokes lines). To detect high v'' (5 to 14) one pumps with red dyes ($\lambda > 600$ nm) and monitors blue-shifted LIF (anti-Stokes lines).

Trickl and Wanner (Ref. 26) have previously shown (in a crossed molecular beam experiment) that the IF(X) vibrational distribution produced from the $IX + F$ reaction differs depending on X as shown in Fig. 25. Note that the $I_2 + F$ and $IBr + F$ reactions produce significant $v' > 9$ while the $ICl + F$ and $CF_3I + F$ reactions do not. There are no other significant differences between

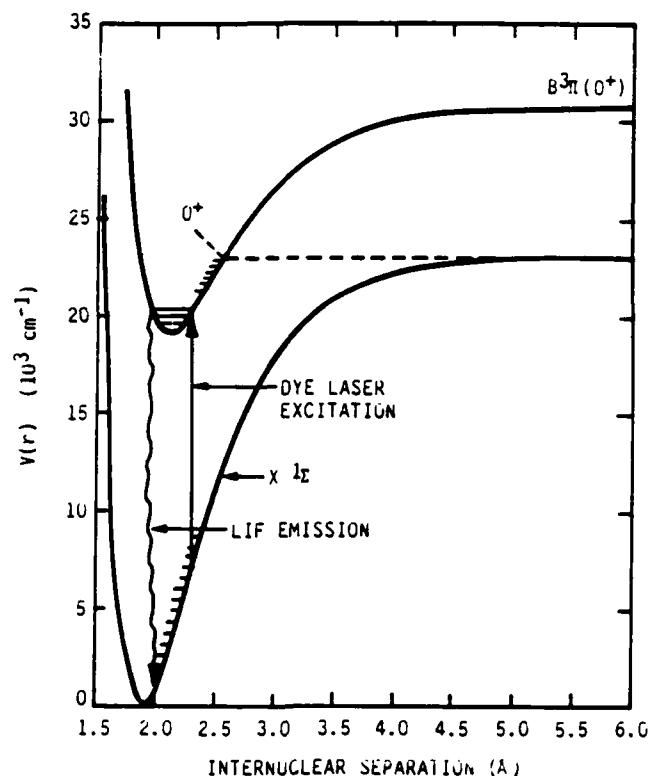
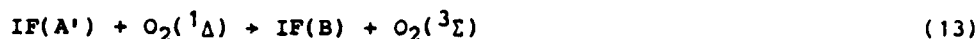
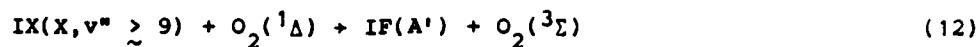


Figure 24. Energy level diagram indicating relevant states involved in LIF detection of IF(X,v).

these reactions. Therefore, comparison of donors should be a critical test of our hypothesis that IF(X,v > 9) is the key species in the first step of the excitation mechanism described below.



If this is an adequate description, then the amount of IF(B) chemiluminescence produced using I₂ should be much greater than that produced using ICl or CF₃I. A direct comparison between the different IF precursors was complicated by the inability to measure the mass flow rate of ICl and IBr. However,

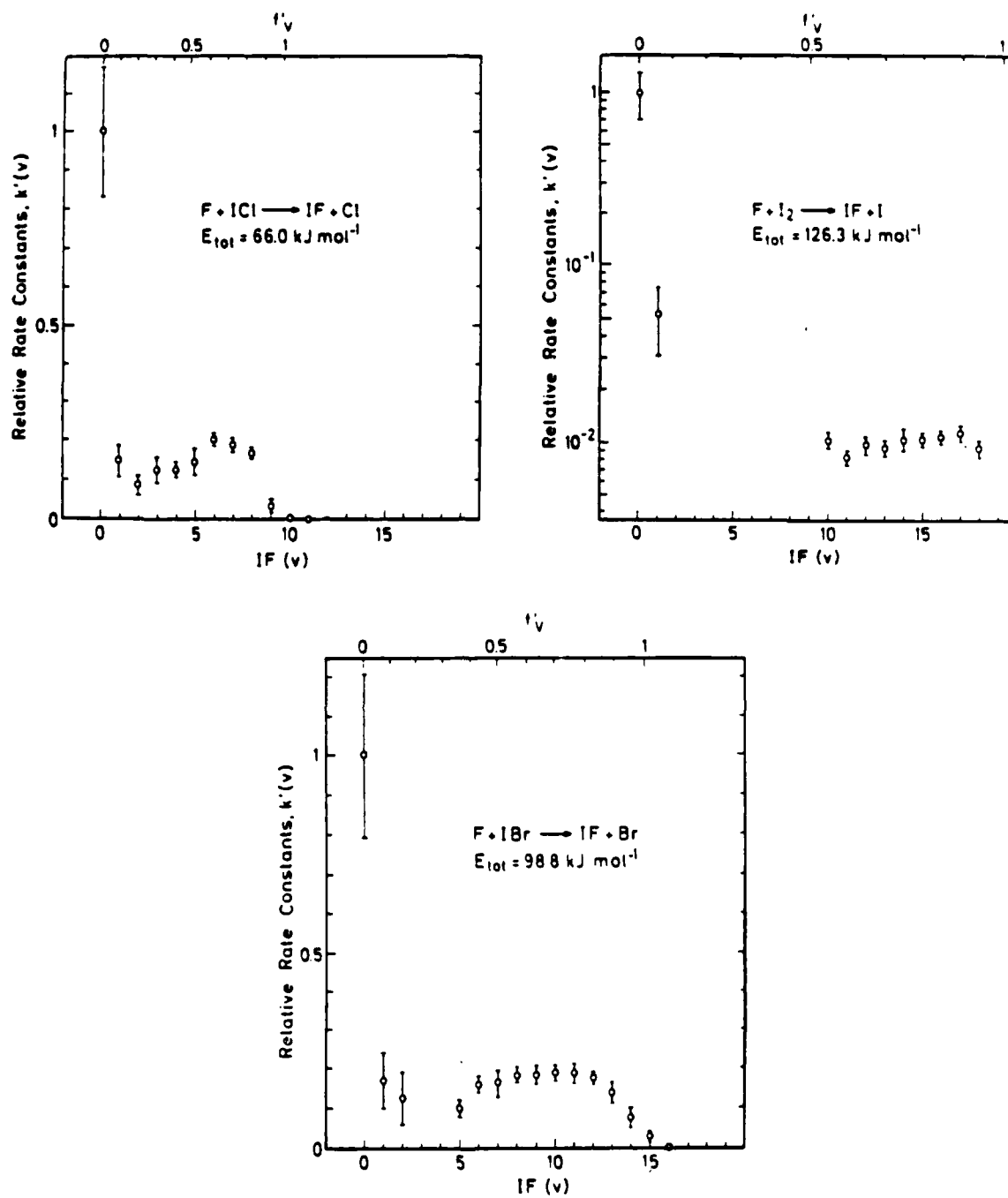


Figure 25. $IF(X,v)$ distribution for $IX + F$ reactions (Ref. 26).

these results can be compared by measuring the relative $IF(X, v'=0)$ produced in each case using LIF as the monitor.

To interpret the LIF results in a more quantitative manner, the following approach has been taken. In general, the LIF signal, I_F , is directly proportional to the number density ($N_{v''}$) of the v'' level excited by the dye laser.

$$IF = KN_{v''} \sigma(v', v'') P(v', v'') \quad (29)$$

where $\sigma(v', v'')$ is the absorption cross section for the $v' + v''$ band, K is a constant, and $P(v', v'')$ is the intensity of the dye laser (photons $\text{cm}^{-2} \text{s}^{-1}$).

In the present experiments an interference filter centered at 500 nm with a 20 nm bandwidth has been used to monitor fluorescence produced by laser excitation of ($v'' > 0$), e.g., excitation of $v' = 4$ from $v'' = 9$. Although it is difficult to determine what fraction of the total fluorescence from $v' = 4$ we observe, if a $v' = 4 + v''$ band is always excited then the LIF signal will be directly proportional to the specific v'' level pumped. A similar argument can be used for any other v' level. In the present experiments $v' = 3$ and 4 has been used. Results for excitation of these two bands are normalized by comparison of the LIF signals observed for pumping of the (3,0), (4,0), (5,0), (6,0), (7,0), and (8,0) bands since each monitors $v'' = 0$. This method allows probing of $v'' = 0, 1, 2, 6, 7, 8, 9, 10, 11, 12, 13, 14$.

To use Eq. (29) we recognize that the absorption cross section $\sigma(v', v'')$ is given by

$$\sigma(v', v'') = \frac{8\pi^3}{3hc} \left(\frac{4\ln 2}{\pi} \right)^{1/2} \left| R_e(v', v'') \right|^2 \frac{q(v', v'') v(v', v'') S_J}{\Delta v_D (2J+1)}$$

where

$|R_e(v', v'')|^2$ is the transition moment

$q(v', v'')$ is the Franck-Condon Factor

$\Delta\nu_D$ is the doppler width

$\nu(v', v'')$ is the frequency of the transition

and

$S_J/(2J+1)$ is the rotational line strength factor and is ~ 0.5 .

We can rewrite Eq. (29) in terms of the relevant parameters

$$\sigma(v', v'') = K_1 |R_e(v', v'')|^2 \nu(v', v'') \quad (30)$$

We can obtain $|R_e(v', v'')|^2$ from Eq. (30).

$$|R_e(v', v'')|^2 = \frac{A_{v', v''}}{(64\pi^4/3h) (\nu(v', v''))^3 q(v', v'')} = \frac{K_2 A_{v', v''}}{q(v', v'') (\nu(v', v''))^3} \quad (31)$$

Thus, we arrive at the expression

$$\sigma(v', v'') = \frac{\hat{\beta} A_{v', v''}}{(\nu(v', v''))^2} \quad (32)$$

where $R(\nu)$ is the dye laser power in microjoules and β is a constant.

The relative number density $N_{v''}$ is determined from

$$N_{v''} = \frac{\kappa I_F(v', v'') (\nu(v', v''))^3}{R(\nu) A_{v', v''}} \quad (33)$$

where κ is a constant that includes all constants described above and is independent of v' and v'' . The $R(\nu)$ are determined from the Laser Precision power meter and the $A_{v', v''}$ are taken from the tables of Ref. 33. Note that we have recognized that the dye laser intensity is proportional to $R(\nu)/h\nu$.

While this technique can be used to compare relative $v'' > 0$, the LIF signals from $v'' = 0$ cannot be directly compared to those originating from $v'' > 1$. This is because two filters are used to observe LIF from $v'' = 0$ ($\lambda = 760$ nm) and from the high v'' ($\lambda = 500$ nm).

3.1.5 Filter calibration--To determine the fraction of IF(X) that is vibrationally excited the relative transmission of the two filters used to observe LIF from $v'' = 0$ ($\lambda = 760 \pm 5$ nm filter) and from the high v'' ($\lambda = 500 \pm 20$ nm filter) must be determined. Since narrow bandpass filters were used to collect the data the relative collection efficiency will differ for each v' (Fig. 26). In addition the transmission curves of the two filters are different.

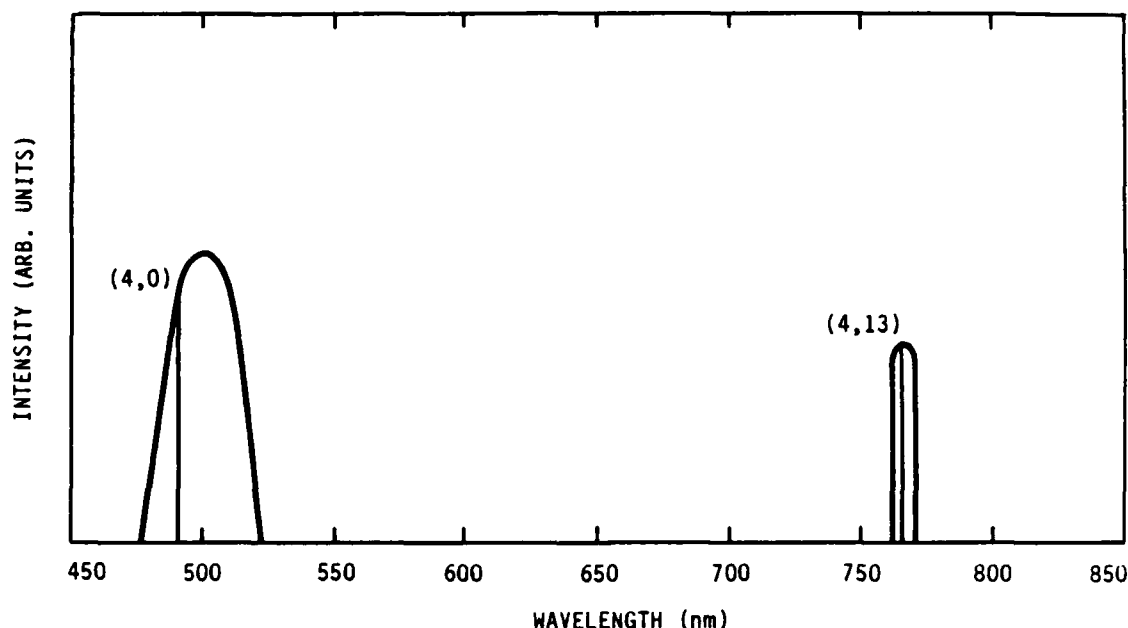


Figure 26. Transmission functions of bandpass filters used to collect LIF data.

To calibrate the two filters, LIF signals resulting from pumping a single (v', v'') transition were measured with each filter while all other conditions were held constant. Transitions for calibration were carefully chosen so that the pump wavelength was not in the range of either filter. This eliminates scattered laser light as a background signal. The I_2 was used as the IF precursor for the calibration measurements. Since the filter at the $\lambda = 760$ nm transmits some I_2 fluorescence an excitation transition was chosen in a region where there was no detectable I_2 fluorescence.

Two distinct transitions, the (3,8) and (4,9), were used to calibrate the filters. Spectra taken using each filter are shown in Fig. 27. In this spectral region two other transitions, the (6,10) and (7,11), are also present. The signal with the $\lambda = 760$ nm filter was too weak to use these transitions for calibration. The spectrum taken with the $\lambda = 500$ nm filter was much more intense than the spectrum taken with the $\lambda = 760$ nm filter. A factor of 20 more sensitivity was needed to record the $\lambda = 760$ nm filter spectrum. The area under each band was integrated with a planimeter to determine the relative intensity of each transition. To determine a calibration factor for $v' = 4$ a ratio of the intensity of the (4,9) using each filter was determined:

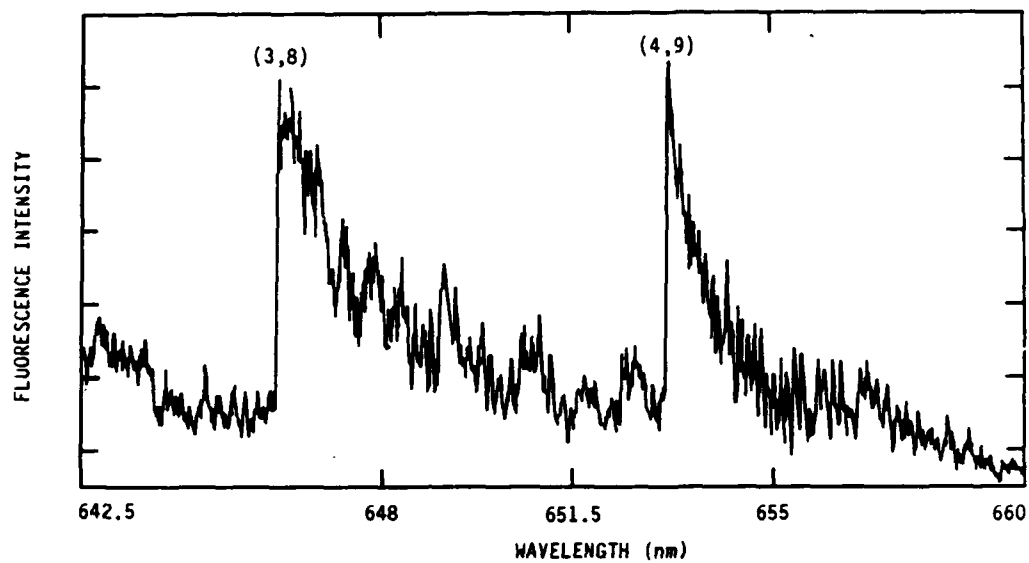
$$\frac{I_{500}(4,9)}{I_{760}(4,9)} = 19.1$$

Similarly a ratio of the for pumping (3,8) was calculated to be 22.0.

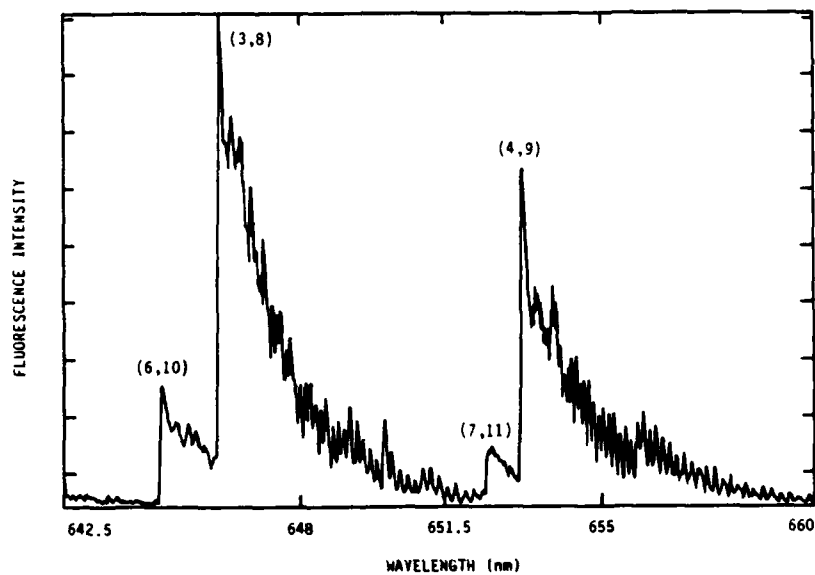
These normalization factors were used to compare the populations in $v'' = 0$ to those in $v'' > 1$ using pump transitions that terminated on $v' = 3$ or 4. Transitions using other v' can be normalized by comparing two transitions with the same v'' . For example the (5,12) can be normalized to the (4,12) for which the v' calibration is known. As previously described, the intensity is first corrected for differences in laser power and absorption cross section. After these corrections, the intensities of the (4,12) and (5,12) would be equal if there was no filter discrimination (Fig. 28). The ratio of $I(4,12)/I(5,12)$ can then be used to normalize the other (5, $v'' > 0$) transitions to $v' = 4$. In this manner normalization factors for $v' = 3, 5, 6, 7$ and 8 with respect to $v' = 4$ were determined. Therefore, all data was normalized to an LIF signal that originated from $v' = 4$.

3.2 RESULTS

3.2.1 Initial LIF results--In our initial studies reactions (16) and (17) were used to produce IF(X).



(a) Observed through the 760 nm filter



(b) Observed through the 500 nm filter

Figure 27. LIF signal.

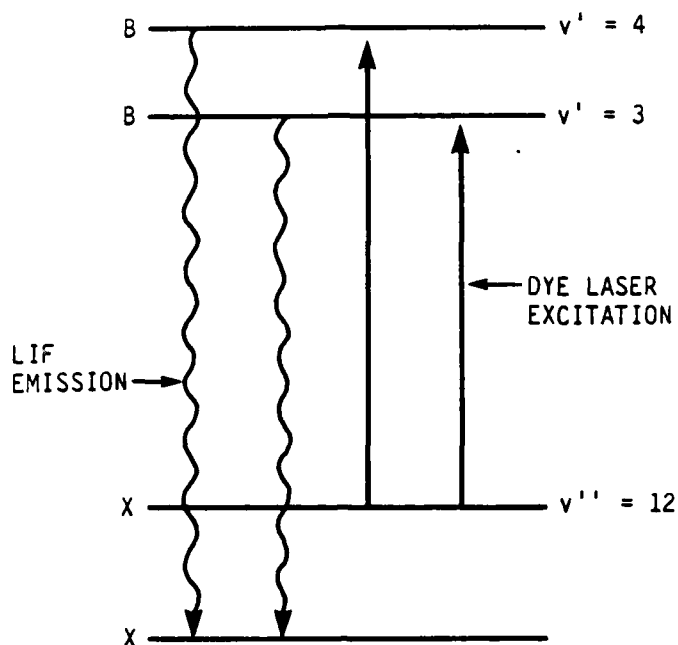


Figure 28. Energy level diagram indicating LIF detection scheme.



The IF^\dagger was seen on the initial attempt. It was encouraging that IF^\dagger could be observed in a flow tube environment. This is an important observation since IF^\dagger must survive long enough to be pumped by an O_2^* molecule. No IF^\dagger was seen when reaction (16) was used to produce IF. In Fig. 29 a comparison is shown of LIF excitation spectra for reactions (16) and (17) both at 0.5 ms reaction time. Although these LIF spectra cover only a small wavelength range of the total that we have studied it is clear that IF^\dagger is absent when reaction (16) is used to produce IF(X) .

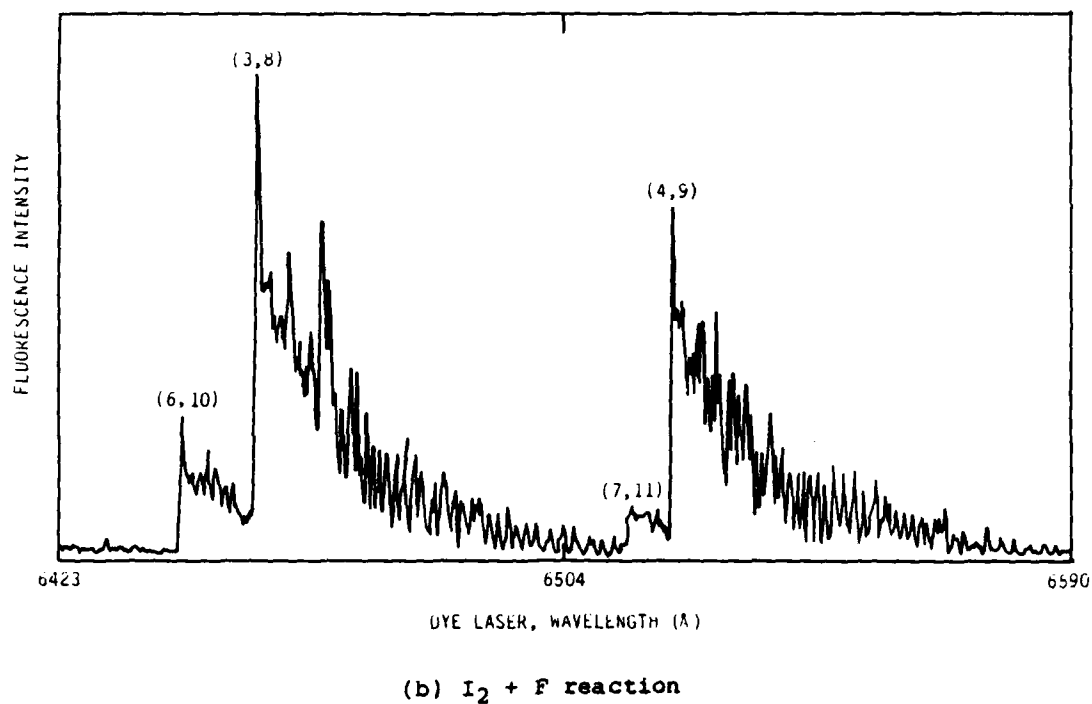
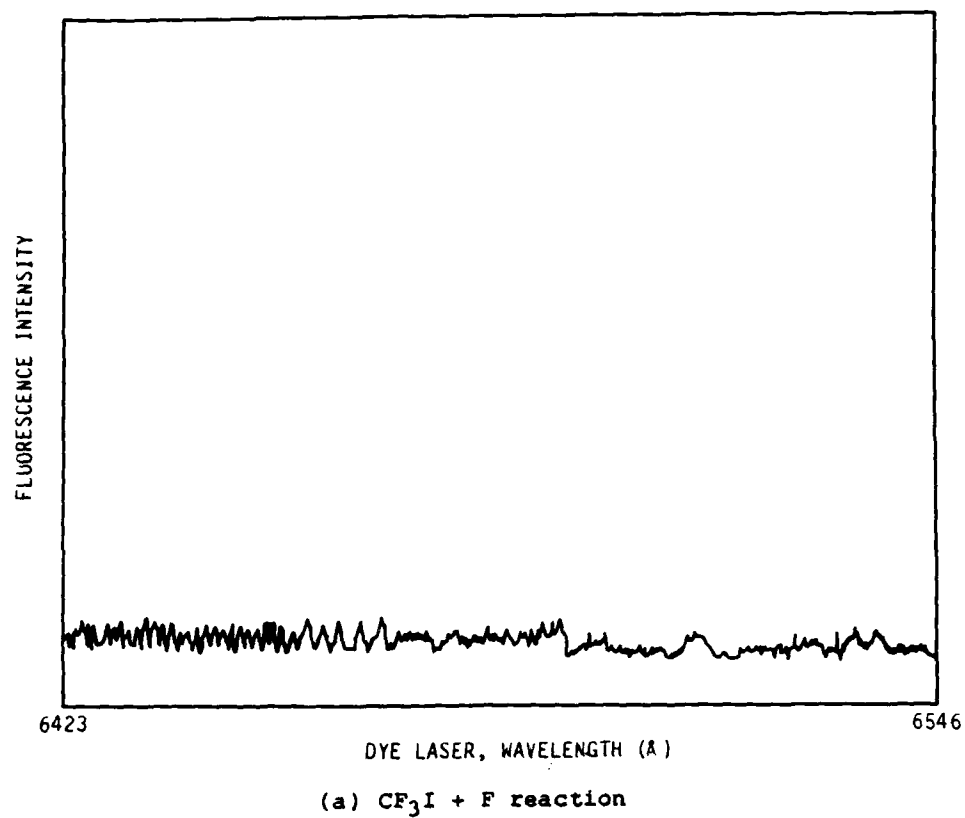


Figure 29. Comparison of LIF excitation spectra using $\text{CF}_3\text{I} + \text{F}$ and $\text{I}_2 + \text{F}$ reactions when dye laser was probing hot vibrational levels in $\text{IF}(X)$.

Some temporal profiles of IF^+ were obtained by varying the I_2 injector location as described in the chemiluminescence experiments. In Fig. 30 the evolution of $v'' = 10$ as a function of reaction time is shown. Also plotted is the $IF(B+X)_{0-4}$ chemiluminescence intensity temporal profile taken under comparable conditions. From Fig. 30 it is seen that the chemiluminescence intensity falls off at a faster rate than does $v'' = 10$. However, it is noted that the observed rate of diminution of $v''=10$ is actually the sum of the rate into $v''=10$ from $v''>10$ and the rate out of $v''=10$ to lower v'' . Consequently, the relaxation rate of $v''=10$, observed by LIF, might be expected to be smaller than the rate of reduction of $IF(B+X)$ emission if $v''>10$ are the critical levels in the O_2^* excitation process.

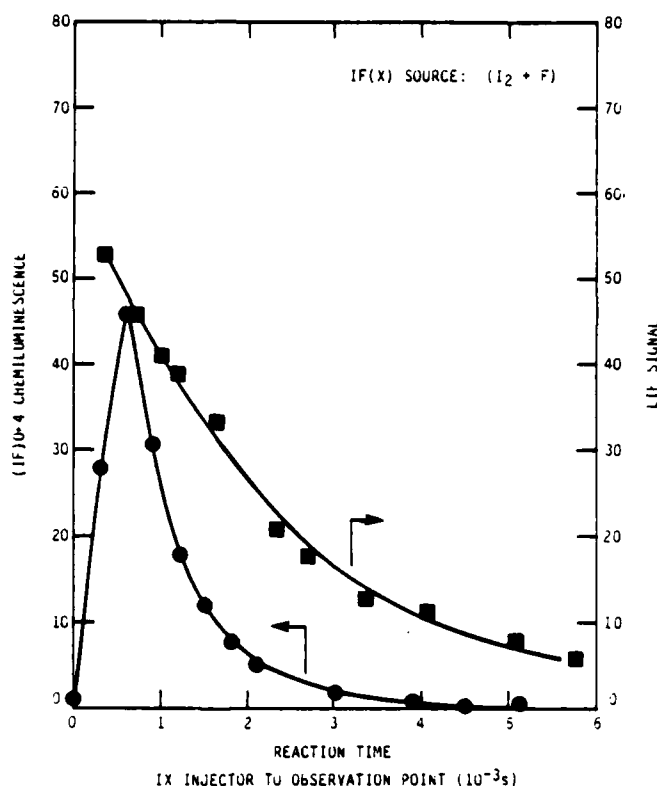


Figure 30. Plot of temporal evolutions of IF^+ and $IF(B+X)$ chemiluminescence intensity. $IF(X)$ produced by $I_2 + F$ reaction. ■ -LIF signal from excitation of $IF^+(X; v''=10)$; ● - $IF(B+X)$ chemiluminescence intensity (data are normalized at one point)

A similar study was done which monitored $v'' = 0$ when CF_3I was used as an iodine donor. These results are presented in Fig. 31. The $\text{IF}(\text{B} \rightarrow \text{X})$ chemiluminescence tracks the profile of $\text{IF}(\text{X}; v=0)$ reasonably well.

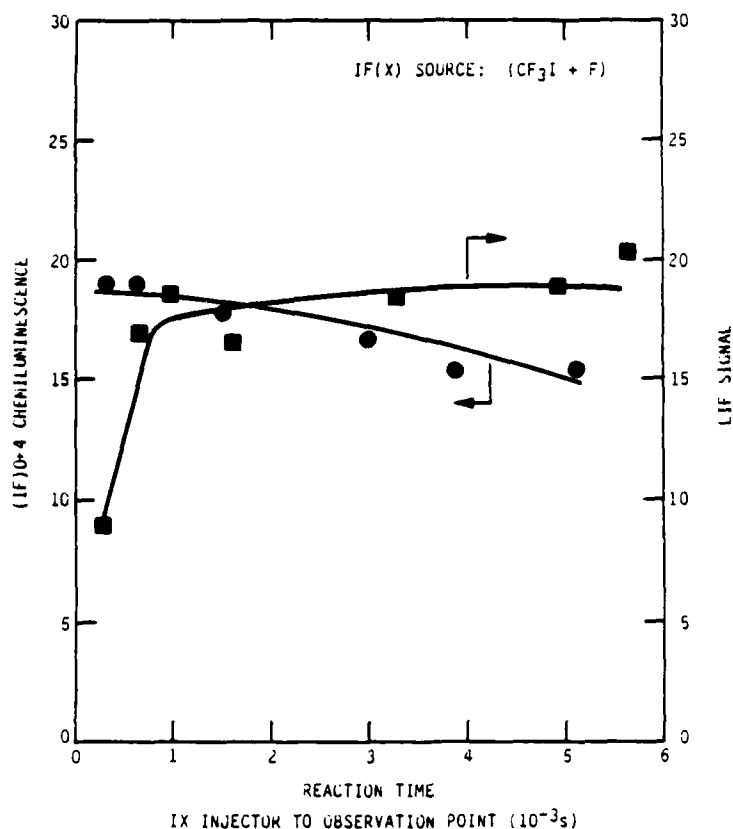


Figure 31. Plot of temporal evolution of $\text{IF}(\text{X}; v''=0)$ and $\text{IF}(\text{B} \rightarrow \text{X})$ chemiluminescence intensity. $\text{IF}(\text{X})$ produced by $\text{CF}_3\text{I} + \text{F}$ reaction. ■ - LIF signal from excitation of $\text{IF}(\text{X}; v''=0)$; ● - $\text{IF}(\text{B} \rightarrow \text{X})$ chemiluminescence intensity (data are normalized at one point)

These results, while not yet quantitative, were suggestive of an active participation of IF^\dagger in the excitation of $\text{IF}(\text{B})$ by O_2^* . Reaction (17) produced readily detectable $\text{IF}(\text{X}; v \leq 12)$ while reaction (16) produced no detectable IF^\dagger with $v > 1$. The evolutions of $v''=10$ and $v''=0$ subsequent to their respective formation by reactions (33) and (34) qualitatively agreed with the temporal profiles of $\text{IF}(\text{B} \rightarrow \text{X})$ chemiluminescence using reactions (16) and (17). At this point in the study it appeared that IF^\dagger was linked to the intense $\text{IF}(\text{B} \rightarrow \text{X})$ chemiluminescence observed in the $\text{F} + \text{I}_2 + \text{O}_2^*$ reaction.

3.2.2 LIF results: complete study--To test the hypothesis of the importance of $v'' > 10$, LIF data were obtained using CF_3I , I_2 , IBr and ICl as iodine donors for IF. Excitation spectra were recorded over a large wavelength region. These data were obtained 0.5 to 5.0 ms downstream of the IF injector. Table 2 summarizes the transitions observed, their calculated wavelengths, and the laser dyes used. A representative selection of excitation spectra of IF formed by the reaction $\text{I}_2 + \text{F}$ are given in Figs. 32, 33, 34, and 35. For comparison excitation spectra for CF_3I , ICl , and IBr are given in Figs. 36, 37, and 38 and 39, respectively. In all four cases strong signals are observed from $v'' = 0$. The intensity of the LIF signal from $v'' > 0$, however, is strongly dependent on the iodine donor used to form IF. As mentioned previously, CF_3I produces no detectable IF^\dagger . For ICl , signals from $v'' = 8$ and 9 are very weak (Fig. 36b). No LIF from $v'' > 9$ could be observed. For both I_2 and IBr , LIF signals from higher vibrations up to $v'' = 14$ were observed (Figs. 34 and 38). Vibrations greater than $v'' = 14$ could not be studied with our laser system.

3.2.3 Analysis of results--Using the equations developed earlier, vibrational distributions in $\text{IF}(X)$ were calculated for the four iodine donors studied. The results of these calculations are given in Figs. 39, 40, 41 and 42. The filter corrections discussed in Section 3 was included in all of these calculations so the ratio $\sum_{v''>0} [\text{IF}(v''>0)]/[\text{IF}(v''=0)]$ is known.

Although LIF is a sensitive monitor for $\text{IF}(v''>0)$ it does present some difficulties in data reduction. These include dye laser power variations and the transmission properties of the filters used to eliminate scattered laser light. The actual dye laser power for each transition was interpolated from readings that were taken periodically during each spectral scan. A 5 percent error is introduced through our accuracy in interpolation. For several transitions the dye laser power was changing rapidly over the spectral range of the transition. In these cases a larger error of up to 20 percent is introduced. The transmission of the filters has been calibrated as described

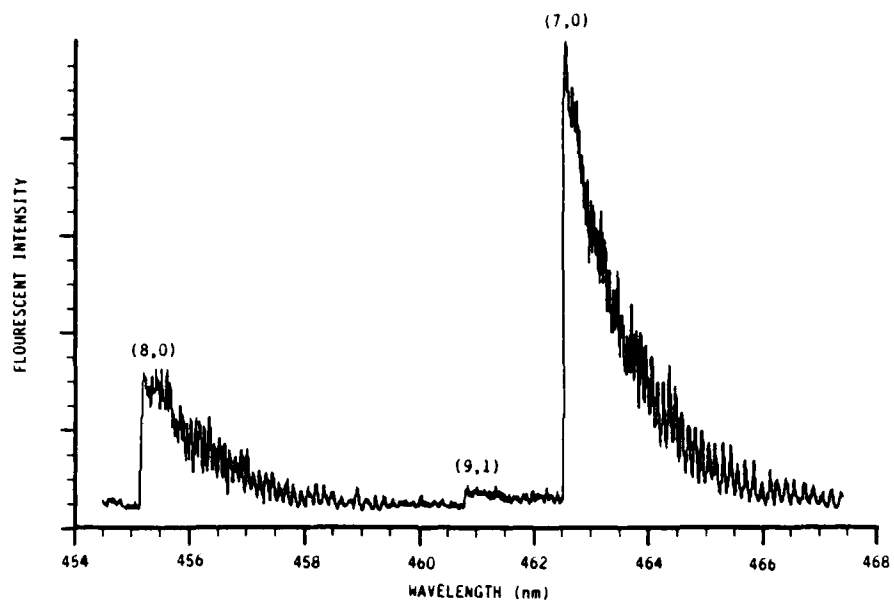
TABLE 2. Transitions in IF(B+X) Observed Using LIF.

(v',v'')	Calculated Wavelength (Å)	Laser Dye
(8,0)	4546.2	Coumarin 460 (C460)
(9,1)	4602.0	C460
(7,0)	4619.5	C460
(8,1)	4674.7	C460
(6,0)	4697.4	Coumarin 480 (C480)
(9,2)	4732.2	C480
(7,1)	4752.2	C480
(5,0)	4780.3	C480
(8,2)	4809.2	C480
(4,0)	4868.1	Coumarin 500 (C500)
(7,2)	4891.3	C500
(5,1)	4922.5	C500
(8,3)	4950.0	C500
(3,0)	4961.3	C500
(6,2)	4973.7	C500
(4,1)	5013.8	C500
(2,0)*	5059.9	C500
(3,1)*	5114.7	C500
(1,0)*	5164.2	C500
(2,1)*	5219.6	C500
(3,5)	5814.7	Rhodamine 590 (R590)
(4,6)	5878.5	R590
(5,7)	5944.3	R590
(2,5)	5950.6	R590

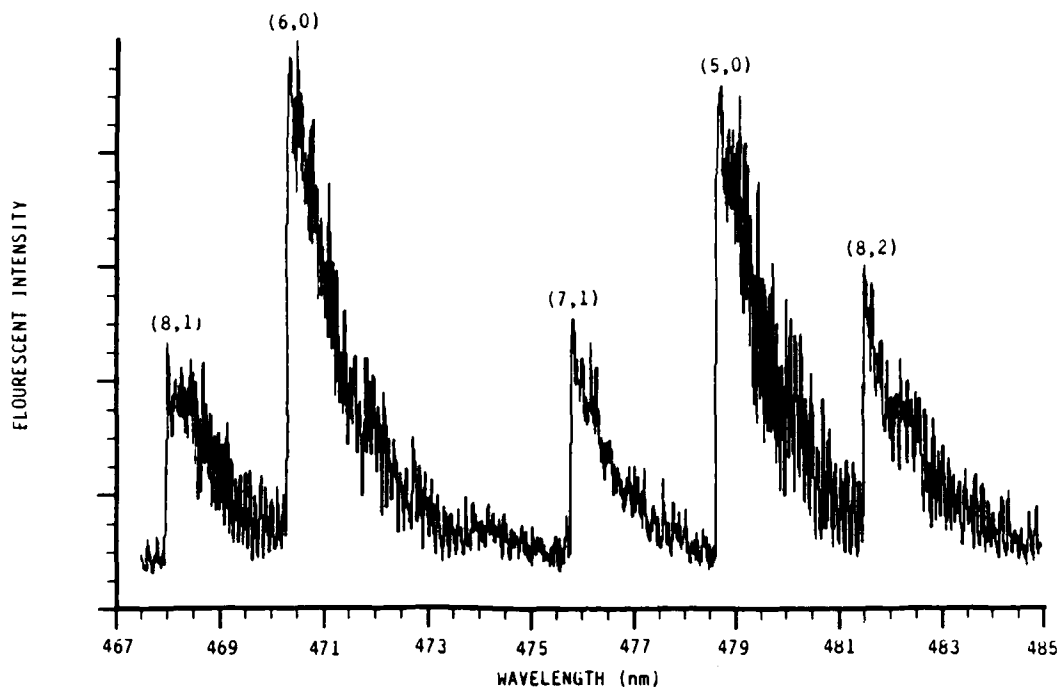
*Not observed using I₂ as iodine donor because of strong I₂ fluorescence.

TABLE 2. Transitions in IF(B+X) Observed Using LIF (Cont.).

(v',v'')	Calculated Wavelength (Å)	Laser Dye
(4,7)	6080.8	Rhodamine 610 (R610)
(7,9)	6083.4	R610
(5,8)	6148.8	R610
(2,6)	6160.4	R610
(6,9)	6219.3	Rhodamine 640 (R640)
(3,7)	6226.8	R640
(4,8)	6295.0	R640
(5,9)	6365.4	R640
(6,10)	6438.4	R640
(3,8)	6451.6	R640
(7,11)	6514.5	R640
(4,9)	6522.1	R640
(5,10)	6595.0	LD690 + Rhodamine 610 (R610)
(2,8)	6619.3	LD690 + R610
(6,11)	6670.6	LD690 + R610
(3,9)	6690.4	LD690 + R610
(7,12)	6749.5	LD690 + R610
(4,10)	6763.4	LD690 + R610
(1,8)	6799.1	LD690 + R610
(8,13)	6832.3	LD690 + R610
(5,11)	6838.9	LD690 + R610
(2,9)	6871.0	LD690 + R610
(4,11)	7020.2	LD700 + Rhodamine 640 (R640)
(1,9)	7064.8	LD700 + R640
(8,14)	7085.1	LD700 + R640
(5,12)	7098.4	LD700 + R640
(2,10)	7139.3	LD700 + R640
(6,13)	7179.7	LD700 + R640
(3,11)	7215.5	LD700 + R640
(7,14)	7263.0	LD700 + R640
(4,12)	7295.0	LD700 + R640

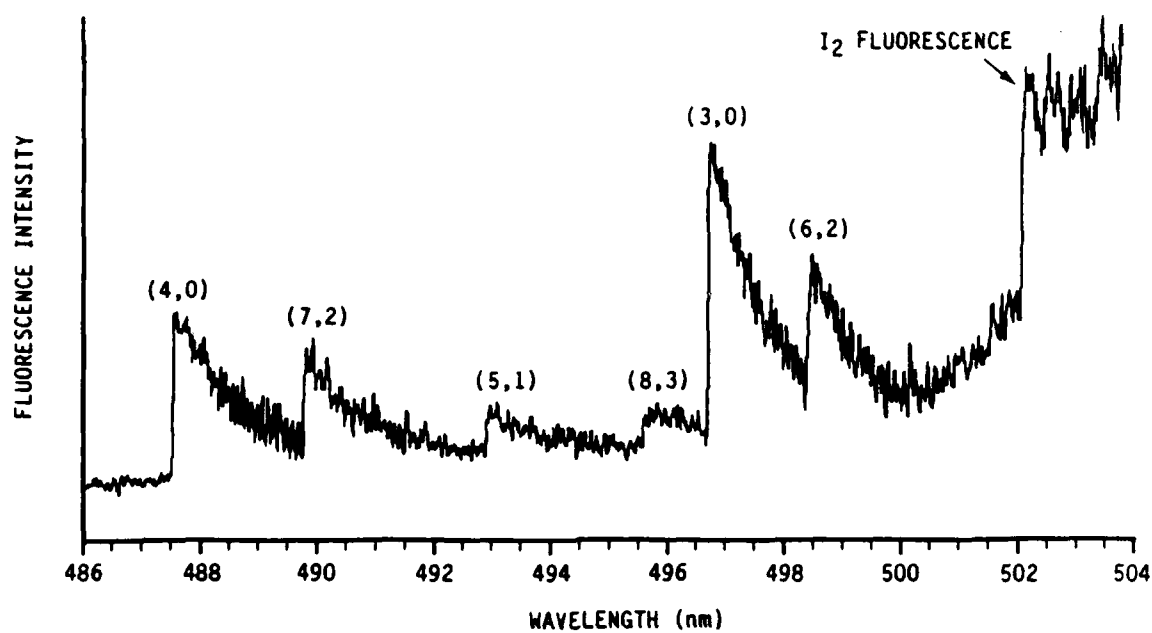


(a) Coumarin 460

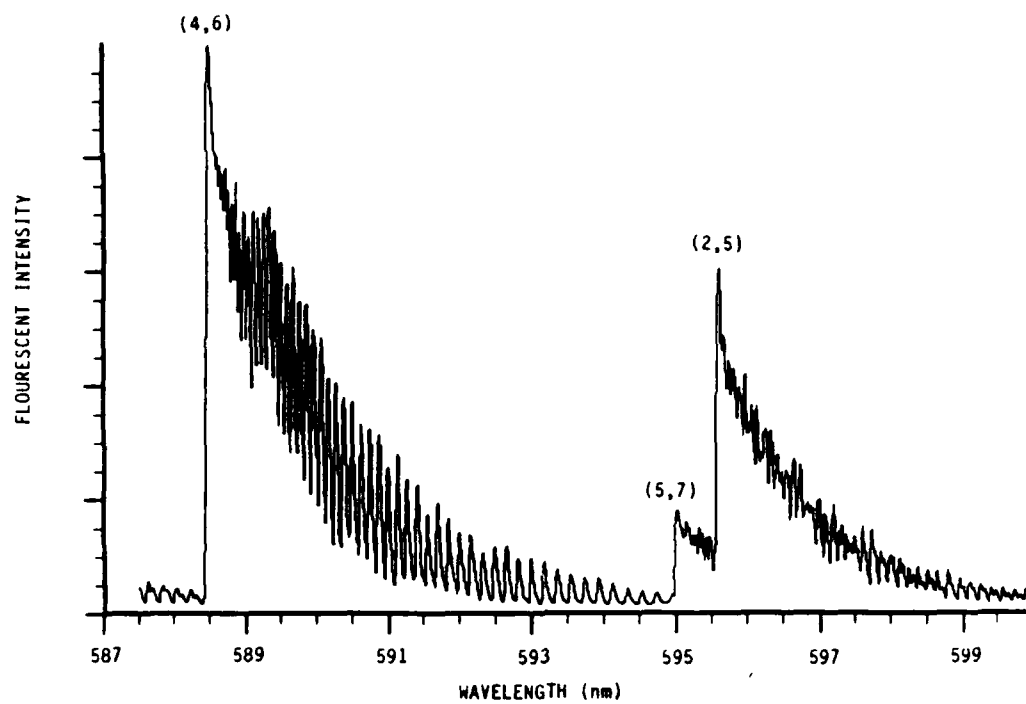


(b) Coumarin 480

Figure 32. LIF of IF. IF(X) formed using $I_2 + F$ reaction

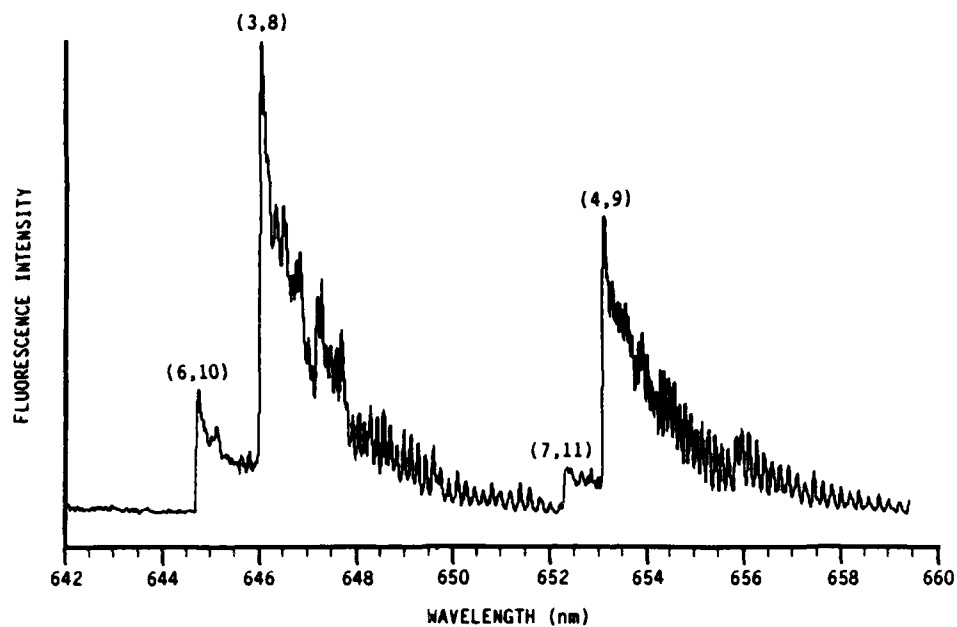


(a) LIF spectrum taken using laser dye Coumarin 500

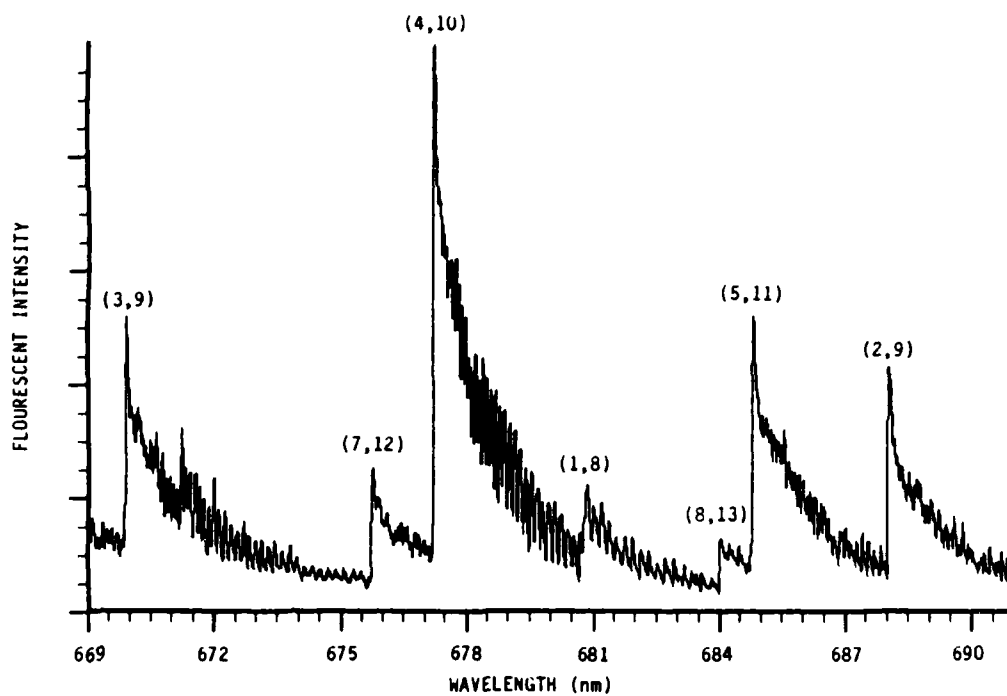


(b) LIF spectrum taken using laser dye Rhodamine 590

Figure 33. LIF of IF. IF(X) formed using I₂ + F reaction



(a) LIF spectrum taken using laser dye R640



(b) LIF spectrum taken using laser dye LDS690 Rhodamine 610

Figure 34. LIF of IF. IF(X) formed using $I_2 + F$ reaction

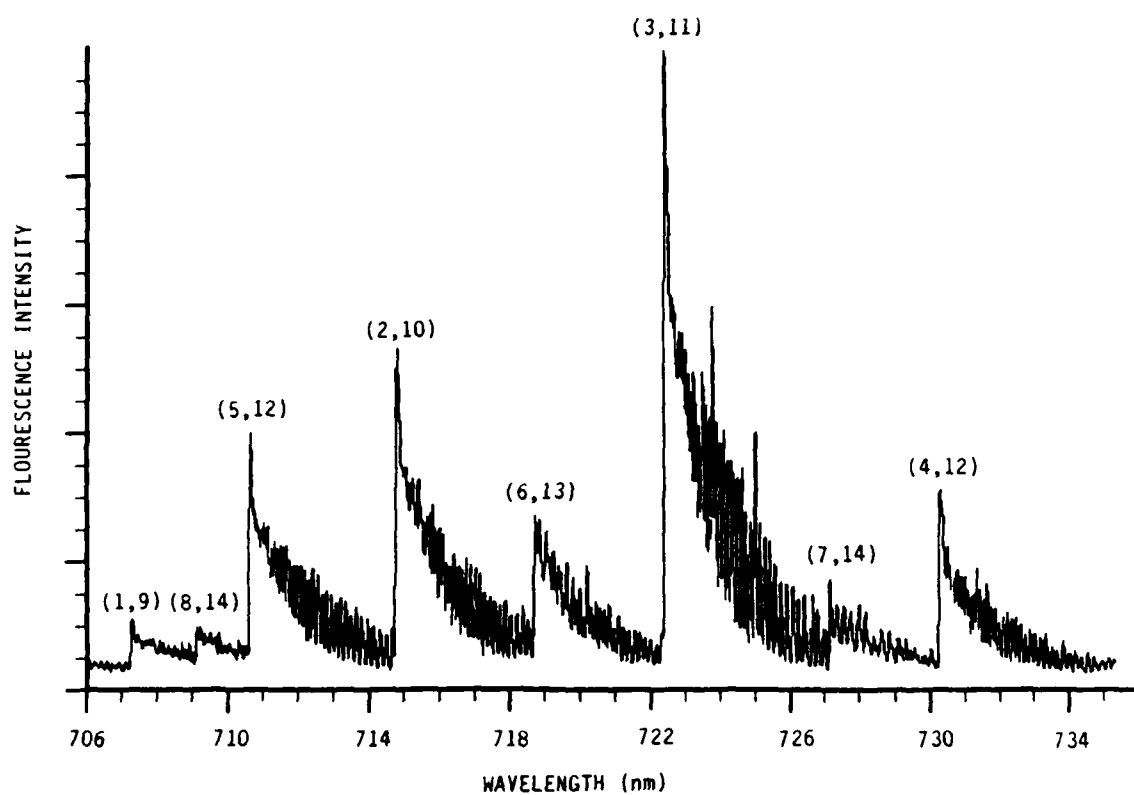
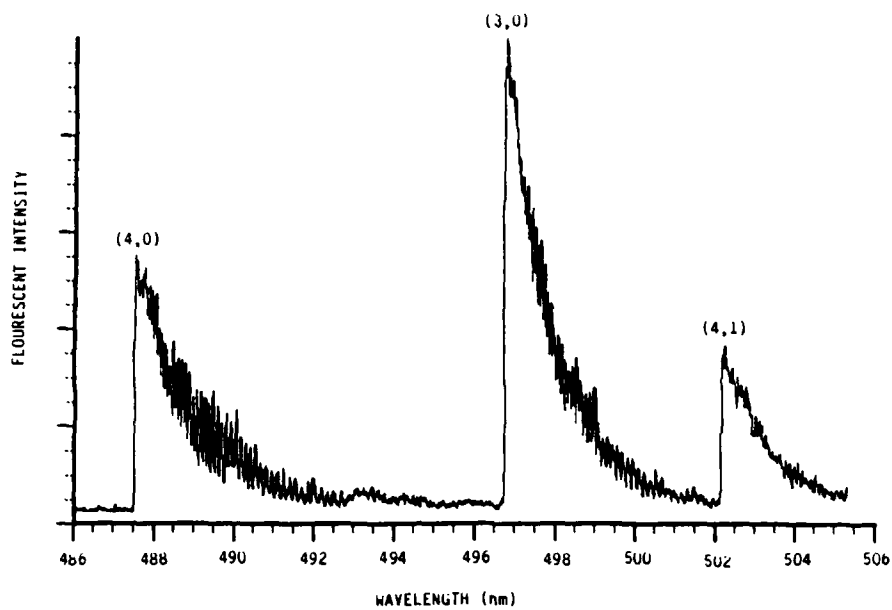
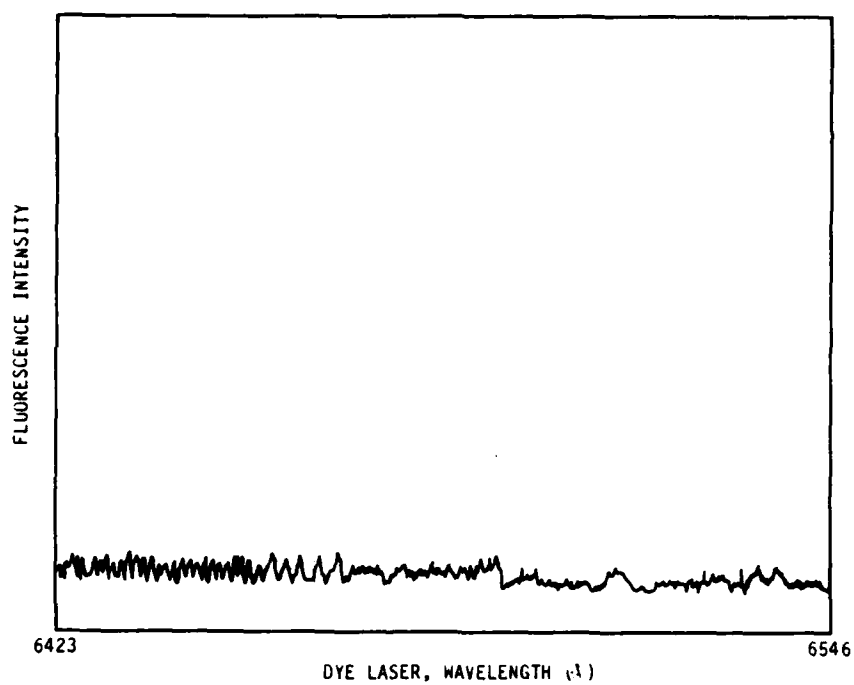


Figure 35. LIF of IF. IF(X) formed using $I_2 + F$ reaction. Spectrum taken using laser dye LD700 + Rhodamine 640.

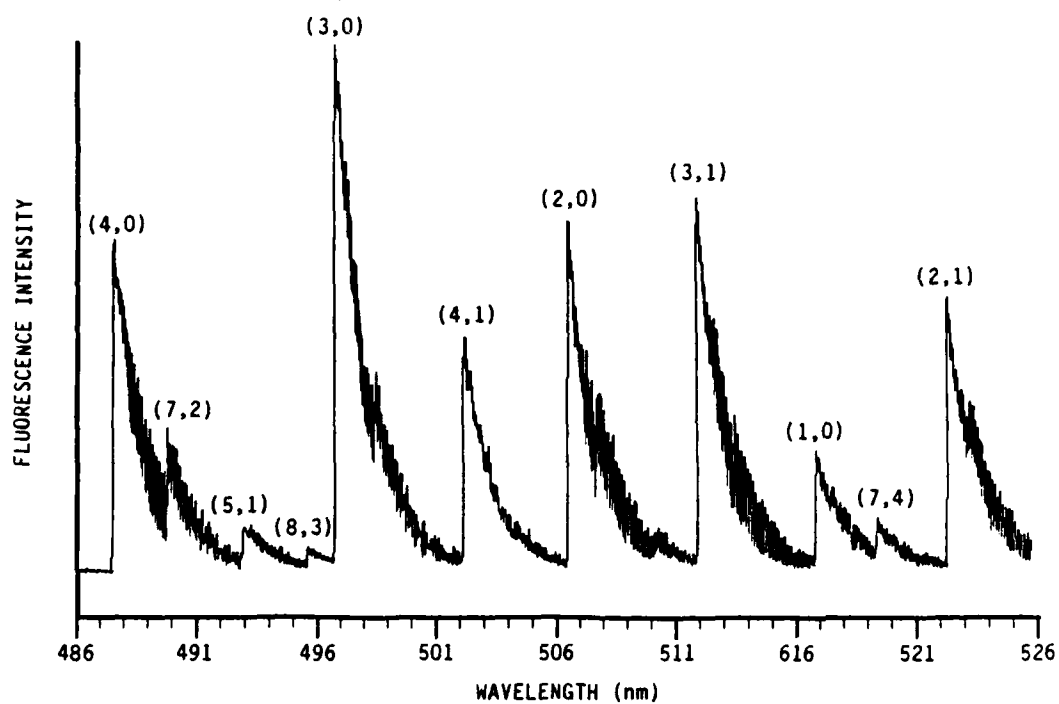


(a) LIF spectrum taken using laser dye Coumarin 500

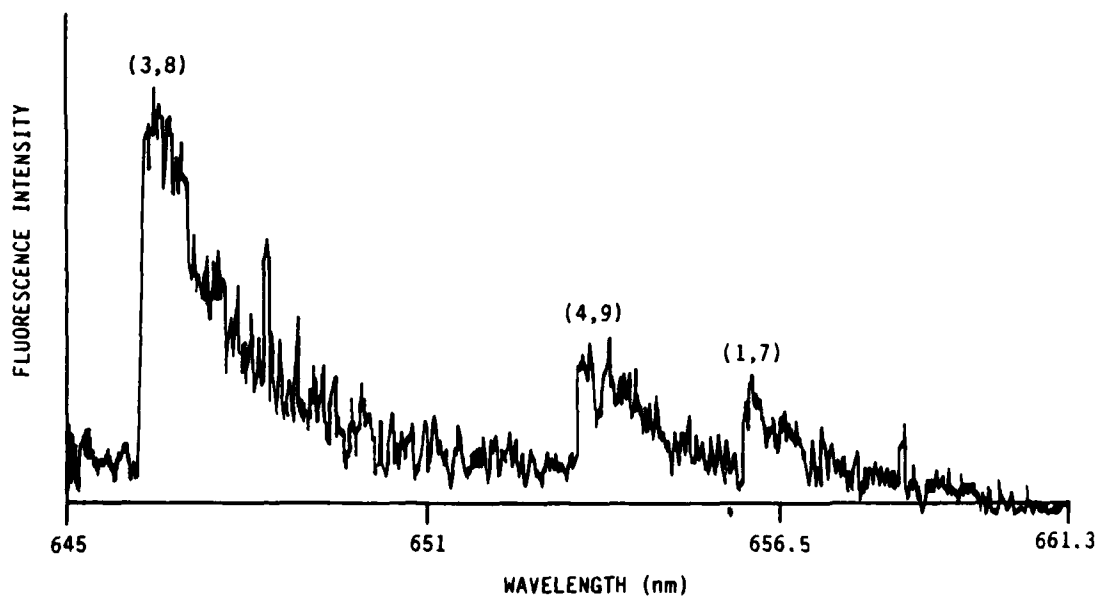


(b) LIF spectrum taken using laser dye Rhodamine 640

Figure 36. LIF of IF. IF(X) formed using $\text{CF}_3\text{I} + \text{F}$ reaction

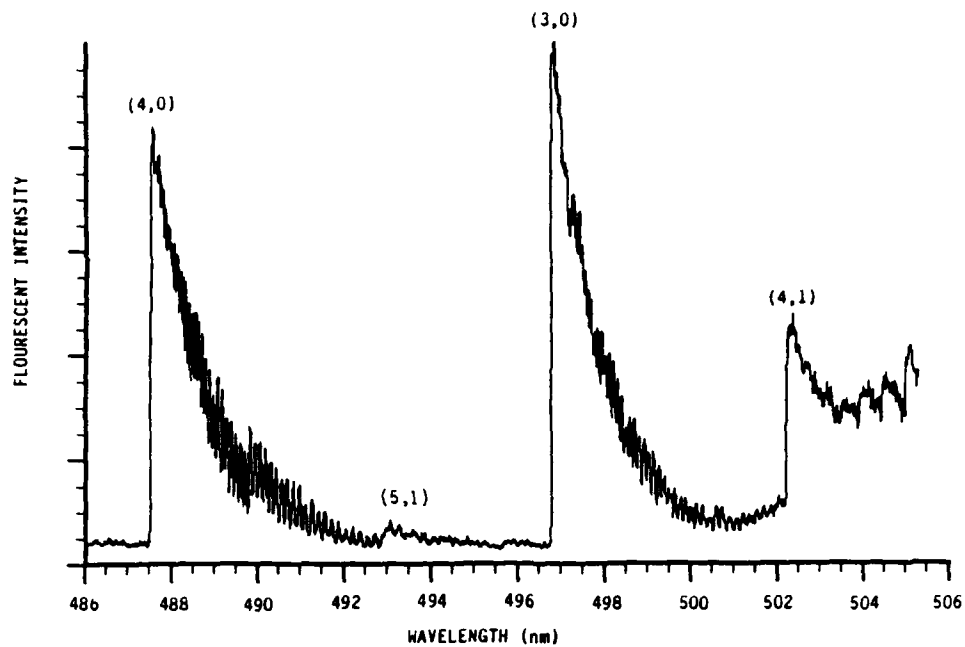


(a) LIF spectrum taken using laser dye Coumarin 500

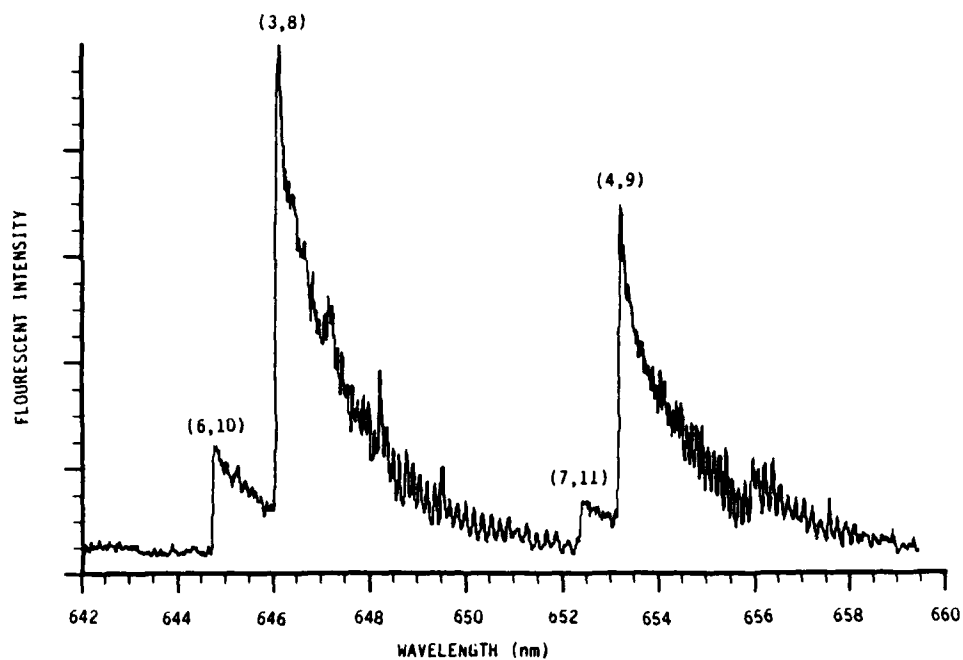


(b) LIF spectrum taken using laser dye Rhodamine 640

Figure 37. LIF of IF. IF(X) formed using ICl + F reaction



(a) LIF spectrum taken using laser dye Coumarin 500



(b) LIF spectrum taken using laser dye Rhodamine 640

Figure 38. LIF of IF. IF(X) formed using IBr + F reaction

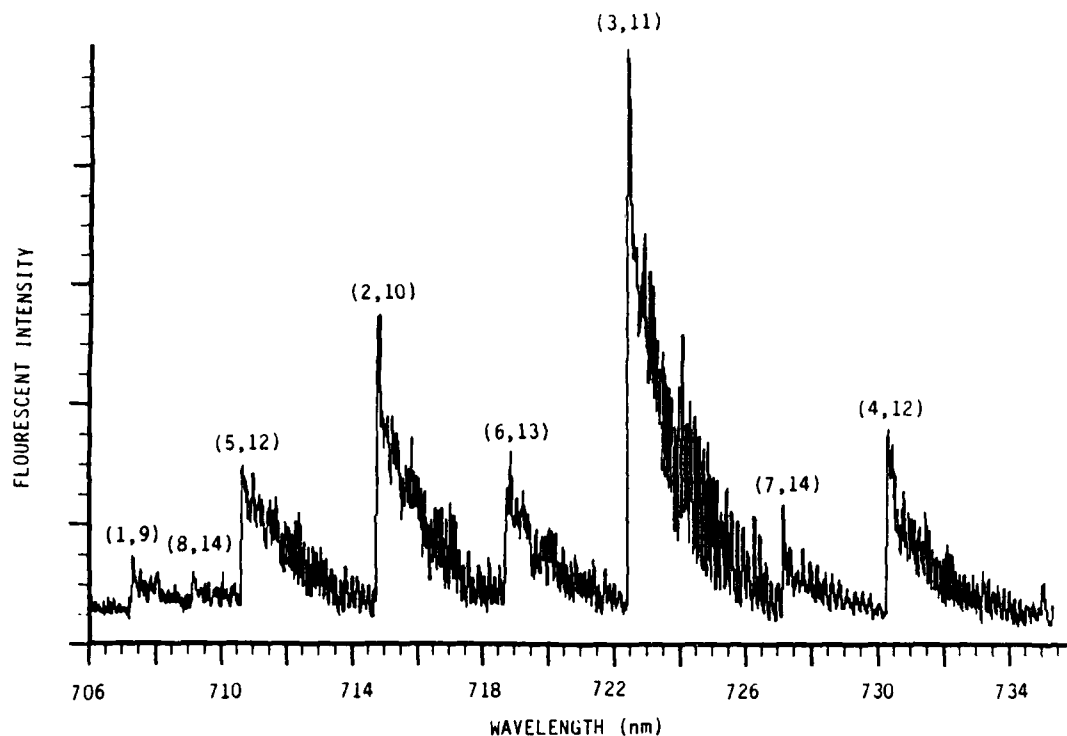


Figure 39. LIF of IF. IF(X) formed using IBr + F reaction. Spectrum taken using laser dye LD700 + Rhodamine 640

previously. Error in the calibration is introduced in the ability to measure accurately the intensity of each transition. The intensity of the strong signals could be measured to within 3 percent but the weaker signals have a 10 percent error uncertainty. For most of the data reduction, the LIF intensity was determined by measuring peak heights from the recorded spectra. The effects of quenching and V-T relaxation are harder to quantify. Both would serve to decrease the vibrational population of higher vibrations and increase the lower vibrations. As will be shown later this would then decrease the observed chemiluminescence signal. Thus, the distributions are almost certainly not nascent. The area under the LIF spectra of several transitions were also integrated. The two methods gave results that agreed to within 9 percent. Overall a combined error of 15 percent is calculated for our ability to connect observed LIF signals to relative populations.

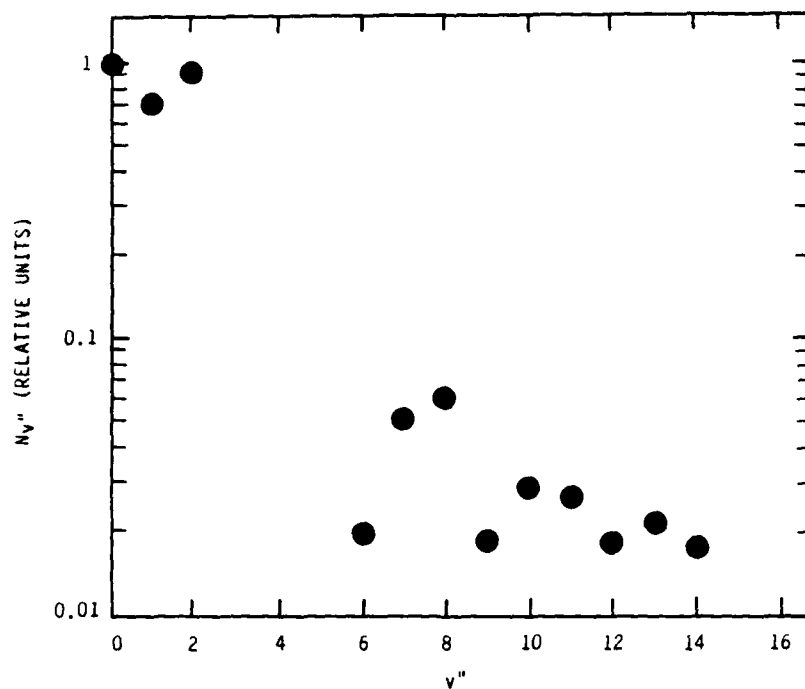


Figure 40. Vibrational Distribution in IF(X). IF(X) formed using IBr + F reaction

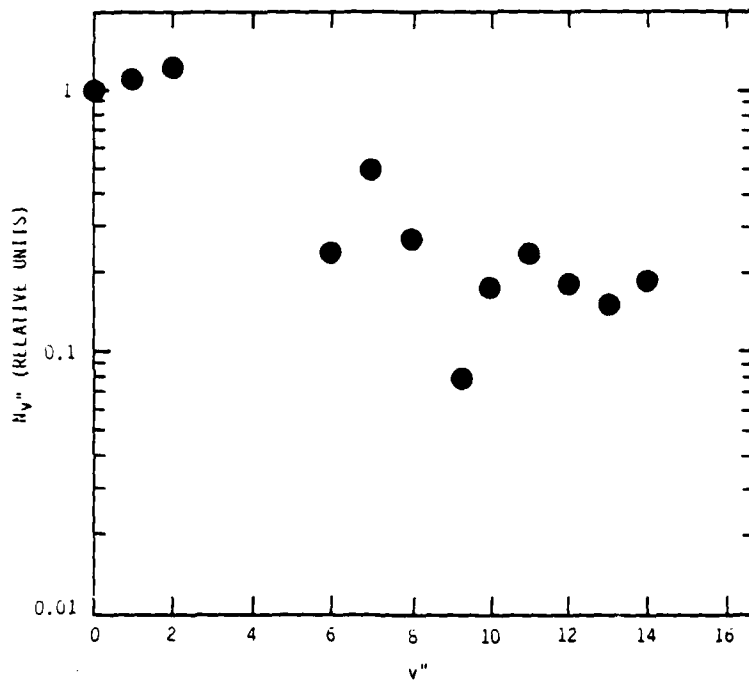


Figure 41. Vibration distribution of IF(X). IF(X) formed using $I_2 + F$ reaction

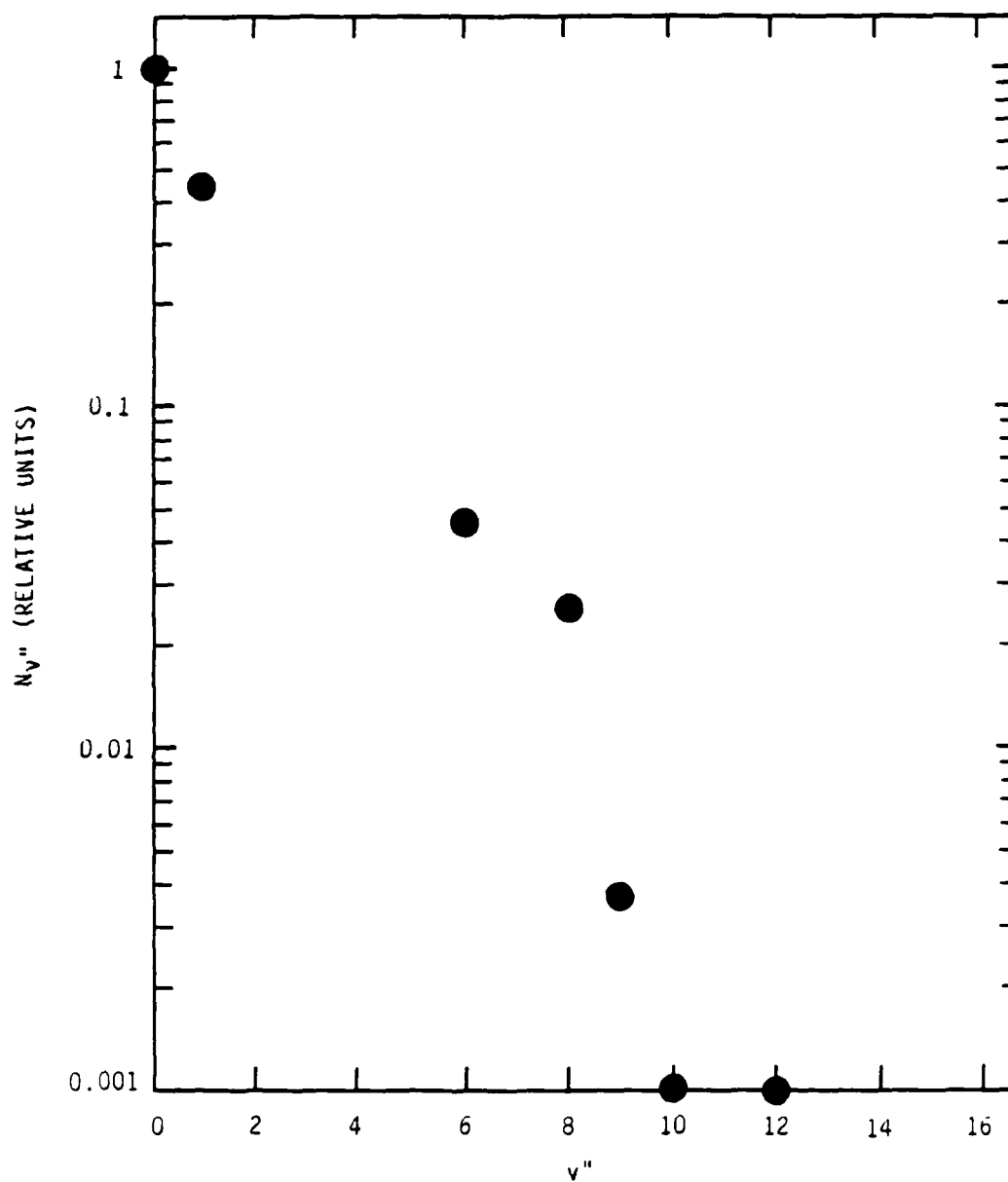


Figure 42. Vibrational distribution of IF(X). IF(X) formed using ICl + F reaction

3.3 CHEMILUMINESCENCE FROM $\text{IF}^\dagger + \text{O}_2^*$

Chemiluminescence spectra of $\text{IF}(\text{B})$ produced by O_2^* pumping were recorded under the same conditions as the LIF spectra for each of the iodine donors studied. Spectra for I_2 , IBr , ICl , and CF_3I are given in Figs. 43, 44, 45, and 46. The vibrational distribution for $\text{IF}(\text{B})$ is similar for all IF donors studied. However, the intensity of the chemiluminescence exhibits a strong dependence on the iodine donor with $I_{\text{I}_2} > I_{\text{IBr}} > I_{\text{ICl}} > I_{\text{CF}_3\text{I}}$. This parallels the LIF results that shows the vibrational population in $v'' > 9$ varied as $\text{I}_2 > \text{IBr} > \text{ICl} > \text{CF}_3\text{I}$. Further evidence of the role of IF^\dagger is seen in the temporal profiles of $\text{IF}(\text{B}+\text{X})_{0-4}$ intensity for each iodine donor obtained by varying the IF injector location (Fig. 47). At long reaction times the amount of $\text{IF}(\text{B})$ formed is comparable for all cases. ICl shows an almost flat response to the variation of reaction time. This is similar to the response observed for CF_3I which was discussed previously. Both of these iodine donors produce little to no $\text{IF}(\text{X}, v'' > 9)$. Thus the $\text{O}_2^1\Sigma$ mechanism is probably operative. At short reaction times the amount of $\text{IF}(\text{B})$ formed is greatly enhanced in the case of I_2 and to a lesser extent for IBr . Both of these iodine donors produce a significant amount of IF in $v'' > 9$. The decrease in intensity at longer reaction times is expected since V-T relaxation will occur and reduce $[\text{IF}^\dagger]$. The LIF results confirm the reduction of $[\text{IF}^\dagger]$ at longer reaction times. In Fig. 48a we show an LIF spectrum using I_2 at a mixing time of 4 ms. For comparison an LIF spectrum taken at a mixing time of 0.7 ms is shown in Fig. 48b. Note the hot vibrational bands are almost completely absent in the long reaction time spectrum. Further, the overall signal from $v''=0$ increases a factor of 7 when going from short to long reaction time. Conversely, chemiluminescence spectra taken under the same conditions show an intensity decrease of a factor of 5 going from short to long reaction time.

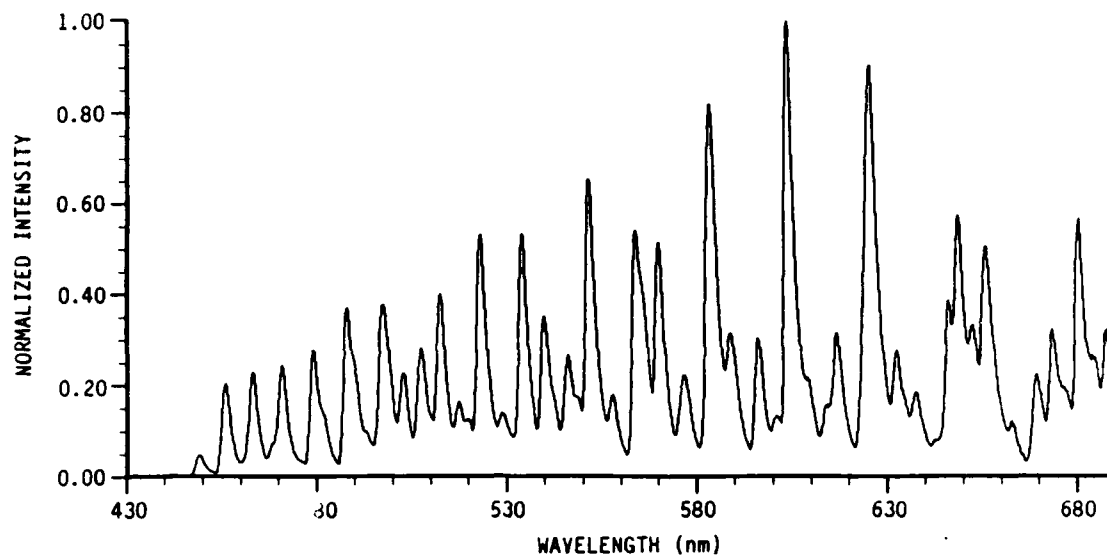


Figure 43. IF(B+X) chemiluminescence from O_2^* excitation. IF(X) formed using $I_2 + F$ reaction

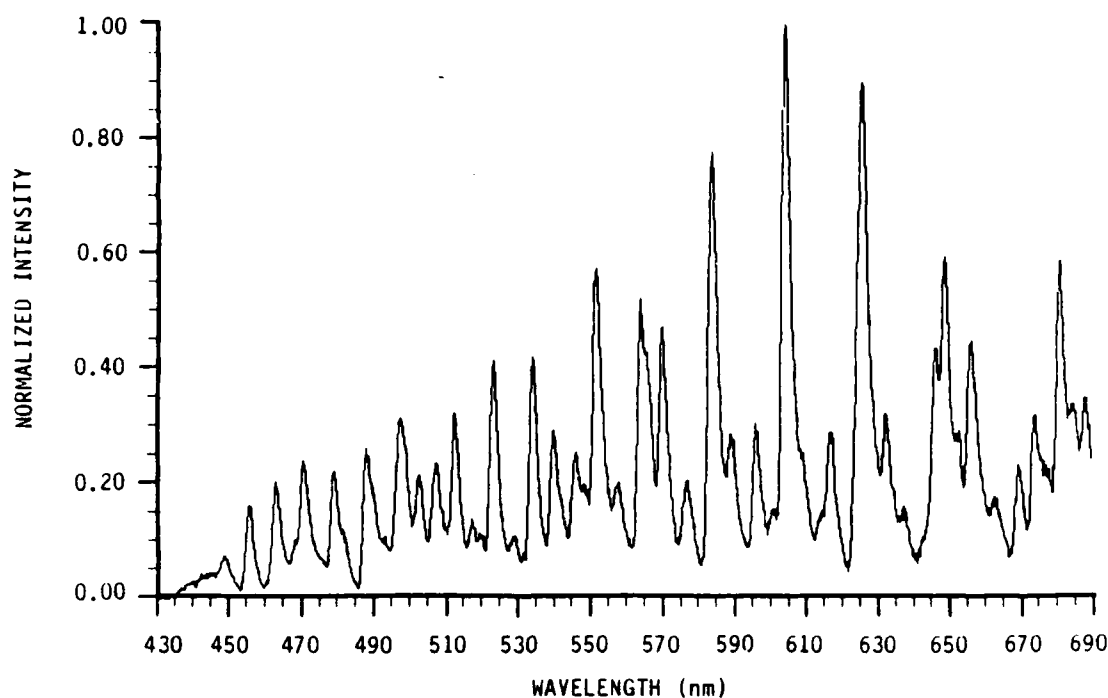


Figure 44. IF(B+X) chemiluminescence from O_2^* excitation. IF(X) formed using $IBr + F$ reaction

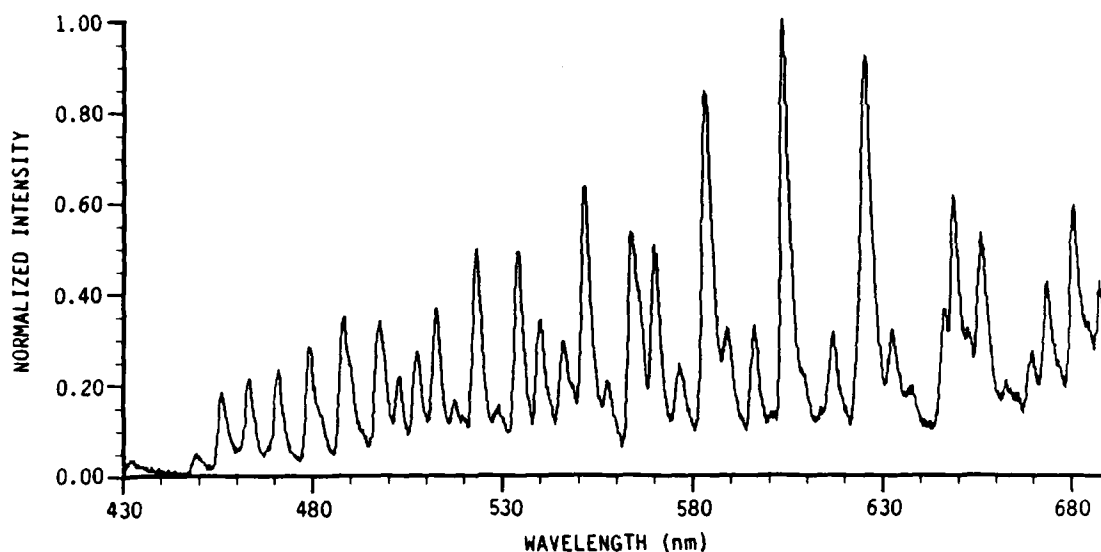


Figure 45. IF(B+X) chemiluminescence from O_2^* excitation. IF(X) formed using ICl + F reaction

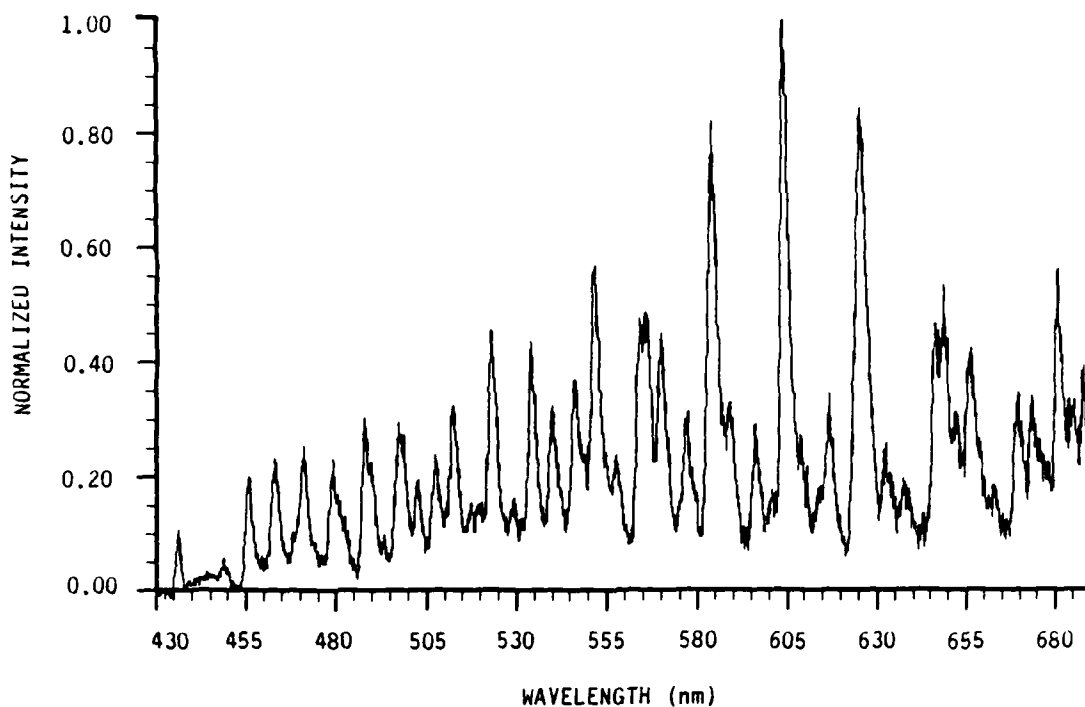


Figure 46. IF(B+X) chemiluminescence from O_2^* excitation. IF(X) formed using CF_3I + F reaction

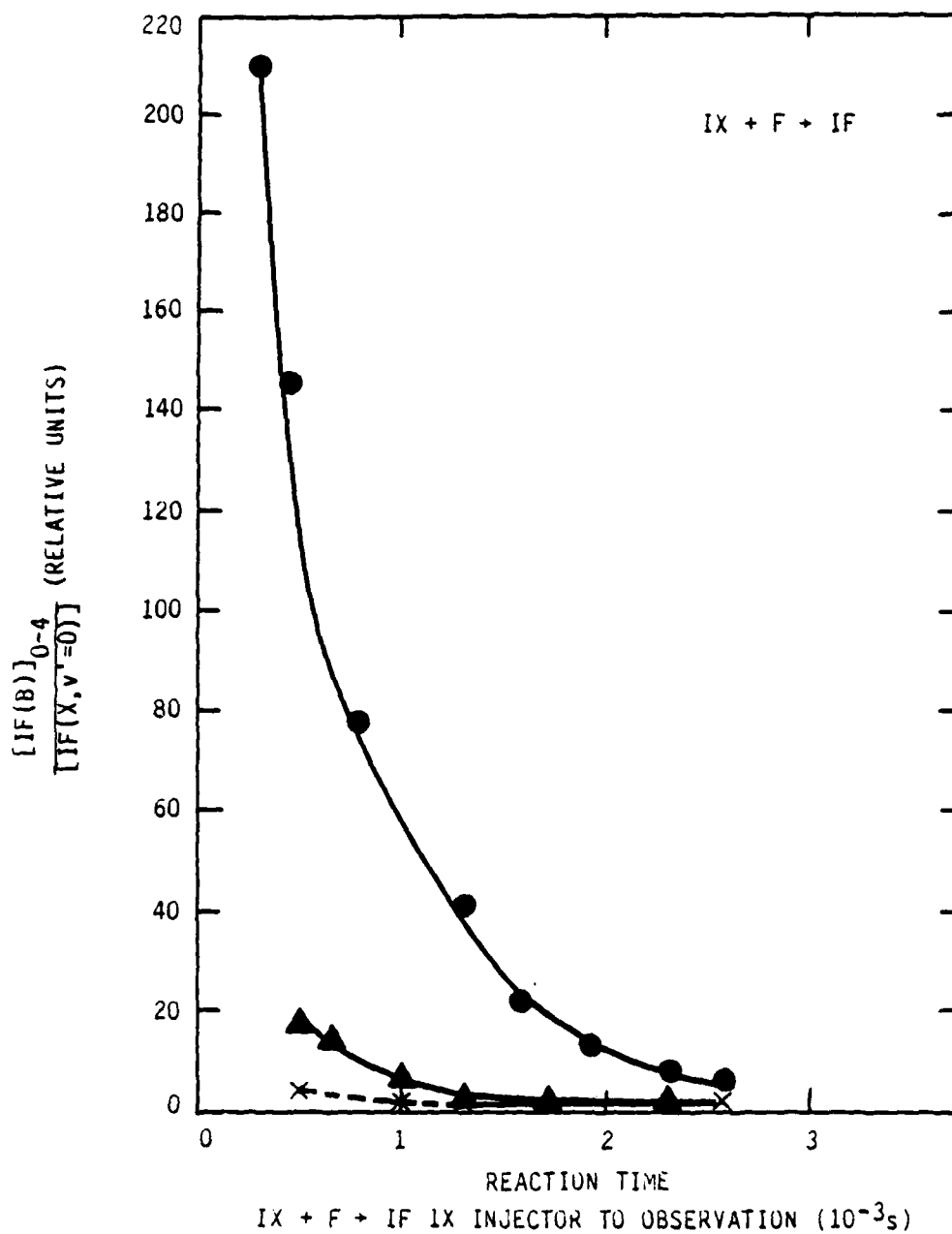
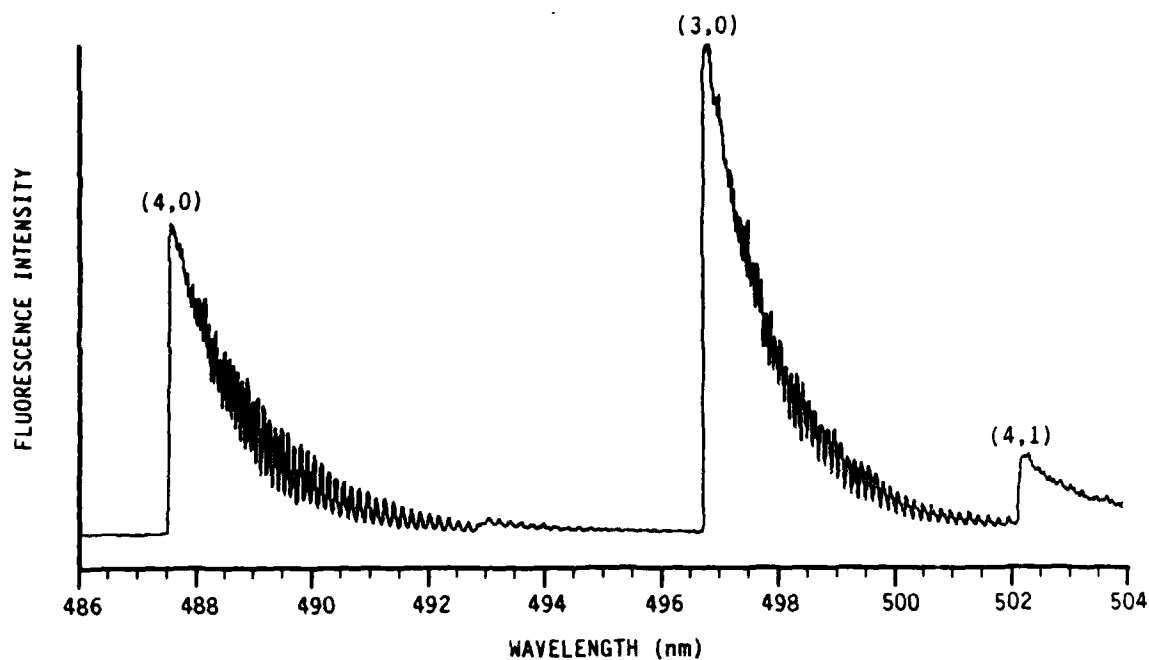
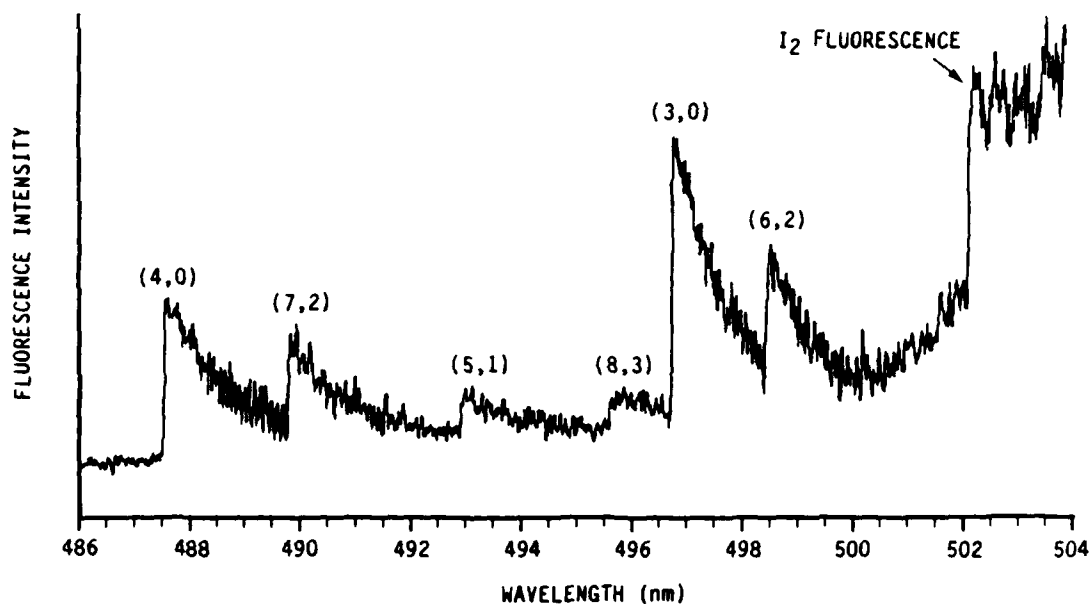


Figure 47. Temporal profiles of $IF(B+X)_{0-4}$ chemiluminescence intensity using iodine donors.

• I_2
 Δ IBr
 \times ICl



(a) Reaction time = 4 ms



(b) Reaction time = 0.7 ms

Figure 48. Excitation spectra for IF(X) resulting from $I_2 + F$ reaction.
a) reaction time = 4 ms; b) reaction time = 0.7 ms

To compare the chemiluminescence intensity for the different iodine donors directly the measured intensity needs to be normalized to the amount of IF^\dagger formed. We are unable to make an absolute determination of the amount of IF^\dagger formed. An estimate of the relative amount of IF^\dagger formed in each case can be determined by summing the population in each vibrational level.

Population of each vibrational level was calculated using the equations derived in Section 3 which include corrections for laser power, transition probability, and filter transmission. The population for each vibrational level could not be determined. In the cases of IBr and I_2 the population could be calculated for $v'' = 0, 1, 2$ and 6 through 14. For ICl $v'' = 2$ and 7 were also omitted from the sum since no measurements were made. The population $v'' = 2$ should be significant so that the calculated population of IF^\dagger is interpolated to be approximately 20 percent lower than the actual value. For CF_3I population from $v'' = 0$ and 1 were summed. Population in higher vibrations are neglected.

To elucidate the importance of $\text{IF}^\dagger(v'' > 9)$ in the excitation of IF(B) by $\text{O}_2(^1\Delta)$ several runs were completed in an attempt to correlate IF(B) production versus the initial IF ground state. For these runs all conditions were held constant with the exception of the IX donor. Plots of IF(B+X) chemiluminescence intensity as a function of $\text{IF(X, } v'')$ were constructed and are summarized in Figs. 49a,b,c. In Fig. 49a the observed chemiluminescence intensity is plotted versus $[\text{IF(X, } v'' = 0)]$ for $(\text{X} = \text{CF}_3, \text{Cl}, \text{Br}, \text{I})$. A similar plot using $[\text{IF(X, } v'' < 8)]$ as the independent variable is shown in Fig. 49b. Examination of these two plots shows essentially no correlation between $[\text{IF(B)}]$ and the relative concentration of $[\text{IF(X)}]$.

In contrast when the data are replotted in Fig. 49c using only $\text{IF(X, } v'' > 9)$ the data show a reasonably well behaved, linear relationship between $[\text{IF(B)}]$ and $[\text{IF(X, } v'' > 9)]$. The intercept is qualitatively consistent with the second excitation process that involves low vibrational levels of IF(X) and $\text{O}_2^1\Sigma$.

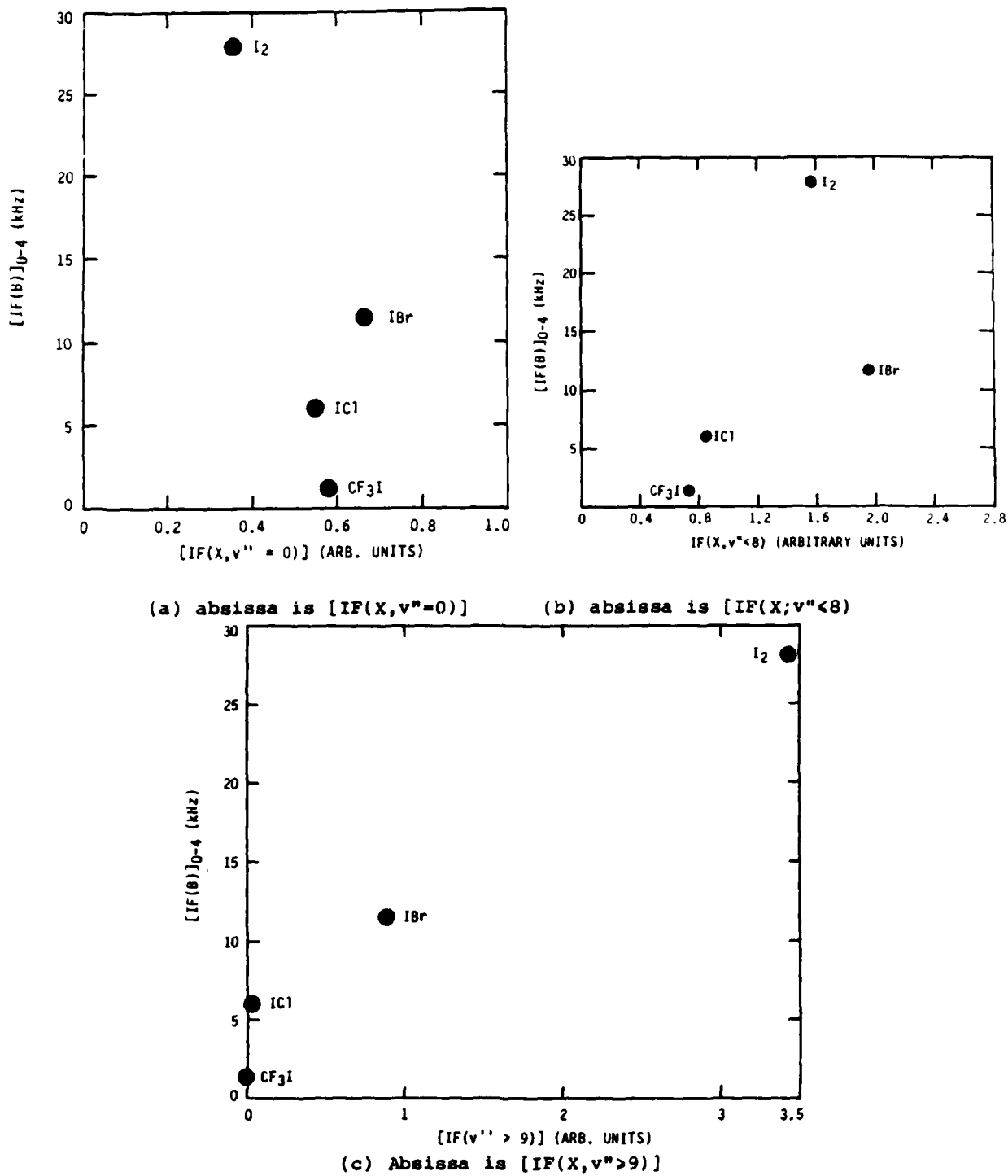


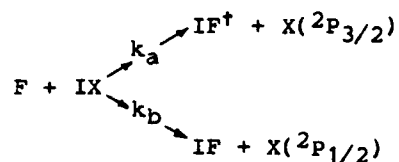
Figure 49. $[IF(B)]$ produced by O_2^+ pumping as a function of IF^+ at constant $O_2(^1\Delta)$.

The importance of IF^{\dagger} is clearly illustrated in these results. A small chemiluminescence signal is observed from vibrationally cold IF. As the amount of vibrationally hot IF is increased the chemiluminescence signal increases.

3.4 COMPARISON WITH PREVIOUS RESULTS

The first attempt to determine the internal energy distribution of the $IF(X)$ formed from $F + IX$ type reactions was reported by Donovan et al. (Ref. 34) in 1980. Using a pulsed dye laser they studied LIF and concluded that the $I_2 + F$ reaction produced a considerable fraction (~60 percent) of $IF(X)$ in vibrationally excited levels. Trickl and coworkers (Ref. 26) performed a similar study using a CW dye laser and reported that, the $F + I_2$ reaction produced $IF(X,v)$ with $v < 19$, but most of the IF (~90 percent) was produced in $v'' = 0$. In addition they found that although fraction of $IF(X,v'' > 0)$ was much higher for the ICl and $IBr + F$ reactions a secondary peak consistently appeared for $IF(X,v'' = 0)$. The vibrational distributions that they observed are reported in Fig. 50 for the convenience of the reader.

From these distributions Trickl and Wanner (Ref. 26) concluded that the $F + IX$ reactions must have two microscopic branches:



where k_b produces an electronically excited halogen atom. This prediction caused a considerable stir since it appeared that the $F + I_2$ reaction might be a convenient source for chemical production of I^* and might produce an I^* laser at $1.315 \mu m$ without the requirements of a chemical oxygen generator. Consequently several groups attempted to confirm this prediction by probing for the presence of I^* . Since the relevant $I(^2P_{1/2} + ^2P_{3/2})$ transition is at $1.315 \mu m$ it can be detected using an intrinsic germanium detector. Setser and coworkers (Ref. 35) used this technique but observed no detectable I^* emission

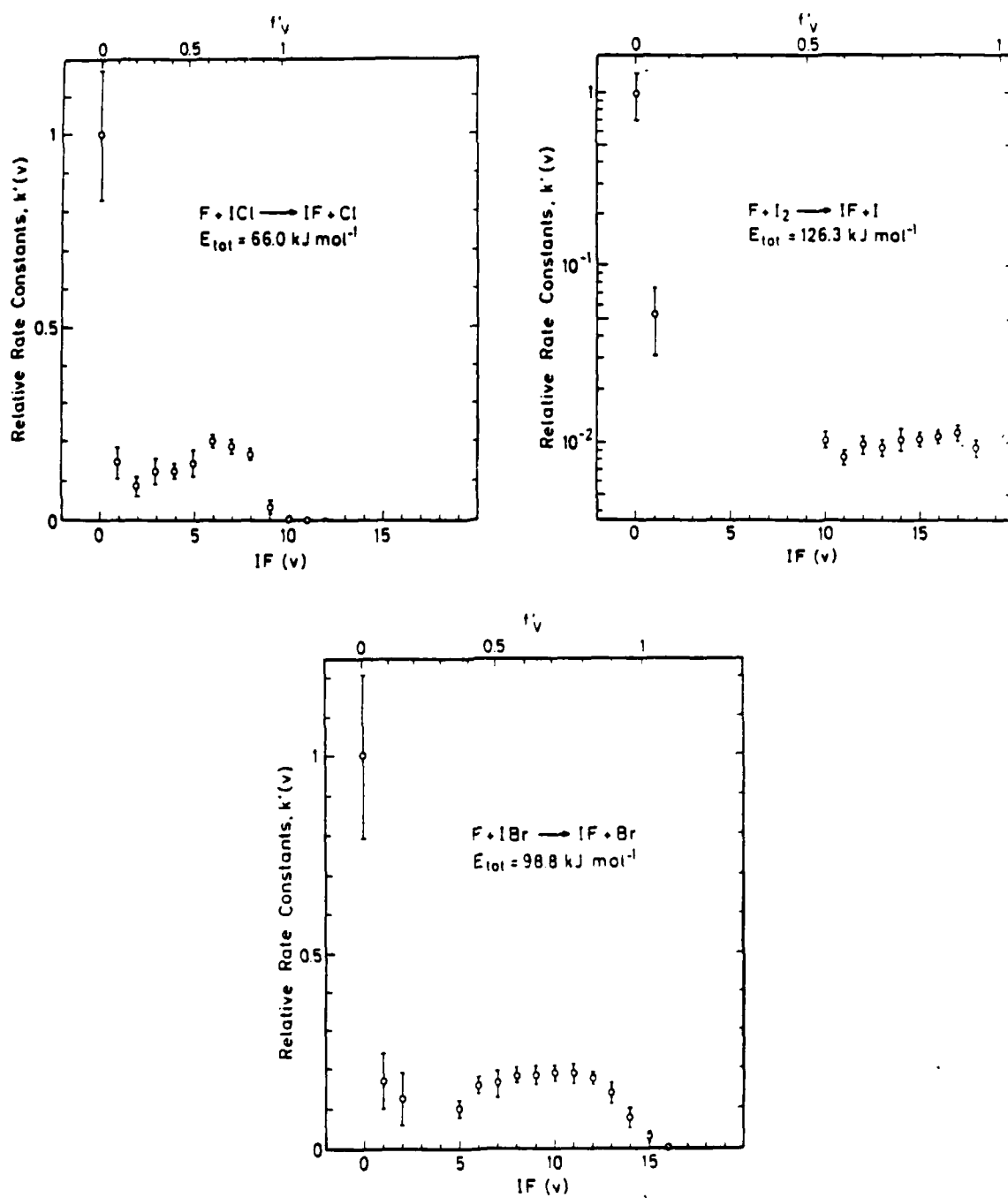


Figure 50. Vibrational distribution for $IF(X)$ produced by $IX + F$.
($X = I, Cl, Br$)

and concluded that the branching to I^* was $<4 \times 10^{-4}$. For the analogous $IBr + F$ reaction they concluded that the branching into Br^* was less than 1 percent. A similar study by Berson (Ref. 36) and his co-investigators used a well established two photon LIF technique for I^* detection, found no detectable I^* and placed an upper limit on the branching at 0.01. These two independent results were both in disagreement with the conclusions of Trickl and Wanner (Ref. 26) in that the predicted $X(^2P_{1/2})$ atoms, associated with the hypothesized $IF(X, v'' = 0)$ production branch, were absent.

The results of the LIF work also disagree with the conclusions of Ref. 26. Since the data in the present work were obtained at relatively high pressure ($P_T \sim 0.8$ Torr) the vibrational v'' distributions should be partially thermalized and indeed should be less nascent than those observed in the crossed beam apparatus of Trickl, et al. Nevertheless, we observed much greater fraction of IF^\dagger than did Trickl and Wanner.²⁶ The results clearly indicate that the fraction $f_v^{IX} = [IF^\dagger]/[IF(v'' = 0)]$ produced from $IX + F$ follows the progression $f_v^{I_2} > f_v^{IBr} > f_v^{ICl}$. Although we could not observe IF^\dagger production to the exothermic limit for the reactions involving either $I_2(v'' = 19)$ or $IBr(v'' = 15)$, we were able to probe the upper limit for the ICl reaction and found no detectable population above $v'' = 9$ which is consistent with Trickl and Wanner.

From a more fundamental viewpoint, it is of interest to note that Fletcher and Whitehead (Ref. 37) performed some classical trajectory calculations of the $I_2 + F$ reaction and predicted that the $IF(X)$ produced would be strongly inverted with a population peak occurring in $v'' = 16$. When normalized to the experimental results of Donovan, et al. (Ref. 34) ($v'' = 1, 2, 3$) and of Trickl and Wanner (Ref. 26) ($v'' = 10-19$) the qualitative agreement is excellent as is indicated in Fig. 51 which is extracted from Fletcher and Whitehead (Ref. 37).

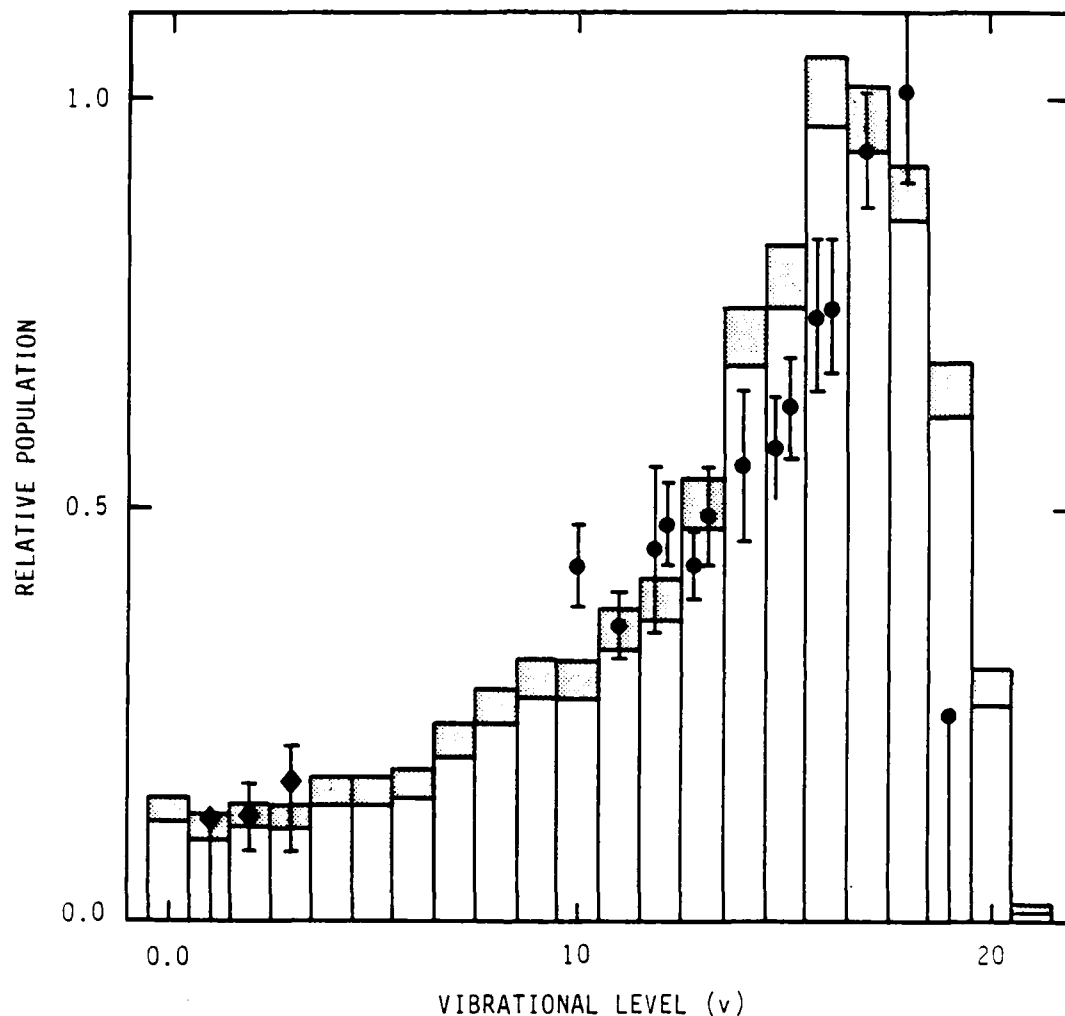


Figure 51. IF produce vibrational state distribution from the trajectory calculations for the reaction $F + I_2 \rightarrow IF + I$ at a collision energy of 8.4 kJ mol^{-1} (histograms). The hatched region represents two standard deviations centered around the calculated population. The calculations are compared with the results of Ref. 26 (solid circles) for $v > 10$; both distributions being normalized at their peaks. The experimental distribution of Ref. 34 is also shown (solid diamonds) and is normalized to the trajectory results at $v = 2$

The failure of the trajectory study to predict a secondary population peak at $v'' = 0$ is of primary importance to the present discussion. Indeed, Fletcher and Whitehead (Ref. 37) rationalized that this difference was because of an alternate reaction channel. This hypothesis was later reiterated by Trickl and Wanner (Ref. 26) in a subsequent paper.

The discrepancy between the results of Trickl and the several experiments has apparently been resolved in a recent study by Vigue, et al. (Ref. 38). They systematically repeated Trickl's experiment, and subsequent to the $I_2 + F$ reaction, they measured $[IF(X, v'' = 0)]/[IF(X, v'' = 13)] = 1.7 \pm 0.7$ in contrast to Trickl and Wanner who reported a value of 103 ± 32 for the same two levels. In addition, Vigue, et al. (Ref. 38) reported that the $[IF(X, v'' = 0)]$ was produced not by the direct $I_2 + F$ reaction but rather by a secondary process within the chamber. This conclusion was derived from the observation that $[IF(X, v'' = 13)]$ was observed only while the F_2 source was on while the corresponding signal for $v'' = 0$ was essentially independent of whether the fluorine source was on. The mechanism of the $IF(X, v'' = 0)$ source is unresolved, but it apparently does not involve the direct $I_2 + F$ reaction.

It is reasonable to extrapolate these results to the ICl and IBr reactions, especially in light of Setser's observation that the upper limit for the branching for Br^* production, which corresponds to the $IF(X, v'' = 0)$ channel, is < 1 percent. If the secondary peak observed by Trickl and Wanner (Ref. 26) at $v'' = 0$ is indeed due to background IF , then one could argue from the energetics of the $IX + F$ reactions that the fraction of IF^+ with $v'' > 9$ would be greatest for $I_2 + F$, and smallest for $ICl + F$, the order that was observed in the present program.

4. MISCELLANEOUS STUDIES

4.1 LIF FROM $D' \rightarrow A'$

An attempt was made to observe LIF from the $D' \rightarrow A'$ transition of IF. The mechanism for IF(B) production by O_2^* excitation involves the A' state as an intermediate. We were hoping to find a method to study the A' state directly. However, the laser system did not work well at the wavelength region of 360 nm needed to probe the transition. Only a few microjoules of laser power were available. A scan was made but no signal was detected.

4.2 REMOVAL OF IF(X,v) BY O_2^*

A qualitative study of the quenching of IF(v) by O_2^* was also performed. The LIF signal from (4,9) was observed under several conditions. First, 150 mTorr of the O_2 was added with no change to the LIF signal observed. Next the O_2 discharge was turned on creating O_2^* . This caused the $v'' = 9$ signal to disappear entirely. This is expected if the O_2^* is pumping the population in $v'' = 0$ up to higher levels. For $v'' = 0$, a 60 percent depletion of LIF signal was observed when O_2^* was present. Thus, although O_2^* depleted IF(X, $v'' = 0$) $v'' = 9$ was much more efficiently reduced. However, it is unknown whether $v'' = 9$ was promoted to IF(A'), and this observation should be investigated more thoroughly.

4.3 ROTATIONAL TEMPERATURE

A rough estimate can be made of the rotational temperature of IF(X,v) by using the spectral fitting computer codes described previously. Two vibrational bands (7,0) and (3,7) were chosen because no other bands overlap them. The computer generated spectra for each band at a variety of rotational temperatures. The generated spectra were then compared to the data to determine the best fit. For $v'' = 0$ the best fit fell between 250 to 300 K while for $v'' = 7$ the best fit was between 300 to 350 K. Because of the flow tube environment a considerable rotational thermalization was expected to occur.

In a crossed-molecular beam study, Vigue and coworkers (Ref. 38) report a rotational temperature of 263 K for $v'' = 0$. For high v'' they observe a non-Boltzmann distribution.

4.4 VIBRATIONAL RELAXATION

Several measurements were made to probe vibrational relaxation in $IF(X)$. The temporal profiles of $v'' = 10, 12$, and 13 were examined for several Ar pressures. This was accomplished by scanning the movable injector. Data from $v'' = 12$ are shown in Fig. 52. Some of the initial rise is due to chemical formation and mixing. The depletion is attributed to vibrational relaxation. The maximum IF^\dagger is depressed by the addition of Ar. Additional data for $v'' = 10$ are shown in Fig. 53. Also plotted is the $IF(B)_{0-4}$ chemiluminescence

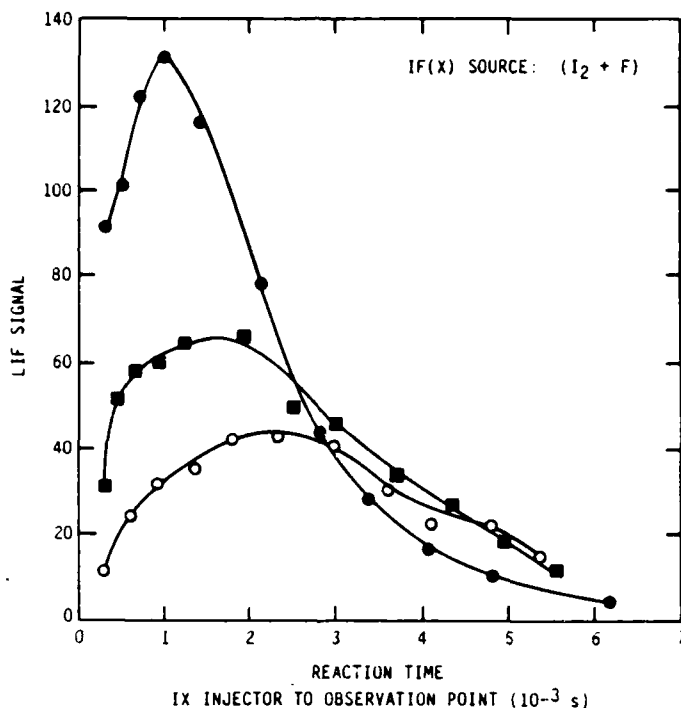


Figure 52. Temporal profile of $v'' = 12$. $IF(X)$ was formed using $I_2 + F$ reaction. ● - total pressure = 0.476 torr; ■ - total pressure = 0.729 torr; ○ - total pressure = 0.945 torr

intensity taken under comparable conditions. From Fig. 53 we observe that the chemiluminescence intensity falls off at a faster rate than does $v'' = 10$. However, we note that the observed rate of diminution of $v'' = 10$ is actually the sum of the rate into $v'' = 10$ from $v'' > 10$ and the rate out of $v'' = 10$ to lower v'' . The log of LIF intensity for LIF from $v'' = 10$ versus reaction time is plotted in Fig. 54. From the linear plot we deduce the decay is first order. Under psuedo first order conditions with the quencher gas in large excess, a kinetic analysis yields a working equation for determining the quenching rate coefficient:

$$\frac{\Delta(\ln I_{\text{LIF}})}{\Delta[Q]} (t) = k_Q$$

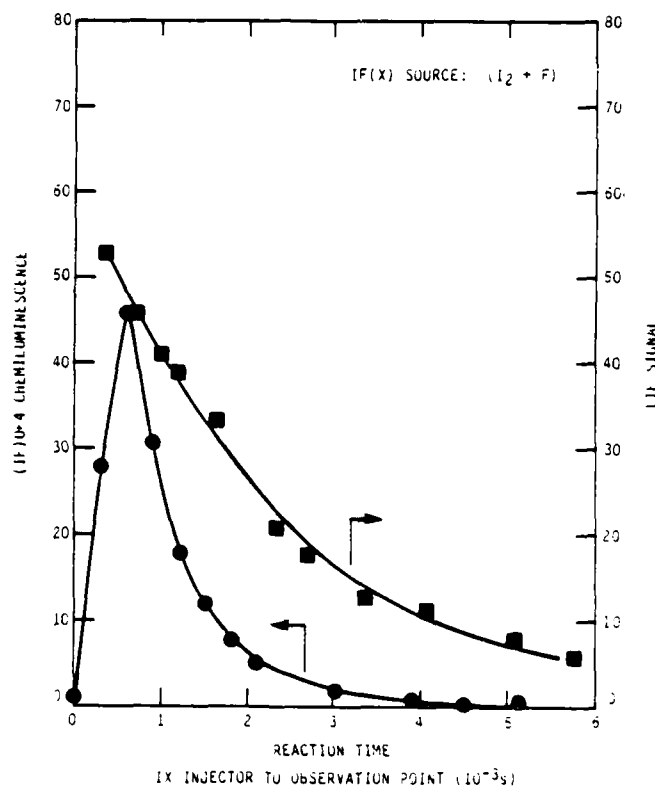


Figure 53. Plot of temporal evolutions of IF^+ and $IF(B+X)$ chemiluminescence intensity $IF(X)$ produced by $I_2 + F$ reaction. - LIF signal from excitation of $IF^+(X; v'' = 10)$; • - $IF(B+X)$ chemiluminescence intensity (data are normalized at one point). Argon pressure was 800 mTorr

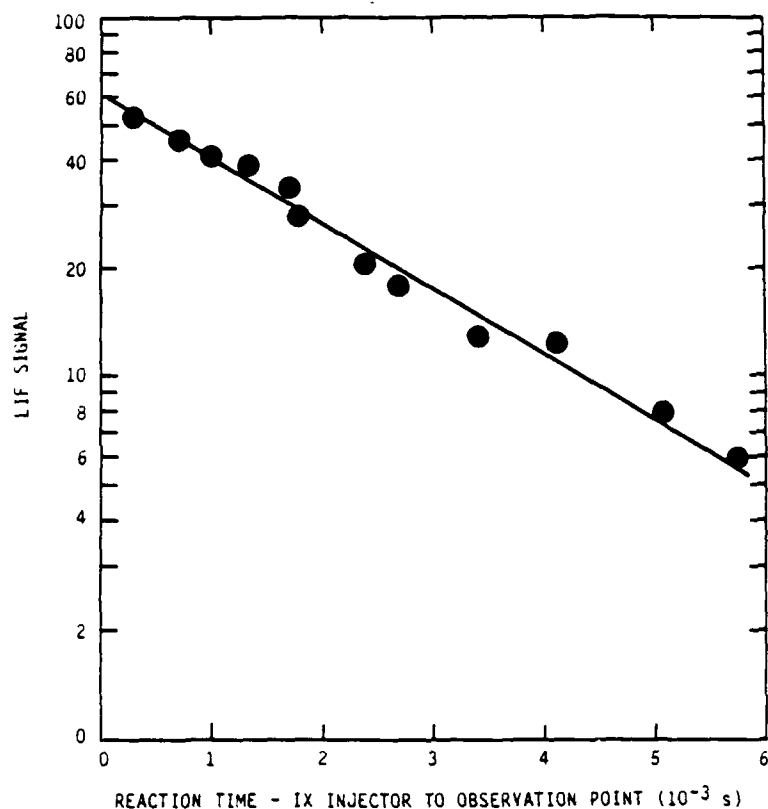


Figure 54. Semi log plot of $[IF(X, v'' = 10)]$ versus reaction time. Data taken from Fig. 54

where $[Q]$ is the concentration of the quenching species (in this case argon), I_{LIF} is the intensity of the LIF signal from $v'' = 10$ and t is the reaction time. The rate for quenching of $v'' = 10$ by Ar determined from the data is $k = 1.8 \times 10^{-14} \text{ cm}^3\text{-molecule}^{-1}\text{-s}^{-1}$. It must be remembered that this is the quenching rate for the net V-T from relaxation into and out of $v'' = 10$. Although the investigation of V-T relaxation of $IF(X, v'' \gg 0)$ is preliminary, it is clear that the LIF techniques developed in this program could be used to determine accurately V-T relaxation rate coefficients.

5. CONCLUSIONS

In this report we describe a multifaceted investigation that appears to confirm that $\text{IF}^\dagger(v'' > 9)$ is an important species in the excitation of $\text{IF}(\text{B})$ by $\text{O}_2(^1\Delta)$. This excitation process displayed a quadratic dependence upon the $\text{O}_2(^1\Delta)$ concentration which suggests a sequential excitation involving an IF reservoir state which is almost certainly $\text{IF}(\text{A}')$. There is a preponderance of evidence to support this hypothesis.

The earlier results of Whitefield et al. (Ref. 13) showed a peak in the population in $\text{IF}(\text{B})$ near $v' \sim 6$. Similar trends were also observed in the present work. This distribution although not nascent may indicate the entrance channel into $\text{IF}(\text{B})$. Since $T_e(\text{A}')$ is $\sim 13490 \text{ cm}^{-1}$ energy transfer from $\text{O}_2(^1\Delta)$ would have energy sufficient to promote $\text{IF}(\text{A}', v' = 0)$ $v' = 5$ of the B state. If $\text{IF}(\text{A}')$ contained any vibrational excitation then higher levels would be accessible.

The LIF results showed that $\text{IF}^\dagger(v'' > 9)$ is the important species in the $\text{O}_2(^1\Delta)$ excitation process. The energy of $\text{O}_2(^1\Delta) + \text{IF}^\dagger(v'' = 9)$ is 13393 cm^{-1} which is very close to the estimate of $T_e(\text{A}')$. Vibrational levels < 9 are sufficiently below this value.

The combined chemiluminescence-LIF experiments showed that when the $\text{IF}^\dagger(v' > 9)$ was reduced by thermalization the efficiency of $\text{IF}(\text{B})$ production was markedly reduced. The results also clearly demonstrated that the I_2 species produced the most IF^\dagger and the strongest chemiluminescence.

A second, much less efficient excitation process was also identified in which vibrational cold IF was excited by $\text{O}_2(^1\Sigma)$. The obvious model is that $\text{O}_2(^1\Sigma)$ energy transfer promotes IF to the A' state and a secondary $\text{O}_2(^1\Delta)$ encounter completes the excitation process.

While the present program has identified that IF^+ is an important intermediate species in the excitation of $IF(B)$ by $O_2(^1\Delta)$, key rate coefficients in the process are essentially unknown. It does appear that the mechanism involving IF^+ is much more efficient than the $O_2(^1\Sigma) + IF$ excitation process.

The determination of the rate of $IF(B)$ production, at $O_2(^1\Delta)$ concentrations much greater than those obtained in the present experiment, would be a valuable experiment to further test the scaling of this interesting system to laser densities. There are other IF precursors that could be investigated that might offer enhanced IF^+ , e.g., C_3H_5I (Ref. 39). The role of $IF(A')$, while strongly indicated from the present results, has not yet been identified in the gas phase. A systematic study of $IF(D' + A')$ laser excitation in an $IF + O_2(^1\Delta)$ flame would be a valuable investigation.

6. REFERENCES

1. Clyne, M.A.A. and McDermid, I.S., "Quantum Resolved Dynamics of Excited States, Part 4. Radiative and Predissociative Lifetimes of IF $B^3\Pi(O^+)$," JCS Faraday II 74, 1644 (1978).
2. Davis, S.J. and Hanco, L., "Optically Pumped Iodine Monofluoride $B^3\Pi(O^+) \rightarrow X^1\Sigma^+$ Laser," Appl. Phys. Lett. 37, 692 (1980).
3. Davis, S.J., Hanco, L., and Shea, R.F., "Iodine Monofluoride $B^3\Pi(O^+) \rightarrow X^1\Sigma^+$ Lasing from Collisionally Pumped States," J. Chem. Phys. 78, 172 (1983).
4. Wolf, P.J., Glover, J.H., Hanco, L., Shea, R.F., and Davis, S.J., "Collisional Dynamics of the IF $B^3\Pi(O^+)$ State. I. Pulsed Excitation Studies of $v'=3$ and 4 at High Pressure," J. Chem. Phys. 82, 2321 (1985).
5. Wolf, P.J. and Davis, S.J., "Collisional Dynamics of the IF $B^3\Pi(O^+)$ State. II. Electronic Quenching at Low Pressures," J. Chem. Phys. 83, 91 (1985).
6. Wolf, P.J. and Davis, S.J., "Collisional Dynamics of the IF $B^3\Pi(O^+)$ State. III. Vibrational and Rotational Energy Transfer," J. Chem. Phys. (in press).
7. Davis, S.J., Hanco, L., and Wolf, P.J., "Continuous Wave Optically Pumped Iodine Monofluoride $B^3\Pi(O^+) \rightarrow X^1\Sigma^+$ Laser," J. Chem. Phys. 82, 4831 (1985).
8. Durie, R.A., "Proc. R. Soc. London Ser. A 207, 388 (1951).
9. Whitefield, P.D. and Davis, S.J., "Rate of the Reaction $I_2 + F_2 \rightarrow$ Products," Chem. Phys. Lett. 83, 44 (1981).
10. Valentini, J., Coggiola, M.J., and Lee, Y.T., Int. J. Chem. Kinet. 8, 605 (1976).
11. Kanler, C.C. and Lee, Y.T., "Crossed Molecular Beam Studies of Chemiluminescent Reactions: $F_2 + I_2$, Br, and ICl," J. Chem. Phys. 73, 5122 (1980).
12. Clyne, M.A.A., Coxon, J.A., and Townsend, L.W., "Formation of the $B^3\Pi(O^+)$ Status of BrF and IF in Atom Recombination in the Presence of Singlet ($^1\Delta$, $^1\Sigma_g^+$) Oxygen," JCS Faraday Trans. II 68, 2134 (1972).
13. Whitefield, P.D., Shea, R.F., and Davis, S.J., "Singlet Molecular Oxygen Pumping of IF $B^3\Pi(O^+)$," J. Chem. Phys. 78, 6793 (1983).
14. Pritt, A.T. Jr., Patel, D., and Benard, D.J., "Iodine Monofluoride Resonant Energy Transfer Chemiluminescence," Chem. Phys. Lett. 97, 471 (1983).

15. Piper, L.G., Marinelli, W.J., Rawlins, W.T., and Green, B.D., "The Excitation of $\text{IF}(\text{B}^3\Pi_0^+)$ by $\text{N}_2(\text{A}^3\Sigma_u^+)$," J. Chem. Phys. 83, 5602 (1985).
16. Daily, M., Hanko, L., and Davis, S.J., (unpublished results).
17. Piper, L.G., Marinelli, W.J., Green, B.D., Rawlins, W.T., Murphy, H.C., Donahue, M.E., and Lewis, P.F., "Kinetics of Iodine Monofluoride Excitation by Energetic Nitrogen," PSI Report TR-460 (Air Force Contract No. F29601-83-C-0051) (February 1985).
18. Setser, D.W., Private communication (1985).
19. Whitefield, P.D. and Berman, M.R., "Oxygen IF Kinetics," AFWL TR-84, Air Force Weapons Laboratory, Kirtland AFB, NM 87117 (1985).
20. Williamson, R.L., Hanko, L., and Davis, S.J., "Intracavity Gain Detection Applied to Pulsed, Transient Inversions in IF," Laser Chemistry (in press).
21. Herzberg, G., Molecular Spectra and Molecular Structure. I. Spectra of Diatomic Molecules, Van Nostrand Reinhold Co., New York (1950).
22. Nicolai, J.P. and Heaven, M.C., "Laser Excitation Spectra for Matrix Isolated IF: Observation of New Low-Lying Electronic States," (submitted to J. Chem. Phys.).
23. Van Benthem, J.H. and Davis, S.J., "Detection of Vibrationally Excited I_2 in the Iodine Dissociation Region of Chemical Oxygen-Iodine Lasers," J. Phys. Chem., 90, 2 (1986).
24. Trickl, T., "Laserspektroskopische Untersuchungen an Jodmonofluorid, gebildet in den Reaktionen von Fluoratomen mit ICl , IBr and I_2 in gekreuzten Molekularstrahlen," MPI Quant. 71 (1983).
25. Trickl, T. and Wanner, J., " $\text{IF}(\text{A} + \text{X}, \text{B} + \text{X})$ Chemiluminescence from the $\text{F} + \text{I}_2\text{F}$ Reaction," J. Chem. Phys. 74, 6508 (1981).
26. Trickl, T. and Wanner, J., "The Dynamics of the Reactions $\text{F} + \text{IX} \rightarrow \text{IF} + \text{X}$ ($\text{X} = \text{Cl}, \text{Br}, \text{I}$): A Laser-Induced Fluorescence Study," J. Chem. Phys. 78, 6091 (1983).
27. Stein, L. and Wanner, J., "Laser-Induced Fluorescence Study of the Reactions of F Atoms with CH_3I and CF_3I ," J. Chem. Phys. 72, 1128 (1980).
28. Trickl, T. and Wanner, J., "High-Resolution, Laser-Induced Fluorescence Spectroscopy of Nascent IF: Determination of X- and B-State Molecular Constants," J. Mole. Spectr. 104, 174-182 (1984).
29. Appleman, E.H. and Clyne, M.A.A., "Reaction Kinetics of Ground State F^2P Atoms," JCS Faraday I, 71, 2072 (1975).

30. Sung, J.P., Bachar, J., and Setser, D.W., "Electronic-to-Vibrational Energy Transfer Studies of Singlet Molecular Oxygen and Hydrogen Halides," AFWL-TR-84-23, AFWL, Kirtland Air Force Base, NM 87117 (1984).
31. Mullar, D.F. and Houston, P.L., J. Phys. Chem. 85, 3563 (1981).
32. Fontijn, A., Meyer, C.B., and Schiff, H.I., "Absolute Quantum Yield Measurements of the NO-O Reaction and Its Use as a Standard for Chemiluminescent Reactions," J. Chem. Phys. 40, 64 (1964).
33. Marinelli, W.J. and Piper, L.G., "Franck-Condon Factors and Absolute Transition Probabilities for the IF ($B^3\Pi_0^+ \rightarrow X^1\Sigma^+$) Transition, JQSRT 34, 321 (1985).
34. Donovan, R.J., Fernie, D.P., Fluendy, M.A.D., Glen, R.M., Rae, A.G.A., and Wheeler, J.R., "Energy Partitioning in the Reaction $F + I_2$," Chem. Phys. Lett. 69, 472 (1980).
35. Agrawalla, B.S., Singh, J.P., and Setser, D.W., "Branching Fraction for $I(^2P_{1/2})$ Formation by the $F + I_2$ Reaction," J. Chem Phys. 79, 6416 (1983).
36. Das, P., Venkitachalam, T. and Bersohn, R., "On the Absence of $I(^2P_{1/2})$ as a Product of the Reactions of F Atoms with HI, I_2 , and ICN," J. Chem. Phys. 80, 4859 (1984).
37. Fletcher, I.W. and Whitehead, J.C., "Classical Trajectory Studies of the Reaction $F + I_2$," JCS Faraday Trans. 2, 78, 1165 (1982).
38. Girard, B., Billy, N., Bouedard, G. and Vigue, J., "LIF Study of the $I_2 + F \rightarrow IF + I$ Reaction: Population of the $v'' = 0$ Level of IF," Chem. Phys. Lett. 136, 101 (1987).
39. Collins, S.T., Trautmann, M., and Wanner, J., "Vibrational-State Distribution of IF from the Reaction $F + 3$ -Iodopropene: An Example of Radical Resonance Energy Participation," J. Chem. Phys. 84, 3814 (1986).